AN INTEIN-LINKED YEAST EXPRESSION PLATFORM FOR CUSTOM FUNCTIONALIZATION OF PROTEINS

By

Carrie J. Marshall

A dissertation submitted in partial fulfillment of

the requirements for the degree of

Doctor of Philosophy

(Chemical and Biological Engineering)

at the

UNIVERSITY OF WISCONSIN-MADISON

2014

Date of final oral examination: August 19, 2014

The dissertation is approved by the following members of the Final Oral Committee:

Eric V. Shusta, Professor, Chemical and Biological Engineering

Sean P. Palecek, Professor, Chemical and Biological Engineering

Regina M. Murphy, Professor, Chemical and Biological Engineering

Jennifer L. Reed, Assistant Professor, Chemical and Biological Engineering

Ronald T. Raines, Professor, Chemistry and Biochemistry

AN INTEIN-LINKED YEAST EXPRESSION PLATFORM
FOR CUSTOM FUNCTIONALIZATION OF PROTEINS

Carrie J. Marshall

Under the supervision of Professor Eric V. Shusta

at the University of Wisconsin-Madison

ABSTRACT

Chemical customization of proteins allows the engineering of proteins that have enhanced properties such as in the creation of antibody-drug conjugates, bispecific antibodies, fluorescent detection molecules, and immobilized proteins for microarrays. Installing chemical functionalities that are bioorthogonal and in a site-specific manner is key to providing consistent and uniform protein modification as well as to preventing deleterious effects on protein structure and activity. One approach for obtaining these site-specific modifications is the reaction of non-self cleaving intein fusion proteins with nucleophiles possessing custom chemical properties. This intein-mediated expressed protein ligation (EPL) method has previously been employed to install a variety of different chemical functionalities onto the carboxy-terminus of target proteins, thus facilitating protein conjugation to fluorophores, surfaces, nanoparticles, and polymers.

While EPL is typically performed using soluble, purified intein-fusion proteins, we have extended these methods to release and chemically modify proteins displayed on the surface of yeast, thereby enabling the facile chemical modification of proteins

directly from an *in vitro* protein engineering platform. To this end, we displayed single chain antibodies (scFvs) and green fluorescent protein (GFP) on the surface of yeast as fusions to the Mxe GyrA intein, thus permitting the simultaneous release of the scFvs and GFP and the insertion of chemical functionalities compatible with click chemistry. For example, proteins were released, alkyne-modified at the carboxy-terminus, and used in a click chemistry reaction to immobilize active proteins on azido-functionalized surfaces. By eliminating laborious protein preparation steps typically required for EPL modification such as reformatting, soluble expression, and purification, this platform provides a particularly powerful tool for the rapid assessment of engineered proteins.

This intein-linked yeast display platform made possible the expression of properly folded scFv-intein fusion proteins, therefore providing for small-scale production of functionalized protein. Preparative scale antibody-intein fusion protein production has typically been performed using bacteria, but this often yields insoluble inclusion bodies that require refolding to obtain active antibody-intein fusion proteins. Therefore, we evolved the Mxe GyrA intein to improve both the display and secretion levels of scFv-intein fusion proteins from yeast. While modest improvements in surface display levels were obtained, we demonstrated that folded, active scFv-intein fusions could be secreted from yeast and that the engineered intein substantially improved scFv-intein secretion levels. Using EPL, the secreted scFv-intein fusion proteins were azide-modified at the carboxy-terminus and site-specifically immobilized onto surfaces via strain-promoted click chemistry. This platform enabled the preparative scale production of active scFv-intein fusion proteins from yeast without any refolding steps, thus providing a robust alternative to bacterial expression systems and permitting a facile

transition of yeast displayed scFv-intein fusions to a system with greater protein production capacity.

Next, we applied these methods to generate and characterize epidermal growth factor receptor (EGFR) scFvs that are capable of recognizing specific isoforms of EGFR. Using the established modification techniques, these antibodies are expected to facilitate the development of a liquid crystal-based assay that can detect EGFR-containing microvesicles shed from cells. Finally, intein-linked yeast display was employed towards development of a clicked bispecific antibody platform enabling combinatorial pairing of antibodies that result from the yeast display antibody identification and engineering platform. Taken together, these methods permit the facile generation of protein conjugates using engineered proteins and enables the rapid integration of large panels of engineered proteins into downstream functional assays.

ACKNOWLEDGMENTS

I would like to express my deep gratitude and appreciation for all the individuals who provided support and encouragement throughout my long academic journey. I owe a great deal to my research advisor, Prof. Eric Shusta, who has served as a mentor to me for these past five years and from whom I have gained tremendous knowledge about research. I particularly appreciated the guidance and advice he provided when needed, as well as the freedom to pursue my own ideas in the development of my career as a scientist. I would also like to express my appreciation for former and current members of the Shusta Lab, especially Dr. Nitin Agarwal, who initiated the project upon which my thesis is based. Dr. Benjamin Tillotson and Thomas Malott both provided tremendous support to me when I was starting in the lab, and in addition to teaching me many useful skills at the beginning of my career, they continued to provide a source of knowledge and advice in the following years. Vanessa Grosskopf was of great assistance when she worked with me as both an undergraduate a Master's student, and her research has helped to strengthen the content of my project. I greatly enjoyed getting to know her over the past several years, and I sincerely miss our daily conversations in the lab. Additionally, Taylor Moelling has worked with me over the past year as an undergraduate student, and I deeply appreciate her hard work and assistance she has provided.

I would like to express my gratitude for the numerous other researchers at UW who have assisted me in the past five years. Although he is no longer with us, I would like to thank Prof. Paul Bertics for guidance with the EGFR assays at the beginning of

my career, and I would especially like to thank Dr. Greg Wiepz for providing further assistance and EGFR reagents necessary to complete the work. Prof. Nicholas Abbott and other members of the Bioengineering Research Partnership (BRP) provided very valuable collaborative assistance on many of my projects. I would also like to express my great appreciation for Prof. Ronald Raines and two members of his group, Dr. Nicholas McGrath and Kalie Mix, whose expertise in chemical synthesis was instrumental to several of my projects. Additionally, the staff at The UW Carbone Cancer Center Flow Cytometry Facility was extremely helpful with sorting for my directed evolution project, and their assistance was essential to the project's success. I would also like to thank additional members of my thesis defense committee, Prof. Regina Murphy, Prof. Jennifer Reed, and Prof. Sean Palecek, and I am very grateful for the time taken to serve on my committee.

Finally, I would like to thank all of my friends and family members who have supported me throughout this journey. I would especially like to thank my parents, Don and Linda Marshall, who provided me with the resources to be successful in my studies, and I know that without their support, none of this would have been possible. Most importantly, I cannot express enough gratitude to my best friend and husband, Mark Lorson, for his unwavering love and encouragement. I could not ask for a more supportive partner in life, and I am excited for the next chapter in ours.

Contents

List of Figures

List of Tables

Chapter 1 – Chemical Modification and Engineering of Proteins

1.1 Introduction

Since the advent of the first recombinant protein therapeutic, scientists have sought to harness the characteristic diversity and complexity of proteins to treat and diagnose diseases. This has led to the creation of a new discipline, protein engineering, that enables the discovery, development, and improvement of novel proteins possessing desired qualities. *In vitro* protein engineering platforms like phage, ribosome, and yeast display have been developed in order to design proteins with desired characteristics including binding specificity, affinity, and enzyme activity. While it has become established that these engineered proteins can be employed in immunoassays for diagnostics or therapeutics for disease treatment, a new generation of protein molecules with increased clinical potential is emerging — protein conjugates. Conjugation provides the ability to expand the intrinsic characteristics of proteins by combining them with molecules containing important functions, such as drugs, polymers, nanoparticles, or other proteins. Furthermore, protein conjugation is expected to facilitate the development of high-throughput diagnostic assays through the creation of microarray chips that are decorated with highly specific and sensitive antibodies. However, thus far the development of protein conjugates and microarrays has been separate from the discovery and engineering of potential protein targets. Conjugates are synthesized using previously engineered proteins, which doesn't permit the simultaneous, application-specific, screening of proteins and conjugates in tandem. Additionally, since protein conjugation is typically performed with soluble, purified

proteins, transitioning large pools of engineered proteins from display platform to a soluble platform would be highly laborious and cumbersome. Thus, current methods to separately engineer and conjugate proteins are not feasible to identify optimum combinations of protein-drug conjugates, bispecific antibodies, or antibodies for microarray chips.

Accordingly, methods to directly incorporate conjugation strategies into protein engineering platforms would be highly desirable for the development of protein therapeutics and diagnostic tools. To this end, we developed a yeast surface display platform that permits the release and chemical modification of engineered proteins through display fusion to a protein splicing element known as an intein (Chapter 2). This intein-based platform enables direct conjugation of proteins to a variety of targets, thus providing a powerful tool for the rapid assessment of engineered proteins. In Chapter 3, we engineer the intein to enhance production of fusion proteins for chemical modification. Through directed evolution, the intein is improved to permit the secretion of soluble fusion proteins from yeast, thereby providing an enhanced platform for protein modification compared to the current bacterial expression systems. Furthermore, the engineered intein improves upon the intein-linked yeast display platform by increasing the attainable yield of functionalized protein via display and by allowing for a facile transition to preparative scale protein production using yeast secretion.

Throughout Chapters 2 and 3, we explore “click”-based chemistries for protein conjugation that are made possible by the intein-fusion platform. In Chapter 2, we employ a copper-catalyzed click reaction to immobilize antibodies onto surfaces and demonstrate antigen capture from purified sources. In Chapter 3, we expand upon this

concept by immobilizing antibodies via catalyst-free click chemistry, and we demonstrate surfaces decorated with the antibodies can be employed to capture different protein isoforms from cell lysates. Finally, in Chapter 5, we explore click reactions with extremely fast kinetics, working toward the creation of a platform that allows high throughput combinatorial bispecific antibody pairings.

In the course of this work, we utilize a cohort of epidermal growth factor receptor (EGFR) antibodies for platform design and to demonstrate the utility of the devised protein conjugation strategies. In Chapter 4, we characterize these antibodies and work towards employing the established conjugation methods to develop a novel liquid crystal assay capable of detecting EGFR biomarkers from cell samples.

This chapter serves to briefly review the literature surrounding the interface of engineering and chemical modification of proteins. Several protein modification strategies will be introduced before focusing upon intein mediated protein functionalization and click chemistry. We will address the current limitations of intein-fusion protein production, discuss alternative recombinant protein expression systems, and explore protein engineering via yeast display.

1.2 Protein Bioconjugation

By linking proteins to molecules with unique properties, bioconjugation offers the opportunity to alter and enhance the therapeutic and diagnostic potential of biomolecules. While there are numerous applications that warrant further development of bioconjugation techniques, one significant example is the emergence of a new class of protein therapeutics known as antibody-drug conjugates (ADCs). ADCs utilize antibody specificity to deliver an attached drug to a particular target, such as tumor

cells, thereby killing the diseased cells while sparing healthy tissue [1]. The potential therapeutic efficacy of ADCs has prompted intense research and development into the field, leading to 30 ADCs in the clinical trial stage [2] and two ADCs on the market as of 2013 [3]. Another noteworthy example of a bioconjugated product is the linkage of polymer structures, particularly polyethylene glycol (PEG), to proteins. These PEG linkers have been shown to improve half life [4-7], solubility, and stability [4] of protein therapeutics while also reducing their immogenicity and antigenicity [4, 6, 7], leading to the FDA approval of nine polymer-protein drugs as of 2011 [5]. Further research has also employed bioconjugation techniques to immobilize antibodies and proteins on surfaces for the development of microarrays [8-11] and biosensors [12-14] that are expected to facilitate high-throughput analysis and diagnostics [15]. Many other applications of bioconjugation exist, including the creation of targeted nanoparticles [16, 17] and bispecific antibodies [18], that further motivate the development of bioconjugation techniques and strategies.

The available techniques to synthesize these protein conjugates usually involve modification of chemical residues within the protein to link a target. The most commonly modified protein residues are lysines, since they tend to be found at the exterior of proteins and contain a reactive primary amine [8, 19]. Among the reagents that will react with primary amines are NHS-esters, which form a stable amide bond to conjugate a NHS-functionalized target to the protein [19] (Figure 1-1). Other reactive chemical residues within a protein that are commonly used in conjugation reactions include thiols, carboxylic acids, and hydroxyl groups. However, since these functional groups are present at multiple locations throughout proteins, these methods led to the random and

heterogeneous functionalization of proteins. A commonly reported problem with random protein modification is a decrease in protein activity caused by alterations of protein binding sites, changes in protein structure and conformation, and steric hindrance between the protein and the newly inserted molecule or surface [4, 5, 12, 20-25].

Figure 1-1: Bioconjugation using NHS-ester reaction with primary amines.
Target molecules containing NHS esters react with the primary amines found on lysine groups to conjugate proteins to a desired target, such as a drug, PEG, surface, or nanoparticle. This representation shows only one conjugation site, but most proteins contain multiple lysine groups that will react with NHS esters.

An alternative strategy to random functionalization is site-specific bioconjugation, wherein a unique residue in the protein is utilized in the chemical conjugation reaction. By controlling the number and site of conjugations, alterations of the active site can be avoided, steric effects are reduced, and homogenous populations of modified proteins are produced, allowing for higher protein activity and more consistent functionalization [12, 20, 22, 26-28]. The importance of site-specific protein conjugation is highlighted by protein immobilization, where numerous studies have reported that the oriented, uniform presentation of antibodies significantly increases antigen binding compared to random orientations [8, 20, 22, 26, 28, 29] (Figure 1-2).

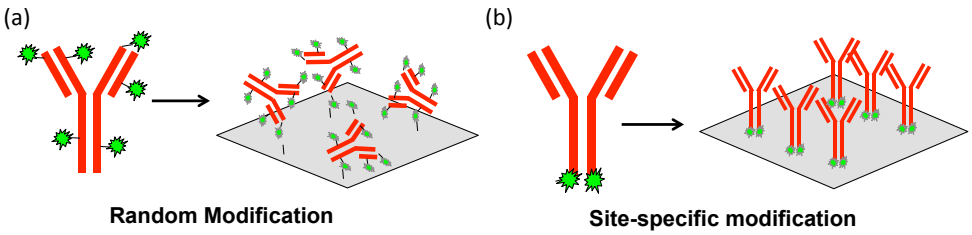

Figure 1-2: Random versus site-specific protein immobilization
(a) Antibodies that are functionalized in a random fashion can contain modifications of binding sites that prevent antigen engagement. Furthermore, the antibodies are not uniformly presented on the surfaces upon immobilization, therefore reducing the accessibility of their binding sites due to steric effects. (b) In contrast, site-specifically modified antibodies can be immobilized in a uniform manner with their binding sites oriented away from the surfaces and other proteins, making the binding sites more accessible and better able to engage antigen.

1.3 Intein-Mediated Expressed Protein Ligation

Site-specific protein conjugation is enabled through the insertion of bioorthogonal chemical groups onto proteins that provide a unique chemical residue in the protein structure [30]. Several methods have been developed to site-specifically install bioorthogonal groups onto proteins. For example, genetic incorporation has been employed to insert nonnatural amino acids containing bioorthogonal functionalities into proteins. Kiik et.al. replaced the amino acid methionine in bacterial cultures with azidohomoalanine, an azide-conjugated methionine analog, thus allowing for incorporation of the azide amino acid during protein synthesis [31]. The azido group was subsequently employed in a Staudinger ligation reaction to result in site-specific protein conjugation [31]. However, a disadvantage of this method is that site-specific chemical modification is only possible if the protein contains just one methionine. Other groups have utilized modified tRNAs that recognize a specific stop codon to incorporate

a nonnatural amino acids [32, 33], but these techniques are highly labor intense and low efficiency [34].

An alternative to genetic incorporation of bioorthogonal groups is chemical incorporation. One of the most powerful and widely used tools for chemical incorporation is expressed protein ligation (EPL) [35, 36]. EPL employs fusion to a protein splicing element known as an intein to generate a unique, reactive thioester on the carboxy-terminus of the target protein. Inteins like the Mxe GyrA intein [37] catalyze a spontaneous, reversible *N*- to *S*- acyl shift at the carboxy-terminus of the target protein to expose a thioester in the protein backbone (Figure 1-3). This particular intein has been modified to block native protein splicing, thereby enabling activation of protein splicing through the addition of a thiol [38]. The exposed thioester reacts with the thiol to release the intein and form thioester on the carboxy-terminus of the target protein (Figure 1-3). This newly formed protein thioester can subsequently be reacted with an amino-terminal cysteine containing a desired modification to covalently link the protein to the modification (Figure 1-3). Previously, this method of EPL has been employed to install unique, reactive chemical functionalities such as alkynes [39-41] and azides [39, 42, 43] or to directly chemically conjugate proteins to molecules like biotin [44, 45], polymers [46], fluorophores [47-49], carbohydrates [49], and surfaces [50].

The EPL modification scheme has also been adapted to install a carboxy-terminal azide onto a protein with a single step reaction [31]. Kalia and Raines synthesized a bifunctional nitrogen nucleophile containing an azide, hydrazine azide, that could attack the thioester formed between RNase A and the intein, thereby releasing the RNAse A and simultaneously installing a carboxy-terminal azide (Figure 1-

3). In a subsequent study, this azide was utilized to site-specifically immobilize RNase A onto surfaces using Staudinger Ligation [51].

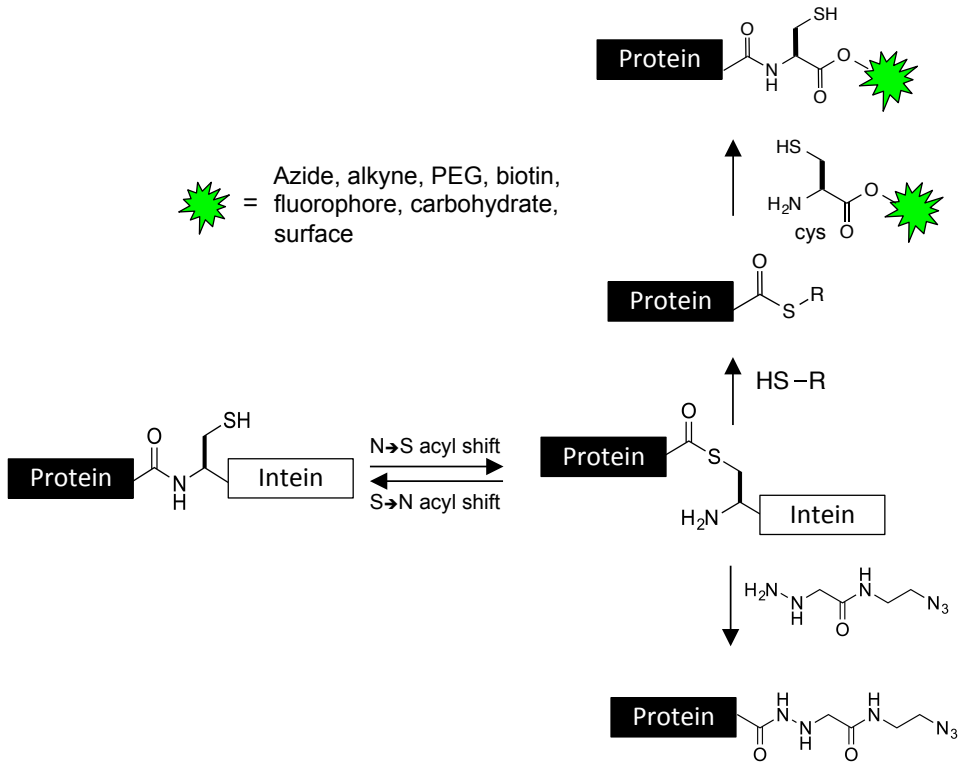

Figure 1-3: Expressed protein ligation (EPL)
EPL can be used to install biomolecules or unique chemical residues onto the carboxy-terminus of proteins. The intein catalyzes a reversible *N*- to *S*- acyl shift in the amide backbone between the target protein and the intein. This exposes a thioester at the carboxy-terminus of the target protein that is susceptible to attack by a nucleophile. Thiols are the most commonly used nucleophile (top), and they will react to release the intein and install a carboxy-terminal thioester on the target protein. Subsequently, an amino-terminal cysteine containing the desired functionality will react with the thioester, forming a native amide bond and covalently linking the protein to the functional group. This process can also be reduced to a single step reacting a bifunctional nitrogen nucleophile, hydrazine azide, with the intein fusion protein [31]. Hydrazine azide will react to release the target protein while simultaneously installing a carboxy-terminal azide (bottom).

1.4 Protein Conjugation via Click Chemistry

Although direct chemical conjugation of proteins to biomolecule targets has been performed with EPL, it is not ideally suited for many applications, since millimolar concentrations of the cysteine reagent are required for efficient conjugation [40, 52]. Therefore, through the use of appropriately functionalized cysteine reagents, EPL has been adapted to insert bioorthogonal chemical functionalities that require lower substrate concentrations for efficient reaction (Figure 1-3). As previously described, EPL can be employed to install click chemistry compatible groups onto proteins in a site-specific manner [31, 39-43, 51]. Click chemistry is an extremely valuable and widely used class of chemical reactions in bioconjugation because of its versatility and chemoselectivity [53]. The classic version of click chemistry involves the reaction between an azide group and a terminal alkyne in the presence of a copper(I) catalyst and is appropriately termed copper(I)-catalyzed azide–alkyne cycloaddition (CuAAC) (Figure 1-6, i) [54]. The CuAAC reaction has been employed in a wide variety of biochemical applications, including conjugation proteins to nanoparticles [41, 43], PEG molecules [55, 56], virus-like particles [57], and surfaces [39, 40, 42, 58]. However, the required copper(I) catalyst can be problematic in some systems, since it is cytotoxic [59, 60] and can cause protein precipitation [23, 61, 62]. Bertozzi and colleagues have since developed a catalyst-free version of the azide click reaction termed strain-promoted azide-alkyne cycloaddition (SPAAC) [63]. By replacing the terminal alkyne with a strained cyclooctyne, the reaction rate of the cycloaddition increases, thereby eliminating the need for the copper(I) catalyst (Figure 1-4, ii). Strain-promoted click is

extremely versatile and bioorthogonal, and it has been employed in numerous applications that require generation of bioconjugates [63-68].

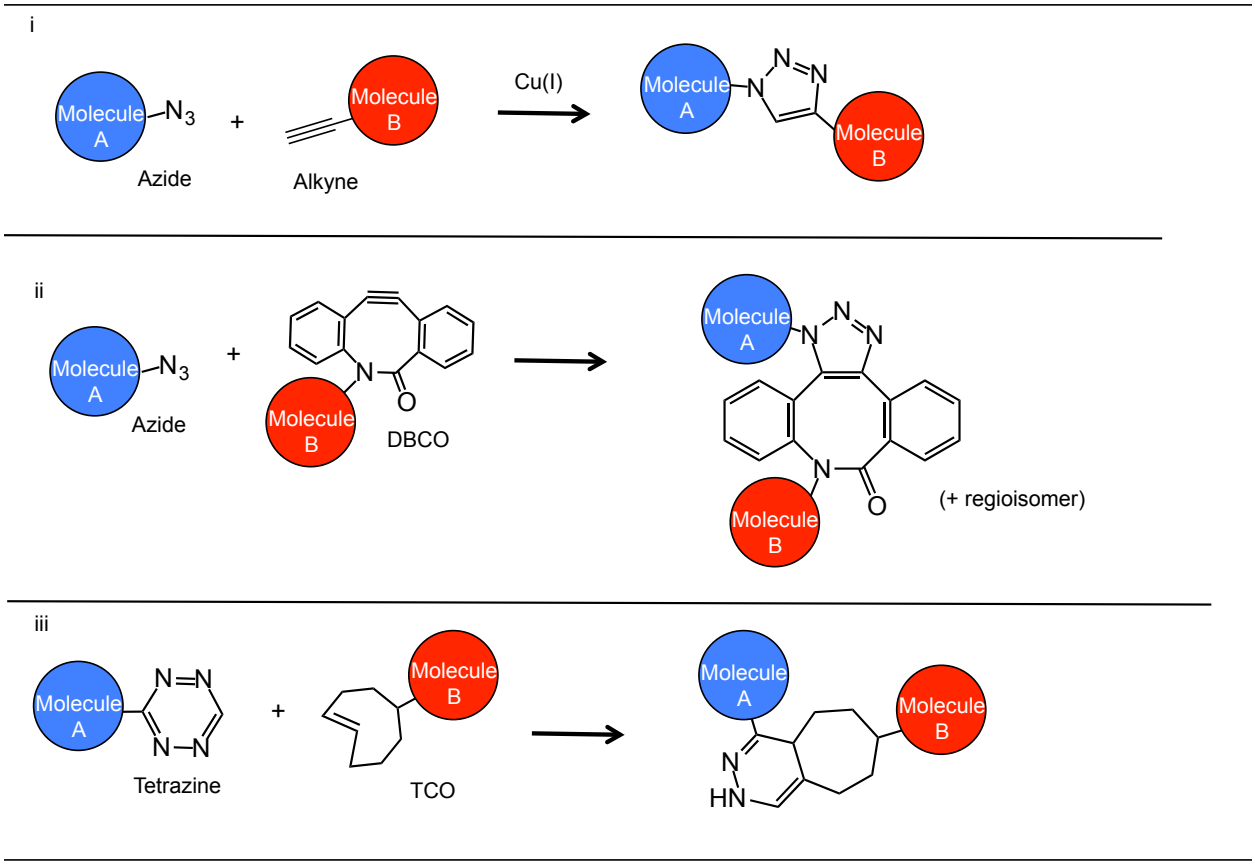

Figure 1-4: Click chemistry reactions
(i) In CuAAC, an azide reacts with a terminal alkyne in the presence of a copper(I) catalyst to yield a triazole linkage. (ii) By replacing the terminal alkyne with a strained alkyne, the azide-alkyne cycloaddition can be modified to eliminate the need for a catalyst. Shown here, in SPAAC, an azide reacts with a DBCO to conjugate two molecules. (iii) Cycloaddition reactions between tetrazines and dienophiles also proceed without a catalyst but, in contrast to SPAAC, these reactions have extremely fast kinetics. A tetrazine-TCO cycloaddition is shown here.

One limitation of this chemistry is the modest reaction rate of the azide-cycloaddition. The second order rate constant for the reaction between azides and one of the most common strained alkynes, dibenzocyclooctyne (DBCO), has been reported to be around 2.1 $M^{-1}S^{-1}$ [69]. This rate is sufficient when reagents are at high

concentrations, but for many biological applications, the proteins and substrates can be in the sub micro-molar range. For example, if two molecules with equimolar concentrations were to be conjugated, reaction and half time ($t_{1/2}$) are represented by

$$A + B \xrightarrow{k} A{:}B$$

$$t_{1/2} = \frac{1}{k[A]_0} \qquad for\ [A]_0 = [B]_0$$

Therefore, if the two reactants were present at concentrations of 1 μM, it would take ~132 hours to reach 50% conjugation.

Other forms of click chemistry have recently been explored to increase the reaction rate of the cycloaddition reaction. One such example is the reaction between tetrazine and dienophiles like *trans*-cyclooctene (TCO) (Figure 1-4, iii), which has exhibited second-order rate constants of up to 2.7×10^5 $M^{-1}S^{-1}$ [70]. Using the previously describe scenario, if two molecules, one conjugated to a tetrazine and the other a dienophile, were reacted at equimolar concentrations of 1 μM, the $t_{1/2}$ would be 3.7 seconds, making the reaction substantially faster than the azide click reactions. The tetrazine-TCO cycloaddition has just recently been employed in a variety bioconjugation reactions, including cell and protein labeling with fluorophores [69, 71, 72], nanoparticles [73], and radioisotopes [70, 73, 74]. However, incorporating these new click groups into proteins has been reliant upon random modification techniques [69, 72] or genetic integration [75], making EPL an attractive alternative to site-specifically incorporate tetrazines and dienophiles.

1.5 Recombinant Protein Expression Systems for Intein-Fusion Proteins

The ability to perform the discussed bioconjugation reactions relies the production of EPL and click chemistry compatible proteins using recombinant expression systems. Since *Escherichia coli* (*E. coli*) is typically able to produce large amounts of heterologous protein at a low cost [76], it is the most common expression system to synthesize intein fusion proteins [31, 40, 43, 44, 46-49, 51, 77-82]. Furthermore, the IMPACT^{TM} kit from New England Biolabs provides a commercially available vector that permits the production of intein fusion proteins in the cytoplasm of *E. coli* [36]. However, there are some challenges associated with intein fusion protein expression in bacteria. First, heterologous protein expression in *E. coli* often results in the formation of insoluble inclusion bodies in the cytoplasm that contain the protein of interest [83, 84]. This is particularly problematic for disulfide bond containing proteins, such as antibodies, because the reducing environment of the cytoplasm does not permit formation of disulfide bridges, resulting in unfolded protein and formation of insoluble protein aggregates [76, 83-85]. Since many intein fusion proteins are produced in this form [46, 47, 77, 80-82], the inclusion bodies must be solubilized and the proteins refolded in order to perform EPL functionalization. Glutathione redox buffers that assist in the formation of disulfide bonds [83] can be used for refolding intein fusion proteins [47, 80, 86], but these buffers can produce an unstable glutathione-thioester on the carboxy-terminus of the protein, leading to subsequent thioester hydrolysis and loss of the thioester functionality [87]. Furthermore, these refolding processes can also result in substantial amounts of misfolded protein. For example, Sydor et.al. reported only 50% of their refolded protein-intein fusions actually contained an active intein, and there

was significant protein aggregation [80]. Additionally, *in vivo* autocleavage of the intein has been reported in the cytosol of *E. coli* [78, 79, 81], resulting in significant loss of the intein fusion. Cui, Li, and colleagues were able to alleviate this issue and reported that mutating threonine at position 3 in the Mxe GyrA to a cysteine (T3C) eliminated the 90% *in vivo* autocleavage observed for one of the proteins [81]. However, as a consequence, subsequent studies have reported a substantial decrease in intein activity with this mutation [77].

To alleviate refolding issues, intein-fusion proteins can be targeted to the bacterial periplasm, where the oxidizing environment enables the formation of disulfide bonds and improves protein folding [88]. Several different inteins have been expressed as folded fusion proteins in the periplasm [89-91], however, many proteins, particularity antibodies, are still produced as unfolded aggregates in the periplasm [76, 92-94], while others are not expressed [76, 95]. Therefore, targeting of intein fusion proteins to the periplasm is not a generalizable method to avoid protein refolding.

Alternative platforms for recombinant protein expression that possess superior protein folding mechanisms are available. However, these systems have rarely been employed for synthesis of intein fusion proteins. One existing study is a recent publication by Möhlmann et.al., who reported that mammalian cells could express IgGs as fusions to the Mxe GyrA intein, and that EPL could be performed to functionalize the antibodies with a biotin [45]. Since mammalian cells are eukaryotic and have more elaborate folding mechanisms compared to *E. coli*, mammalian cell protein expression would be one viable alternative. Another frequently used organism for recombinant protein expression is yeast. *Saccharomyces cerevisiae*, commonly known as baker's

yeast, is a eukaryotic, single cell organism that is often used to synthesize proteins that are difficult to express in *E. coli* [96]. Yeast contain more sophisticated protein folding and processing machinery compared to *E. coli*, and, therefore, they are more capable of producing folded, active proteins [76]. Yet, unlike mammalian cells, yeast can grow and divide quickly on simple media and their genetics are easily manipulated [97]. Previously, yeast have been used to successfully produce folded proteins such as single chain antibodies [98-100], green fluorescent protein [100, 101], epidermal growth factor receptor [102], antibody fusion proteins [103], and human fibronectin domains [104].

In addition to advantages in recombinant protein production, a powerful yeast-based protein engineering platform, known as yeast surface display (YSD), has been developed [105]. In YSD, the protein of interest is expressed as a fusion to a yeast anchor protein that tethers the construct to the outer yeast wall. The most common anchor system is the a-agglutinin system developed by Boder and Wittrup [105] that employs fusion to Aga2p (Figure 1-4). Aga2p forms disulfide linkages with Aga1p to covalently anchor the protein of interest to the yeast surface [106]. Since ~10^4-10^5 constructs per yeast are displayed on the surface, expression and activity of the target protein can conveniently be analyzed using quantitative flow cytometry. Furthermore,

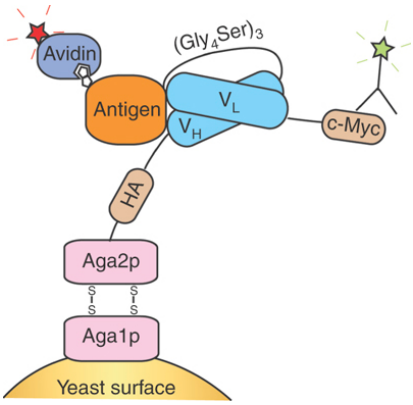

Figure 1-5: Yeast surface display schematic
A protein of interest (shown here as a single chain antibody) is displayed as a fusion to Aga2p. Aga2p forms disulfide bonds with Aga1p to covalently link the construct to the yeast surface. From [107].

yeast surface display can be employed to quantitatively screen protein libraries using fluorescence activated cell sorting (FACS) [107]. Previously, libraries of up to ~10^9 clones have been screened to identify novel proteins [108, 109] or to improve protein properties such as expression [110], stability [110], and affinity [105, 111-113].

1.6 Generation of Soluble Proteins from a Display Platform

By combining a robust protein engineering platform with the ability to synthesize difficult to express proteins, the yeast expression system provides a potential opportunity to expand the utility of intein-mediated protein functionalization. As we describe in Chapter 2, by installing an intein residue into the yeast display construct, engineered proteins could be directly released to generate soluble, chemically functionalized proteins for use in downstream assays. A few existing studies have employed similar concepts to combine surface display engineering platforms with soluble protein assays. Recently, Chen et.al. developed a platform that permitted the release of mammalian cell surface displayed proteins to generate soluble proteins [114],

thus enabling screening using both surface display and soluble protein assays without cumbersome intermediate steps to transfer proteins between platforms. Furthermore, previous efforts have also been made to generate soluble proteins from yeast surface display platforms. For example, Boder and Wittrup demonstrated that DTT could reduce the disulfide bonds between Aga1p and Aga2p, thereby releasing the displayed protein from the yeast surface [105]. Additionally, by inserting a factor Xa recognition site between Aga2p and surface displayed GFP, it has been shown that the factor Xa enzyme could selectively release the GFP to generate soluble protein [115]. However, unlike a system that would employ intein-based protein release, these techniques only permit the generation of soluble proteins from the display platform, and to date, none of these studies have also combined the capability to site-specifically functionalize the released protein.

1.7 Summary

Chemical modification of proteins is critical to the development of the next generation of protein therapeutics and diagnostics. Intein-mediated EPL provides an attractive method to chemically modify proteins in a site-specific manner, and, by employing EPL to install click chemistry compatible groups, proteins can be conjugated to a variety of targets. Currently, there are limitations to the production of soluble intein fusion proteins in bacteria that not only make it laborious to functionalize proteins, but also insurmountable to apply these techniques to large panels of engineered proteins. By producing intein fusion proteins in yeast, we believe that we can improve upon the existing expression system through enabling integration of these facile chemical

functionalization techniques into a display protein engineering platform and through enabling the secretion of active soluble intein fusion proteins from yeast.

Chapter 2 : Facile Chemical Functionalization of Proteins through Intein-Linked Yeast Display

This chapter was adapted from: Marshall, C. J., Agarwal, N., Kalia, J., Grosskopf, V. A., McGrath, N. A., Abbott, N. L., Raines, R. T., and Shusta, E. V. “Facile chemical functionalization of proteins through intein-linked yeast display”, *Bioconjugate chemistry,* 2013. 24: 1634-1644. Here we establish and characterize an intein-linked yeast display method that enables site-specific functionalization of antibodies and proteins from an engineering platform.

2.1 Introduction

The capability to append unique chemical functionalities to proteins is valuable for a variety of applications, including protein immobilization [39, 44, 51, 116-118], therapeutic drug delivery [55, 119, 120], and imaging [65, 121]. Inserting these chemical functionalities into proteins in a site-specific manner is often preferred over nonspecific modifications to provide uniformly modified protein populations while minimizing potential deleterious effects on native protein activity [28, 118, 119, 122, 123]. One approach that has been employed for site-specific protein modification is the reaction of a non-self cleaving intein fusion protein with nucleophiles possessing desired chemical properties [31, 39, 41, 44, 45, 51]. Non self-cleaving inteins have been engineered to block native protein splicing activity, enabling an exogenous nucleophile to catalyze protein release. Typically, a sulfur nucleophile is used to cleave the target

protein from the intein moiety, forming a thioester intermediate at the C-terminus of the target protein [38, 124]. The thioester can subsequently be reacted with an N-terminal cysteine or cysteine derivative to form a native amide bond [49]. Using this method of expressed protein ligation (EPL), functional groups such as tyrosine analogs [125], biotin [39, 44, 49], azides, and alkynes [39] have been installed at the C-terminus of proteins. This traditional two-step approach was reduced to a single reaction step by employing a nitrogen nucleophile bearing an azido group, hydrazine azide, that could cleave the intein while installing a C-terminal azide on the protein, obviating the need to form the thioester intermediate [31, 51].

Such intein-mediated chemical functionalization strategies are typically performed at a preparative scale with soluble, purified proteins [31, 38, 47-49, 51, 80, 125]. It would, however, be desirable to integrate these modification strategies into a protein engineering platform, such as yeast surface display, where multiple clones could be evaluated rapidly on a small scale and in a high-throughput manner. In this way, intein-mediated release of engineered proteins from display platforms would permit the downstream analysis of many clones as soluble proteins without tedious preparation steps such as subcloning, expression, and purification. Furthermore, the ability to simultaneously append unique chemical functionalities to the C-terminus of the protein could allow for rapid integration into a variety of protein-based assays such as immobilization, imaging, and drug conjugation.

In this study, we have extended intein-mediated chemical functionalization approaches to proteins displayed on the surface of yeast. Intein fusion proteins displayed as active proteins on the yeast surface were released and subsequently

chemically functionalized to be compatible with EPL and click chemistry. The released and functionalized proteins were used directly for immobilization on surfaces without any protein purification steps, and immobilized antibodies demonstrated specific capture of their target antigens.

2.2 Materials and Methods

2.2.1 Yeast Strains and plasmids

Yeast surface display was performed using *Saccharomyces cerevisiae* strain EBY100 [105] (*MAT*a *AGA1::GAL1-AGA1::URA3 ura3–52 trp1 leu2Δ1 his3Δ200 pep4::HIS3 prb1Δ1.6R can1 GAL*). The pCT4Re yeast surface display vector was created by insertion of the constructs shown in Figure 2-1a into the pCT-302 yeast surface display vector [105] between the *GAL1-10* promoter and the alpha factor terminator sequences using the restriction sites *Eco*RI and *Xho*I. The Mxe GyrA intein sequence was subcloned from the pTXB1 vector (New England Biolabs). The anti-fluorescein single-chain antibody (scFv) (4-4-20) was subcloned from the pCT-302 vector [105], creating pCT4Re-4420, and the yeast enhanced green fluorescent protein (GFP) was subcloned from the pCT-GFP plasmid [101], creating pCT4Re-GFP. The anti-epidermal growth factor receptor (EGFR) scFv, scFv2, was subcloned from the pCDNA3.1-scFv2 plasmid generously donated by Dr. Winfried Wels [126] to create pCT4Re-scFv2. An N-linked glycosylation site that appears in the scFv2 amino acid sequence (N-x-T) was altered to prevent N-linked glycosylation by changing the asparagine residue to a serine (S-x-T) with the Quikchange II Site-Directed Mutagenesis Kit (Agilent). Yeast were transformed using the LiAc/ssDNA/PEG method [127] and transformants were selected on tryptophan and uracil deficient SD-CAA agar

plates (20.0 g/L dextrose, 6.7 g/L yeast nitrogen base, 5.0 g/L casamino acids, 10.19 g/L $Na_2HPO_4 . 7H_2O$, 8.56 g/L $NaH_2HPO_4 . H_2O$, 15 g/L agar).

2.2.2 Yeast growth and surface display induction

Yeast cells were grown in 50 mL SD-CAA medium (20.0 g/L dextrose, 6.7 g/L yeast nitrogen base, 5.0 g/L casamino acids, 10.19 g/L $Na_2HPO_4 . 7H_2O$, 8.56 g/L $NaH_2PO_4 . H_2O$) overnight at 30°C, 260 rpm. The following day, cultures were reset to an optical density at 600 nm (OD_{600}) of 0.3 and grown for ~4 h in SD-CAA until a culture density OD_{600}=1.0 was reached. Surface display was induced by replacing the media with 50 mL SG-CAA (20.0 g/L galactose, 6.7 g/L yeast nitrogen base, 5.0 g/L casamino acids, 10.19 g/L $Na_2HPO_4 . 7H_2O$, 8.56 g/L $NaH_2PO_4 . H_2O$) for 20 h at 20°C, 260 rpm. Following induction, an OD_{600} of ~2–3 was typically reached, corresponding to a total culture of ~$1x10^9$–$1.5x10^9$ yeast. The medium was removed, and the yeast were washed in PBS containing 0.1% w/v bovine serum albumin (BSA) (PBS-BSA).

2.2.3 Flow cytometry

The following immunolabeling steps for flow cytometry analysis were carried out at 4°C using $2x10^6$ yeast per labeling experiment. Surface display expression levels were evaluated by incubating induced yeast with an anti-FLAG rabbit polyclonal antibody (Sigma–Aldrich, diluted 1:500 in PBS-BSA) for 30 min, washing once with PBS-BSA, and secondary labeling with anti-rabbit allophycocyanin (APC) (Invitrogen, diluted 1:500 in PBS-BSA) for 30 min followed by a final wash with PBS-BSA. To evaluate the binding of 4-4-20 to fluorescein, yeast were incubated with 10 μM fluorescein isothiocyanate-functionalized dextran in PBS-BSA (FITC-dextran, Sigma–

Aldrich) for 30 min and washed once with PBS-BSA to remove non-specifically bound antigen. To evaluate the binding of scFv2 to EGFR, yeast were incubated with purified human EGFR (4 μg/mL in PBS-BSA, purified human EGFR was generously donated by Greg Wiepz, Biomolecular Chemistry, University of Wisconsin-Madison) for 1 h, followed by a PBS-BSA wash to remove unbound protein. Yeast were subsequently incubated with anti-EGFR mouse antibody cocktail Ab-12 (Lab Vision Corporation, diluted 1:200 in PBS-BSA) for 30 min, washed once with PBS-BSA, and labeled with anti-mouse PE (Sigma–Aldrich, diluted 1:40 in PBS-BSA) for 30 minutes followed by a final wash with PBS-BSA. GFP activity was assessed by measuring the GFP fluorescence of the yeast at 488 nm excitation. The fluorescence of the immunolabeled yeast cells was measured using a FACSCalibur flow cytometer (Becton Dickinson), and the geometric mean fluorescence intensities of the protein expressing populations were quantified with the FlowJo software package to determine relative display levels and activity.

For absolute quantitation of surface expression levels, Quantum Simply Cellular^{TM} anti-mouse IgG microbeads (Bangs Laboratories) were used. Yeast displaying the scFv-intein and GFP-intein constructs were incubated with mouse anti-FLAG antibody (Invitrogen, diluted 1:200 in PBS-BSA) for 30 min and washed once with PBS-BSA. The microbeads were also incubated and washed under the same conditions. The yeast and microbeads were subsequently incubated with anti-mouse Alexa 647 (Invitrogen, 1:500 dilution in PBS-BSA) for 30 min, washed once with PBS-BSA, and analyzed via flow cytometry.

2.2.4 SDS-PAGE and Western blotting of reacted proteins

Protein samples were resolved on 12.5% w/v SDS-PAGE gels. Samples were boiled for 10 min prior to resolution on the SDS-PAGE gels for non-reducing conditions. For reducing SDS-PAGE, 1 mM 2-mercaptoethanol was added to the sample buffer and the samples were boiled for 10 min prior to resolution on the gels. Gels were either stained with Coomassie blue, or the proteins were transferred to a nitrocellulose membrane for Western blot analysis. To detect the FLAG tag, membranes were probed with anti-FLAG M2 mouse monoclonal antibody (Sigma–Aldrich, diluted 1:3000), followed by anti-mouse HRP conjugate (Sigma–Aldrich, diluted 1:2000). For detection of biotinylated proteins, membranes were probed with anti-biotin mouse monoclonal antibody Ab-2 clone BTN.4 (Lab Vision Corporation, diluted 1:500), followed by anti-mouse HRP conjugate. Membranes were subsequently developed with ECL reagents and exposed to Hyperfilm (GE Healthcare). For quantitative Western blotting, the band intensities were measured using the NIH ImageJ program, and the slopes of the unsaturated band intensities versus exposure time were compared to determine the relative amounts of protein.

2.2.5 Hydrazine release of yeast surface-displayed proteins

For protein release with hydrazine, induced yeast (~$1x10^9$ cells containing an estimated total of ~40–140 pmole scFv or GFP) were suspended in 500 µl MOPS-NaOH (0.5 M) buffer at pH 8.0 containing NaCl (0.50 M), EDTA (0.10 mM), 0.1% w/v BSA (added as carrier to prevent non-specific adsorption losses after protein release), and 500 mM of either azide-terminated hydrazine (synthesized as described previously[31]), or a simple hydrazine, ethyl hydrazinoacetate hydrochloride (Sigma–

Aldrich). The reaction was carried out for 3 days at room temperature with gentle rotation. Subsequently, the yeast were removed by centrifugation, and the supernatant containing the released proteins recovered. The samples were dialyzed against PBS using a Slide-A-Lyzer dialysis cassette (Pierce) to remove unreacted hydrazine. To purify the hydrazine-released proteins, the dialyzed solution was added to 25 µl of anti-FLAG M2 resin (Sigma–Aldrich) and incubated for 2 h at room temperature with gentle rotation. The FLAG resin was subsequently washed three times with 500 µl PBS to remove unbound proteins. The proteins were eluted by incubating with 50 µl of 100 µg/mL 3x FLAG peptide (Sigma–Aldrich) in PBS for 30 min, followed by 3 serial incubations for 10 min each in the same buffer.

To perform the CuAAC reactions, the following was added to 100 µl solution of hydrazine-released proteins in PBS: 5 µl of 5 mM alkyne biotin (Invitrogen) in DMSO, 2.5 µl of 4 mM $CuSO_4$ (Thermo-Fisher) in water, 5 µl of 1.6 mM TBTA ligand (Sigma–Aldrich) in 80% v/v tert-butanol, and 5 µl of 100 mM sodium ascorbate (Sigma–Aldrich) in water. The reactions were carried out for 1 h at room temperature.

2.2.6 MESNA release and EPL of yeast surface-displayed proteins

Release of the scFvs with the sulfur nucleophile was conducted by suspending induced yeast cells (~$1x10^9$ cells containing an estimated total of ~40–140 pmole scFv or GFP) in 500 µl HEPES (50 mM pH 7.2) containing 0.1% w/v BSA and 50 mM 2-mercapthoethanesulfonic acid (MESNA, Sigma–Aldrich). Initially, this reaction was carried out for 20 h at room temperature followed by yeast removal by centrifugation and recovery of the supernatant containing the released proteins. To analyze the mechanism of release via MESNA, yeast expressing pcT4Re-GFP constructs were

reacted with MESNA for 45 min at room temperature prior to yeast removal. The proteins were either frozen at -20°C to prevent further reaction, or the proteins were allowed to react in the MESNA solution in the absence of yeast for an additional 20 h at room temperature. Where indicated, the *N*-linked glycans were removed from the samples with EndoH (New England Biolabs) for 1 h at 16°C. Since the 45 minute protocol led to nearly complete removal of all surface displayed fusions, all further MESNA experiments were carried out using the 45 minute, 20 h approach. When necessary, a cysteine reagent was added during the 20 h step to perform EPL, as described below.

Three cysteine reagents were used in this study to perform the EPL reactions, cysteine azide (Anaspec), cysteine alkyne (Anaspec), and Bio-P1, an N-terminal cysteine peptide containing a biotin (synthesized by the University of Wisconsin Biotechnology Center based upon the Bio-P1 peptide from New England Biolabs. Sequence: NH_2-CDPEK(Bt)DS-$CONH_2$). Proteins were released from yeast displaying scFv-intein or GFP-intein fusion proteins with either simple hydrazine (3 days) or MESNA (45 min), and the supernatants containing released proteins were separated from the yeast by centrifugation. For biotinylation, 15 µl of 15 mM Bio-P1 in PBS was added to 100 µl of the released protein products and allowed to react for 20 h at room temperature. To generate azide and alkyne proteins, either 3 µl of 800 mM cysteine azide in PBS or 3 µl of 800 mM cysteine alkyne in PBS was added directly to 500 µl of the released protein products and the reactions were allowed to proceed for 20 h at room temperature. The reactions were subsequently dialyzed against PBS with a Slide-A-Lyzer dialysis cassette to remove unreacted cysteines.

The azide and alkynyl functionalization of the EPL proteins was evaluated via CuAAC reaction. To 100 µl of azide protein, alkyne protein, or protein thioester, the following was added: either 5 µl of 5 mM alkyne biotin in DMSO or 5 µl of 5 mM azide biotin (Invitrogen) in DMSO, 2.5 µl of 4 mM $CuSO_4$ in water, 5 µl of 1.6 mM TBTA ligand in 80% v/v tert-butanol, and 5 µl of 100 mM sodium ascorbate in water. The reactions were carried out for 1 h at room temperature.

2.2.7 Immobilization of alkynyl proteins on agarose beads

Azide-functionalized surfaces were generated using NHS-activated agarose beads (Thermo-Fisher). The agarose beads (250 µl) were washed three times with PBS to remove the storage buffer. The beads were resuspended in 1 mL PBS, and a PEG-azide containing a primary amine, O-(2-aminoethyl)-O′-(2-azidoethyl)nonaethylene glycol (Sigma–Aldrich), was added to the suspension to a final concentration of 100 mM. The mixture was incubated for 2 h at room temperature followed by an overnight incubation at 4°C with gentle rotation. The beads were washed three times with PBS to remove the PEG-azide reagent, and unreacted NHS groups were quenched by incubating the agarose beads in 1 M Tris buffer (pH 7) for 2 h at room temperature. The beads were subsequently washed 3 times in PBS-BSA and resuspended in PBS-BSA.

Alkynyl proteins (100 µl) were added to 5 µl of azide-functionalized beads along with 2.5 µl of 4 mM $CuSO_4$ in water, 5 µl of 1.6 mM TBTA ligand in 80% v/v tert-butanol, and 5 µl of 100 mM sodium ascorbate in water. The reaction was incubated for 16 h at room temperature with gentle rotation. The reacted beads were washed three times with 500 µl of PBS-BSA. To assay for immobilized proteins bearing a FLAG tag, the

agarose beads were incubated with anti-FLAG rabbit polyclonal antibody (1:2000 dilution in PBS-BSA) for 1 h, washed three times in PBS with 0.1% w/v Tween (PBST), incubated with anti-mouse Alexa 594 (1:500 dilution in PBS-BSA) (Invitrogen) for 30 min, and washed three times in PBST. To assay 4-4-20 activity, protein-loaded agarose beads were incubated with 10 μM FITC-dextran in PBS-BSA for 30 min and washed three times in PBST. To assay scFv2 activity, protein-loaded agarose beads were incubated with purified human EGFR (4 μg/mL in PBS-BSA) for 2 h, washed three times with PBST, immunolabeled with anti-EGFR antibody cocktail Ab-12 (1:200 dilution in PBS-BSA) for 1 h, washed three times with PBST, immunolabeled with secondary anti-mouse Alexa 488 antibody (1:500 dilution in PBS-BSA) for 30 min, and washed three times with PBST. The agarose beads were subsequently imaged with an Olympus IX70 fluorescence microscope, and bead-associated fluorescence was quantified with a Tecan Infinite M1000 fluorescent microplate reader.

2.3 Results

2.3.1 Surface display of intein fusion proteins

The scFv, GFP, scFv-intein and GFP-intein fusions were expressed as fusion partners to Aga2p, as in standard yeast surface display [105] (Figure 2-1a). However, while most yeast display systems employ fusion to the C-terminus of the Aga2p, the display constructs used here are fused to the N-terminus of Aga2p to allow for intein-mediated protein release from the yeast surface (Figure 2-2b). The resultant constructs enable display of unmodified scFv or GFP or display of the same proteins fused to the N-terminus of the Mxe GyrA intein, a genetically modified intein that undergoes nucleophile-induced protein splicing at its N-terminus[37] (Figure 2-1a). Three different

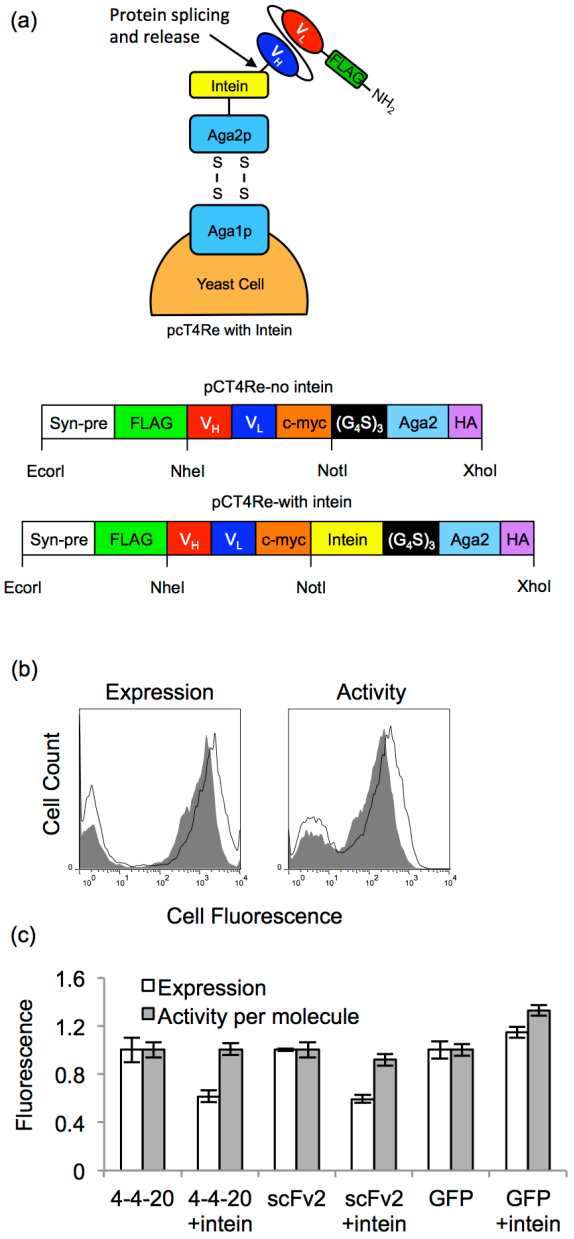

Figure 2-1: Expression and activity of yeast surface-displayed intein-fusion proteins
(a) Yeast surface display construct pCT4Re anchors the C-terminus of the Aga2p-protein fusions (shown here as Aga2p-scFv fusions) to the surface via disulfide bonds. A FLAG epitope tag is expressed on the N-terminus of the construct to represent full-length expression. In the intein-containing construct, the Mxe GyrA intein is expressed on the C-teminus of the target protein. The non-intein construct is identical except it contains no intein. (b) Using flow cytometry, expression of target proteins in the pCT4Re construct (black line in the histograms) and the pCT4Re construct with intein (solid gray in the histograms) was detected with a FLAG-tag antibody (shown for scFv2). These expression levels corresponded to ~24,000 4-4-20-intein constructs, ~48,000 scFv2-intein constructs, and ~86,000 GFP-intein constructs per yeast. Activity of the proteins in the pcT4Re (black line in the histograms) and the pcT4Re with intein (solid gray in the histograms) constructs was also evaluated by detecting binding to the scFv

antigens at saturating concentrations or by measuring GFP fluorescence (shown for scFv2). (c) The geometric mean fluorescence of the FLAG-positive yeast populations was quantified to determine relative expression levels, and these values were normalized to the pCT4Re construct without intein for each protein. Activity per molecule was determined by ratio of the geometric means for activity (binding or fluorescence) to FLAG expression levels, and normalized to the pCT4Re construct without intein. Plotted are the mean ± SD for yeast display results from three independent yeast transformants.

target proteins were evaluated: GFP [101], anti-fluorescein scFv 4-4-20 [105] ,and anti-epidermal growth factor receptor (EGFR) scFv2 [126]. First, the effects of intein fusion on protein display and activity were evaluated. Each of the proteins was successfully displayed on the surface (Figure 2-1b and 2-1c), with the two scFvs, 4-4-20 and scFv2, having ~40% reduced expression when displayed as a fusion to intein, and GFP expression being unaffected by intein fusion (Figure 2-1c). The activity of the displayed proteins was determined by evaluating scFv binding to cognate antigen (4-4-20, fluorescein and scFv2, EGFR), or by measuring the GFP fluorescence. While expression was attenuated for 4-4-20 or scFv2, the proteins displayed as intein fusions exhibited nearly the same activity per molecule as the proteins displayed without intein (Figure 2-1c), indicating that the presence of the intein did not negatively impact the function of the displayed protein.

2.3.2 Intein-mediated release and C-terminal functionalization of surface-displayed proteins

Key to intein-mediated release and functionalization, a spontaneous, reversible *N*- to *S*- acyl shift occurs at the amino-terminal cysteine of the Mxe GyrA intein backbone, forming a thioester that is susceptible to nucleophilic attack. Reaction with the nucleophile releases the protein from the intein, and hence, from the yeast surface

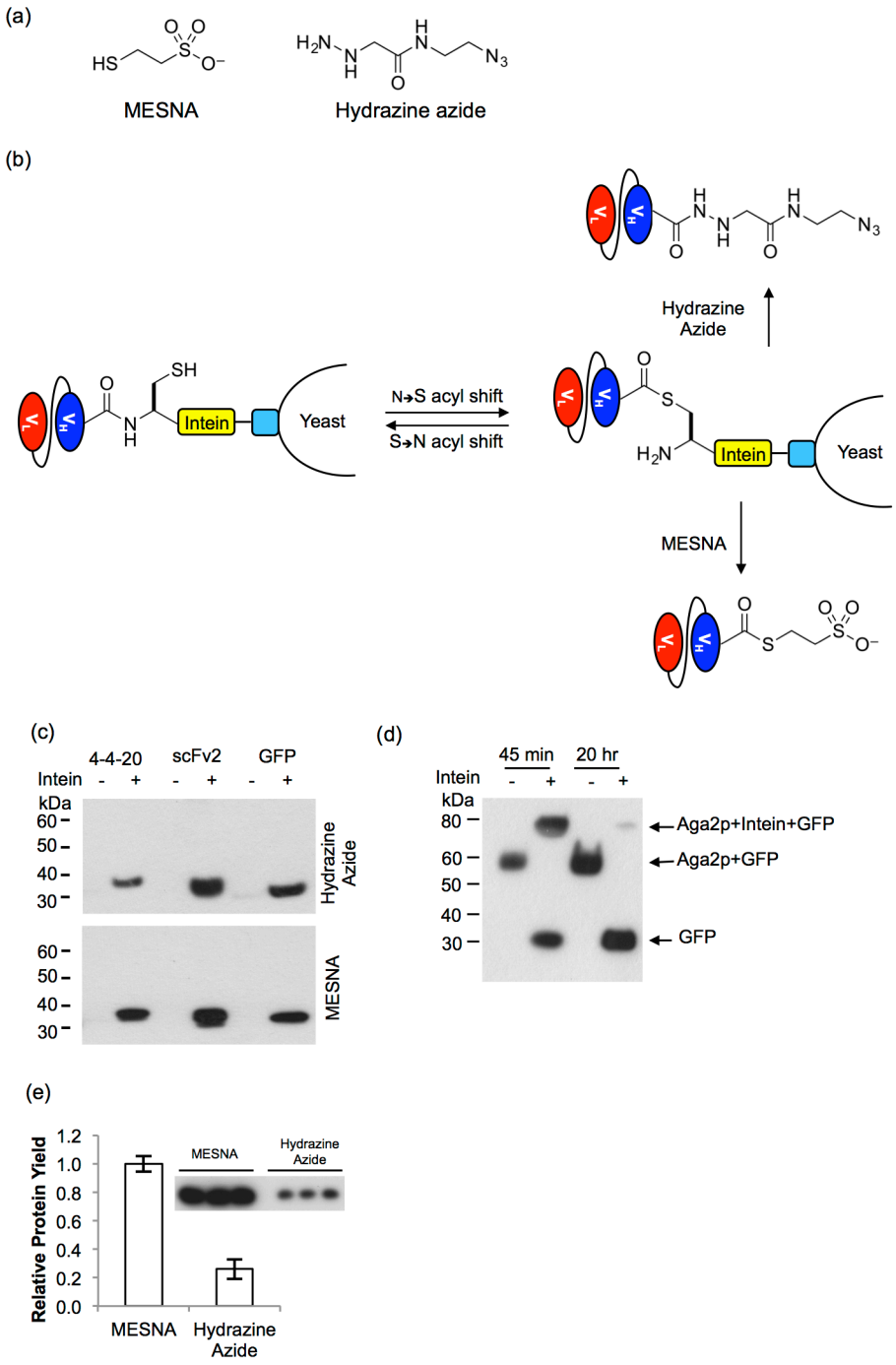

Figure 2-2: Intein-mediated protein release

(a) Two nucleophiles were used to release the proteins, 2-mercapthoethanesulfonic acid (MESNA), and a hydrazine azide. (b) For intein-mediated protein release, the intein facilitates an *N*- to *S*-acyl shift to generate a thioester. Nucleophilic attack results in protein release from the display construct while a functional group is simultaneously appended to the C-terminus of the protein. When MESNA is used to release the protein, a thioester is installed on the protein of interest; when the hydrazine azide is used, an azido group is installed. (c) Western blots of the

supernatants obtained after incubating protein-displaying yeast with the hydrazine azide for 3 days or MESNA for 20 h, probed with an anti-FLAG antibody to detect the presence of released target protein. Prior to Western blotting, proteins were resolved by SDS-PAGE using nonreducing conditions to prevent unwanted intein-mediated protein release by the beta-mercaptoethanol nucleophile present in reducing SDS-PAGE sample buffer. Released scFv or GFP at their unfused ~30-kDa size were only detected when intein was present. (d) GFP-displaying yeast with and without intein were reacted with MESNA for 45 min and the resulting supernatant removed from the yeast and incubated for an additional 20 h where noted. Anti-FLAG Western blots performed under nonreducing conditions to compare the MESNA-released GFP products after reaction for 45 min and 20 h. The released proteins were first deglycosylated with EndoH revealing Aga2p-GFP (~55 kDa) fusion release in the absence of intein (compared to 2-2c -intein without deglycosylation). Release of both Aga2p-intein-GFP (~75 kDa) and unfused GFP (~30 kDa) is observed when MESNA reacts with the yeast for 45 min, but upon allowing the reaction to proceed an additional 20 h, GFP is nearly quantitatively released from the intein. (e) Quantitative Western blot analysis was used to determine the relative amount of proteins released, and revealed that the 20-h reaction with MESNA releases 4 times more protein than does the 3-day reaction with the hydrazine azide. Plotted are means and standard deviations for three independent reactions originating from three independent yeast surface display transformants.

display construct (Figures 2-2a and 2-2b). The ability of the thiol and hydrazine nucleophiles to promote intein-mediated release of target proteins from the yeast surface was evaluated. Two different nucleophiles were compared in this study, a nitrogen nucleophile containing an azido group, hydrazine azide [31], and a sulfur nucleophile, 2-mercapthoethanesulfonic acid (MESNA) [38] (Figure 2-2a). After treating yeast displaying either scFv or GFP with the nucleophiles, Western blotting with an anti-FLAG antibody demonstrated that both nucleophiles release the yeast-displayed protein from the intein in a 3-day reaction for the hydrazine azide or a 20-h reaction for MESNA (Figure 2-2c).

Since MESNA is also a reducing agent and potentially capable of reducing the disulfide bonds between Aga1p and Aga2p (Figure 2-1a), the contribution of intein-mediated release versus disulfide-bond reduction was assessed. Intein-release typically requires an overnight reaction for completion [37], and thus, an abbreviated

MESNA reaction was examined to determine if GFP-intein-Aga2p fusions are released via disulfide reduction. Yeast displaying GFP-Aga2p or GFP-intein-Aga2p fusions were reacted with MESNA for 45 min, and the supernatant containing released proteins was removed from the yeast. Given that glycosylation can cause Aga2p fusion proteins to have diffuse bands at high molecular weights on Western blots that are difficult to detect [101] (Figure 2-2c), samples were treated with glycosidase prior to Western blot analysis. An anti-FLAG Western blot revealed that with or without intein, MESNA released GFP from the yeast surface within 45 min, consistent with disulfide bond reduction (Figure 2-2d). When the released proteins were allowed to further react in the MESNA solution for 20 h after yeast removal as performed in Figure 2-2c, GFP was nearly completely released from the intein-Aga2p fusion. As expected, the increased reaction time had no effect on the non-intein construct, as MESNA did not release GFP from Aga2p in the absence of intein (Figure 2-2d). These results indicate that MESNA first releases the displayed proteins from the yeast surface by reducing the disulfide bonds between Aga1p and Aga2p and/or by intein-mediated reaction, and subsequently further reacts with intein to completely release the scFvs or GFP from the rest of the display construct. Likely, because of this dual release mechanism, the treatment with MESNA removed nearly 90% of the fusions from the yeast surface, while treatment with hydrazine azide only removed 20% of the fusions from the yeast surface, as determined by flow cytometry. This resulted in the MESNA reaction yielding ~4 times more released protein than the hydrazine azide reaction, as determined by a quantitative Western blot (Figure 2-2e).

Following intein-mediated release of the yeast surface displayed proteins, the carboxy-terminal functionalization of the proteins was confirmed by further reacting the released proteins with biotinylated reagents (Figure 2-3a). After 3 days, the hydrazine-released proteins were separated from the yeast by centrifugation and subsequently reacted with a biotin alkyne in a copper-catalyzed azide–alkyne cycloaddition (CuAAC) (Figure 2-3b). Anti-biotin Western blotting demonstrates that when the displayed proteins were released with a non-azido hydrazine, there was no reaction with the biotin alkyne, as expected (Figure 2-3c). However, when performing the CuAAC reaction with the hydrazine azide-released proteins, multiple proteins reacted with the biotin alkyne reagent (Figure 2-3c). Thus, although the target protein was released by nucleophile treatment (Figure 2-2c), other yeast proteins are also non-specifically released (Supplemental Figure 2-1), a subset of which were functionalized by the hydrazine azide (Figure 2-3c). This issue could be resolved by purifying the hydrazine-azide released proteins with anti-FLAG resin prior to reaction with biotin alkyne, as was demonstrated for GFP, resulting in azide-dependent biotinylation of the released protein (Figure 2-3d).

To examine thioester functionality of the MESNA-released proteins, these proteins were reacted with a biotinylated peptide having an N-terminal cysteine (Figure 2-3a) in an EPL reaction (Figure 2-3b). Following the initial 45-min reaction with MESNA, released proteins were separated from the yeast by centrifugation. The intein-release reaction via MESNA was allowed to proceed for an additional 20 h in the presence of the biotinylated cysteine peptide to complete the EPL reaction. Anti-biotin Western blotting demonstrates specific biotinylation of the thioester scFvs and GFP but

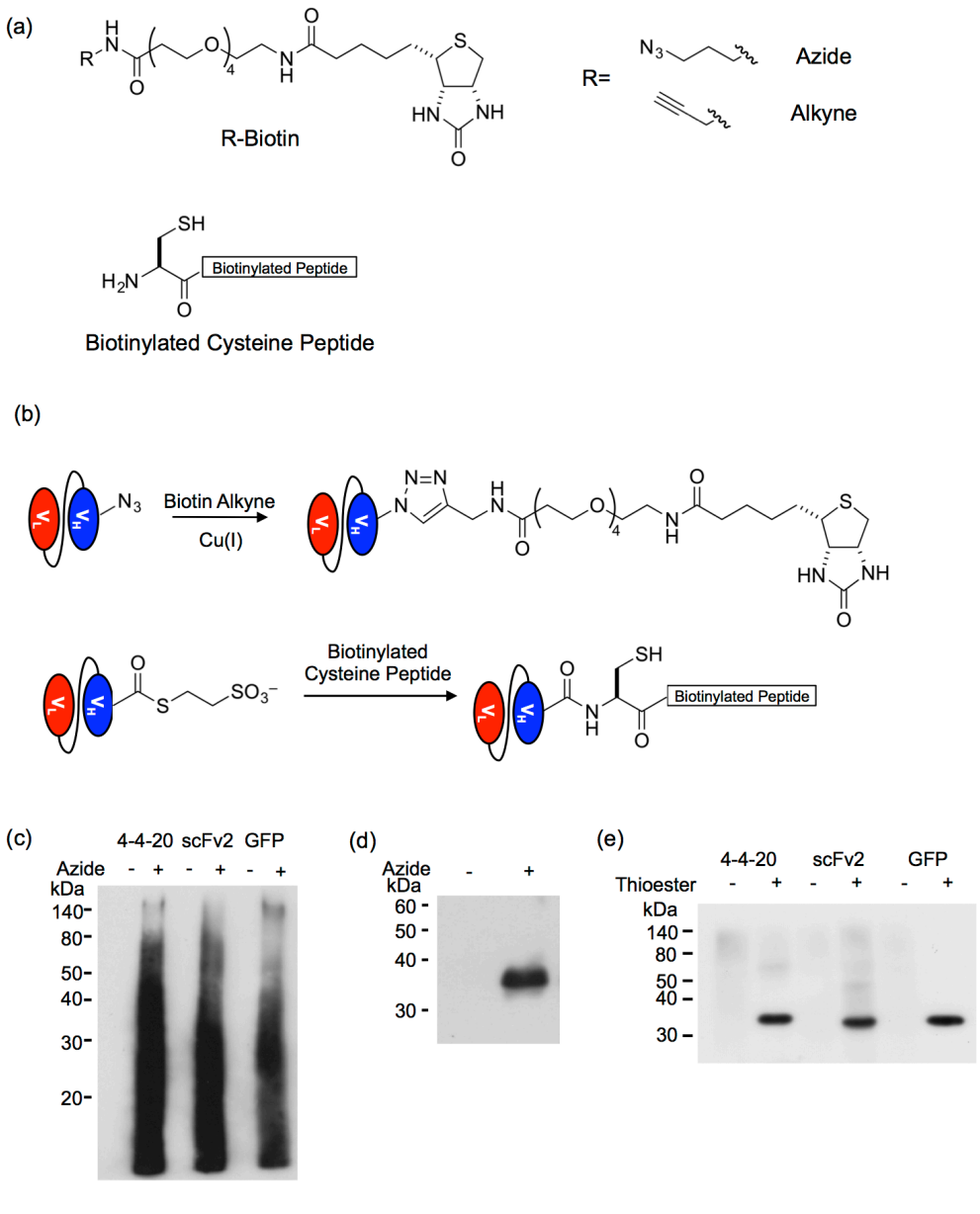

Figure 2-3: Site-specific biotinylation of released proteins
(a) Structures of the biotinylation reagents, biotin alkyne, biotin azide and cysteine-terminated biotinylated peptide. (b) The biotin alkyne reacts with the azide-functionalized proteins obtained via cleavage reaction with the hydrazine azide in a copper-catalyzed azide–alkyne cycloaddition (CuAAC) reaction. The protein thioester obtained by the cleavage reaction with MESNA reacts with a N-terminal cysteine peptide in an expressed protein ligation (EPL) reaction. (c) A Western blot of the CuAAC reaction probed with an anti-biotin antibody reveals that multiple proteins react with the biotin alkyne when the hydrazine azide is used to release the proteins from the yeast surface. When a non-azido hydrazine is used to cleave the proteins, no reaction with the biotin alkyne is detected. (d) The hydrazine-released products were subjected to FLAG tag purification before CuAAC reaction with biotin alkyne. A Western blot of the reaction probed an anti-biotin antibody reveals biotinylation corresponds to the hydrazine-azide released proteins

(shown for GFP only). (e) An anti-biotin Western blot of the EPL reaction between the protein thioesters and biotinylated cysteine peptide shows specific biotinylation of the released protein. Hydrazine-released proteins were reacted with the biotinylated cysteine peptide as a non-thioester negative control to demonstrate that the reaction is specific to the thioester.

no biotinylation of proteins released with hydrazine that lack a thioester moiety (Figure 2-3e). In contrast to the results achieved with the hydrazine azide, the main biotinylated product of the EPL reaction corresponded to the target protein. Although MESNA will release other yeast proteins because of its reducing character (Figure 2-2d and Supplemental Figure 2-1), the thioester functionality was selectively added to the target protein via the intein-mediated reaction. These results further demonstrate that although MESNA does initially release the yeast-displayed constructs via disulfide bond reduction (Figure 2-2d), the subsequent MESNA-mediated release of the scFv or GFP from the remainder of the display construct produces specific carboxy-terminal functionalization of the target protein. Thus, protein release with MESNA eliminates the need for protein purification prior to use in downstream applications. Although the hydrazine azide proved useful to release and chemically functionalize purified intein fusion proteins [31, 51], its use with yeast surface displayed proteins is less advantageous because subsequent protein purification steps are necessary (Figure 2-3d). This disadvantage, along with the greater absolute efficiency of the MESNA release, led us to move forward with the MESNA-EPL approach.

2.3.3. Azide and alkyne functionalization of thioester proteins

While EPL with the thioester functionalized proteins in solution can yield specific modification of a protein, it would be desirable to adapt these methods for site-specific

immobilization of proteins on surfaces. The protein thioester formed is not ideally suited for protein immobilization applications via EPL since millimolar concentrations of the reactants are typically required for efficient conjugation [52, 128]. This has previously resulted in inefficient thioester surface immobilization reactions because these concentrations are difficult to obtain on surfaces [41]. As an alternative that is compatible with the MESNA-mediated release approaches, it is possible to employ EPL reactions to append azido and alkynyl groups onto the MESNA-released proteins. Subsequently the azide and alkyne functionalities can be used to immobilize proteins on surfaces since CuAAC reactions require lower concentrations of substrates than does EPL [39-41, 52]. Thus, by performing the EPL reaction with cysteine azide or cysteine alkyne in solution, high concentrations of the derivatized cysteine can be used to drive efficient functionalization of the proteins.

To generate these CuAAC-compatible proteins, proteins released after the initial 45-min MESNA reaction were separated from the yeast by centrifugation, and MESNA-mediated intein release was allowed to proceed for an additional 20 h in the presence of either cysteine azide or cysteine alkyne (Figure 2-4a and 2-4b). Resultant protein functionalization was detected by reacting the azido proteins with biotin alkyne (Figure 2-3a) and the alkynyl proteins with biotin azide (Figure 2-3a) in a CuAAC reaction, followed by anti-biotin Western blotting analysis of the reaction. The CuAAC reaction resulted in biotinylation of the target proteins that were functionalized with an azide or alkyne (Figure 2-4c); whereas, MESNA-released proteins that had not been reacted with the cysteine reagents and used as non-alkyne and non-azido negative controls were not functionalized. Although other yeast surface proteins are released in the

MESNA reaction and are present in the subsequent reaction mixtures (Supplemental Figure 2-1), the primary products of the EPL and CuAAC reactions correspond to biotinylated target protein. However, more non-specific biotinylation of yeast proteins was observed when EPL was performed with the cysteine azide followed by CuAAC with biotin alkyne than with the opposite chemical orientation (Figure 2-4c). Thus, by functionalizing the proteins with an alkyne via EPL followed by CuAAC with an azide target, protein functionalization is achieved with high specificity and no purification or post-processing after release from the yeast surface.

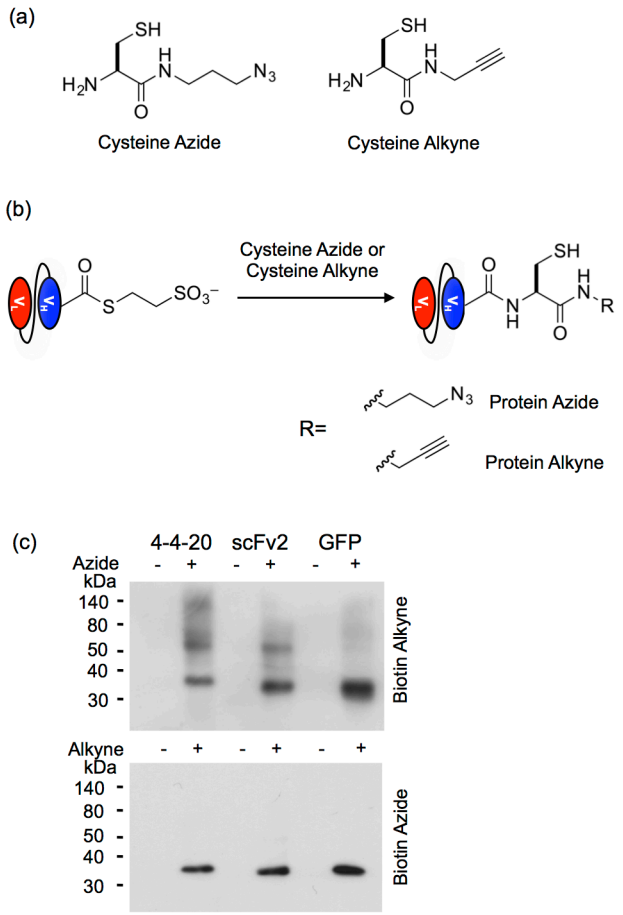

Figure 2-4: Azide and alkyne functionalization of thioester proteins via EPL

(a) Cysteine azide and cysteine alkyne were used in the EPL reaction. Biotin alkyne and biotin azide (shown in Figure 2-3a) were used to detect the chemical functionalization. (b) Thioester proteins obtained though the MESNA-release reaction react with cysteine azide or cysteine alkyne to install an azide and alkyne, respectively, on the C-terminus of the protein. The azide-functionalized protein is subsequently reacted with the biotin alkyne in the presence of Cu(I) via CuAAC to yield biotinylated protein. Similarly, the alkyne-functionalized protein reacts with biotin azide to yield biotinylated protein. (c) Western blots of the CuAAC reactions probed with an anti-biotin antibody demonstrate biotinylation only when the azide or alkyne is present in the protein. Proteins containing only the thioester modification were used as negative controls lacking azide and alkyne functionalization.

2.3.4 Immobilization of alkyne-functionalized proteins

Previous studies have demonstrated a greater reaction efficiency by immobilizing alkynyl proteins on azido surfaces than reacting azido proteins on alkynyl surfaces [39]. Given this result and the higher specificity of the CuAAC reaction in solution with the alkynyl protein, protein immobilization was performed with the alkynyl proteins (Figure 2-4c). Azido-functionalized agarose beads were reacted with either the alkynyl protein or the control, thioester proteins, under CuAAC conditions. Substantial protein immobilization in terms of FLAG epitope tag detection was observed only when the reaction was performed with a protein containing a carboxy-terminal alkynyl group (Figure 2-5a). Quantification revealed that 10–13 fold more scFv or GFP was present on the beads when the reaction was performed with scFv alkyne or GFP alkyne compared to scFv or GFP without the alkyne (Figure 2-5a), indicating that >90% of the alkynyl protein immobilization is site-specific and mediated via the alkyne.

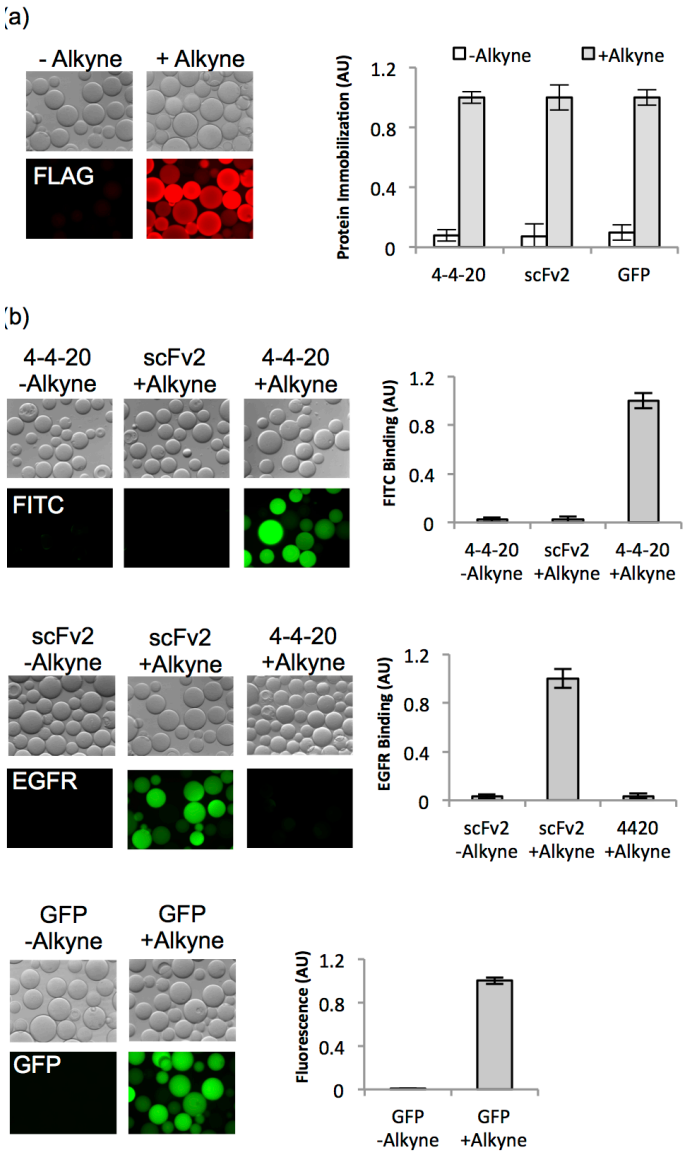

Figure 2-5: Immobilization and activity of alkynyl proteins
(a) Proteins released and functionalized with alkyne as described are further reacted with the azide functionalized agarose beads via CuAAC. Microscopic images indicate the presence of immobilized proteins by immunofluorescent labeling of the FLAG tag. Protein immobilization is quantified by measuring the total bead fluorescence. The fluorescence reading was independently normalized to the alkyne-linked protein for each of the three proteins, and represents the mean ± SD values of the immobilization reaction performed with proteins released from 6 independent yeast transformants, thereby representing the full measure of method variability. (b) Fluorescent microscope images demonstrate the activity of immobilized proteins on agarose beads. Top panel: Beads reacted with alkyne 4-4-20 exhibit binding to the 4-4-20 ligand, FITC-dextran, while beads reacted with non-alkyne 4-4-20 or alkyne scFv2 did not bind fluorescein. Middle panel: Binding of EGFR to immobilized proteins is detected with an anti-EGFR antibody. Immobilized alkyne scFv2 was shown to bind its ligand, EGFR, while beads reacted with alkyne 4-4-20 or non-alkyne scFv2 do not demonstrate binding to EGFR.

Bottom panel: Beads exhibit GFP fluorescence only when reacted with alkyne GFP. Protein activity is quantified by measuring the resultant fluorescence intensity of the beads and the fluorescence values are independently normalized based upon the signal for alkynyl protein binding its respective antigen (or GFP fluorescence). Plotted are the mean ± SD of activity measurements from three independent bead immobilization reactions.

Following confirmation of site-specific protein immobilization, the activity of the proteins conjugated to the beads was evaluated to ensure that the protein release and modification strategies did not have deleterious effects upon protein activity. In particular, scFvs contain two intrachain disulfide bonds that are critical for their stability and proper folding [129], and so the exposure to thiol-based reagents such as MESNA and cysteine alkyne could in principle reduce these disulfide bonds, causing the protein to unfold and become inactive. Using the various combinations of activity (GFP) and antigens (4-4-20, FITC and scFv2, EGFR), it was demonstrated that proteins indeed retained activity and antigen specificity after immobilization on the beads. Azido beads loaded with alkyne-conjugated 4-4-20 specifically bound fluorescein, while beads loaded with alkyne-conjugated scFv2 instead specifically bound EGFR (Figure 2-5b). GFP fluorescence was also detected on beads loaded with alkyne-conjugated GFP (Figure 2-5b). Although a small amount of non-specific protein immobilization was detected with anti-FLAG immunofluorescence labeling (Figure 2-5a), the adsorbed proteins appeared to exhibit little to no antigen binding or GFP fluorescence, indicating the importance of site-specific immobilization for the activity of these proteins (Figure 2-5b). Antigen binding selectivity was greater than 30:1 for the alkyne-immobilized scFvs compared to beads loaded with negative control scFv or non-alkyne containing scFvs (Figure 2-5b). Similarly, site-specific GFP immobilization yielded 100-fold more fluorescence than did non-alkyne containing GFP (Figure 2-5b). These results suggest

that the requisite MESNA release, cysteine alkyne EPL, and CuAAC reactions are collectively compatible to yield functional scFv and GFP.

2.4 Discussion

Intein-mediated protein functionalization strategies permit the addition of unique chemical functionalities to the C-terminus of proteins. In this study, we have demonstrated that target proteins displayed as intein fusion partners on the surface of yeast can be released by appropriate nucleophiles and subsequently functionalized to be compatible with EPL and CuAAC chemistries. The optimized release and chemical modification strategy illustrated in Figure 2-6 enabled facile and rapid functionalization of the C-terminus of our target proteins with alkynes while obviating the need for purification steps for downstream applications. To this end, we obtained >90% CuAAC-mediated immobilization of the alkynyl proteins on surfaces and demonstrated that the functionalization and immobilization strategies produced active antibodies that were capable of binding antigen.

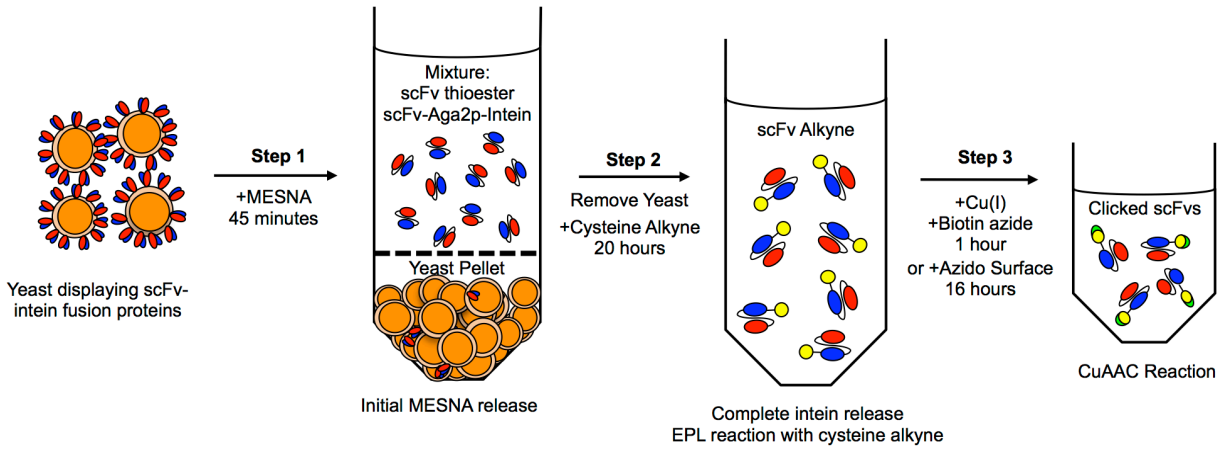

Figure 2-6: Intein-based release and functionalization method
The overall intein-based release and functionalization method is performed in three steps, as shown in this example for an scFv. Step 1: Yeast displaying scFv-intein fusion proteins are

reacted with MESNA for 45 min. Step 2: Released proteins in the MESNA solution (a mixture of scFv-thioesters and scFv-intein-Aga2p fusions) are removed from the yeast and cysteine alkyne is added. This reaction proceeds for 20 h to complete release of the scFv from intein and to conjugate the alkyne via EPL. Step 3: The alkyne-conjugated scFvs are reacted in a CuAAC reaction with biotin alkyne for 1 h or with an azido surface for 16 h.

Typical intein-mediated functionalization procedures are performed using soluble, purified proteins [31, 40, 41, 44, 45, 47, 48, 51, 80]. The techniques described in this study provide a facile alternative for obtaining small amounts of modified protein by directly releasing and reacting intein fusion proteins that are displayed on the surface of yeast. Whereas proteins that contain disulfide bonds such as scFvs are often expressed as insoluble inclusion bodies in prokaryotic organisms like *E. coli* [76], we displayed the intein fusions as folded, active proteins on the yeast surface. This eliminated protein solubilization and refolding procedures that not only require multiple steps to obtain soluble protein, but that can also result in inactive intein fusion proteins incapable of nucleophile-mediated release [47, 87]. However, in contrast to nucleophile-mediated release with soluble proteins, performing the reactions directly on the yeast surface generates the possibility that the nucleophile will react with other proteins present on the yeast surface. These undesirable side reactions were observed when the hydrazine azide was used to release the target proteins from the yeast surface. Although the hydrazine azide is known to react chemoselectively with purified protein thioesters [31, 51], the lack of chemoselectivity apparent in Figure 2-3c is likely due to the formation of hydrazones with carbonyl groups on glycosylated proteins that are secreted by yeast cells during the 3 day reaction or that reside on their surface. This competitive reaction would not confound the use of the hydrazine azide in the release of proteins displayed on the surface of *E. coli* or other cells that do not glycosylate their

proteins. In contrast, yeast displayed protein released with MESNA contained a carboxy-terminal thioester capable of undergoing an EPL reaction, which led to uniquely functionalized scFv or GFP, thus obviating the need to perform any protein purification. Therefore, by directly releasing and modifying surface displayed proteins, we have eliminated intermediate protein preparation steps including inclusion body solubilization, protein refolding, and protein purification to provide a simplified protein functionalization method.

Yeast surface display is a powerful protein engineering technique that can be used to perform high-throughput selections of scFv clones from large libraries in order to identify novel antibodies from naïve libraries [108, 130] or to fine-tune antibody properties such as affinity, stability, and specificity [112, 131, 132]. By releasing and functionalizing proteins displayed on the yeast surface, we have integrated these intein-mediated protein modification strategies into a protein engineering platform, potentially enabling downstream analysis of engineered clones as modified, soluble proteins without time-consuming intermediate steps. This platform could prove particularly useful to analyze panels of engineered clones where protein subcloning, soluble expression, and purification become limiting factors for clonal fitness assessment. Furthermore, standard enzymatic approaches for protein release from the yeast surface [105, 115] and functionalization methods such as biotinylation [133] would yield proteins that are immobilized or conjugated in a noncovalent fashion. In contrast, our strategy results in protein release and insertion of CuAAC-compatible groups that instead can enable stable, covalent conjugation of released proteins to many different linkers, proteins, surfaces and nanoparticles [41, 52, 62, 134, 135]. In addition, the general approaches

employing EPL chemistries described here could also be used for covalent introduction of numerous other useful chemical functionalities [49, 136].

The methods described in this study would be especially well suited for applications where small amounts of protein are sufficient for downstream analysis. Based upon the surface expression of our proteins (Figure 2-1b, 24,000-86,000 fusions per cell), it is possible to obtain between ~14 μg and ~58 μg of protein using a 1 L yeast culture and a 20-h surface display induction time. As one example, typical microarrays require antibody spotting at concentrations ranging from 25 to 400 μg/mL [10, 137, 138] and spotting volumes between 50 and 350 pL [9, 138, 139], and the amount of released protein would permit, at a minimum, 100,000 array spots. Thus, it is conceivable that by using the intein-linked yeast surface display method, a large selection of novel scFv clones could be expressed, released, functionalized, and immobilized in parallel to rapidly generate an antibody microarray. In conclusion, a combination of yeast surface display with intein-based tools provide a facile method for direct chemical functionalization of proteins, likely enabling a variety of downstream applications.

2.5 Supplemental Data

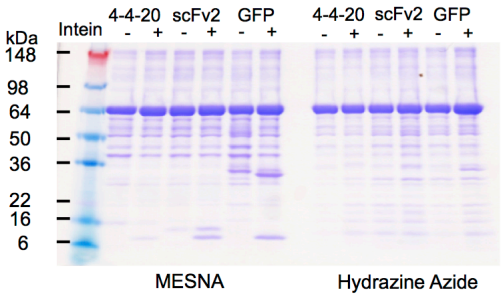

Figure 2-7: Coomaisse gel comparing hydrazine and MESNA release.
A Coomaisse-stained SDS-PAGE gel demonstrates that many yeast proteins are present in the mixture resulting from yeast reaction with MESNA or hydrazine azide. These yeast proteins

may be the result of protein released from the yeast surface by the nucleophiles or protein secreted from the yeast during the course of the reaction. The intense protein band at ~64 kDa represents BSA that acts as a carrier protein in all release reactions.

Chapter 3 – An Evolved Mxe GyrA Intein for Enhanced Production of Fusion Proteins

Chapter 3 continues to develop the intein-linked yeast display platform and extends EPL chemical modification strategies to secreted yeast proteins. We engineer the Mxe GyrA intein to improve surface display of scFv-intein fusion proteins, and consequently, the engineered intein facilitates the secretion of soluble scFv-fusion proteins from yeast, thus enabling chemical modification of scFvs at a preparative scale. This chapter serves both to provide an alternative to traditional bacterial expression systems and to enable the facile transition of surface displayed intein fusion proteins to a secretion platform. This chapter is to be submitted for publication as Marshall, C. J., Grosskopf, V. A., Moehling, T.J., Tillotson, B.T., Wiepz, G.J., Abbott, N. L., Raines, R. T., and Shusta, E. V. “An Evolved Mxe GyrA Intein for Enhanced Production on Fusion Proteins”.

3.1 Introduction

Therapeutic and biochemical properties of antibodies can be enhanced by custom chemical functionalization that enables modifications such as small molecule drug conjugation [140, 141], PEGylation [142, 143], and conjugation to nanoparticles [141, 142, 144]. Expressed protein ligation (EPL) is one common approach to chemically modify proteins in a site-specific manner. In EPL, the target protein is expressed as a fusion partner to a protein splicing element known as an intein [47, 89, 145]. Intein-mediated protein splicing is activated by the addition of a thiol nucleophile

that releases the target protein from the intein while simultaneously producing a carboxy-terminal thioester intermediate on the target protein. Subsequently, this carboxy-terminal thioester can be reacted with an appropriately functionalized amino-terminal cysteine to covalently attach the desired chemistry to the carboxy-terminus of the target protein.

Intein fusion proteins are most often expressed in the cytoplasm of *E.coli* [31, 39, 41, 47, 80, 87, 146]. One disadvantage of cytoplasmic expression is the formation of insoluble inclusion bodies that contain inactive intein-fusion proteins, therefore requiring solubilization of the inclusion bodies and refolding of the protein [47, 77, 80, 87, 146]. Glutathione redox buffers that are typically used to refold disulfide-containing proteins like antibodies can react with the thioester intermediate formed by the intein, thereby releasing it from the target protein and forming an unstable glutathione thioester on the carboxy-terminus of the target protein [87]. This unstable glutathione thioester can subsequently be hydrolyzed leading to loss of the thioester functionality [47, 87]. Additionally, *in vivo* autocleavage of the intein has been observed during protein expression, resulting in up to 90% loss of the intein for some fusion proteins [48, 81]. These factors have combined to hamper antibody-intein fusion protein production using bacteria [47, 89].

Yeasts provide a possible alternative to bacterial expression systems given their eukaryotic quality control machinery. Recently, scFvs were displayed as fusions to the Mxe GyrA mini-intein on the surface of *Saccharomyces cerevisiae* [145]. Contrasting with bacterial protein-intein fusion platforms, yeast displayed scFv-intein protein fusions were properly folded and capable of engaging their antigenic targets. However, surface

display levels of the scFvs were reduced by ~40% when fused to intein compared to the unfused antibody. In addition, surface display of heterologous proteins is not ideally suited for protein production at a preparative scale since protein expression on the yeast surface is limited to ~100,000 display constructs per yeast [105, 107], producing on the order of 70 μg of scFv per liter of yeast culture [145], while baseline scFv secretion in yeast is in the multi-mg per liter range [100, 103]. The yeast display levels of scFv-intein proteins could potentially be improved via directed evolution, as has been previously reported for a variety of proteins [131, 147]. Moreover, improvements in yeast display often translate to improvements in secretion titer [110, 148, 149]. While directed evolution approaches have been employed to engineer catalytic properties of inteins such as temperature, pH, and ligand dependence [150-153], intein-fusion protein expression levels have not been a target for improvement.

Therefore, in the current study, we sought to improve the production of scFv-intein fusion proteins both as displayed and secreted proteins. Directed evolution of the Mxe GyrA intein was employed as an scFv-intein fusion, and the yeast surface display levels of scFv-intein fusion proteins were restored to that of the unfused scFv. Furthermore, we demostrated that the engineered intein dramatcially improves secretion of scFv-intein fusion proteins from yeast, and, since the secreted proteins are folded and active, the scFvs can be directly functionalized and site-specifically immobilized via EPL and click chemistry.

3.2 Materials and Methods

3.2.1 Yeast strains and plasmids

Saccharomyces cerevisiae strain EBY100[105] (*MAT*a *AGA1::GAL1-*

AGA1::URA3 ura3–52 trp1 leu2Δ1 his3Δ200 pep4::HIS3 prb1Δ1.6R can1 GAL) was used for surface display, and strain YVH10[99] *(MAT*α *PDI1::GAPDH-PDI1::LEU2 ur*a3-52 *trp1 l*eu2Δ1 *his*3Δ200 *pep*4::*HIS*3 *prb*1Δ1.6R *ca*n1 *GAL)* was used for protein secretion. The unfused and intein-fused pCT4Re vectors[145] were used as a backbone for surface display of the scFvs (Figure 3-1a). Constructs pCT4Re-4420, pCT4Re-4420-intein, pCT4Re-scFv2, pCT4Re-scFv2-intein, pCT4Re-GFP, and pCT4Re-GFP-intein were generated in a previous study [145]. Anti-epidermal growth factor receptor mutant vIII (EGFRvIII) scFv, MR1 [154] (GenBank accession number U76382), was synthesized by IDT DNA Technologies and subcloned into the pCT4Re constructs to create pCT4Re-MR1 and pCT4Re-MR1-intein. An scFv that binds the external domain of EGFR, 2224 [155], was synthesized by Life Technologies based upon the sequence provided in patent US 20100009390 A1 [156] and subcloned into the pCT4Re constructs to create pCT4Re-2224 and pCT4Re-2224-intein. RBE4 binding scFvs selected in a previous study [130] were subcloned into the pCT4Re vectors to generate pCT4Re-scFvA, pCT4Re-scFvA-intein, pCT4Re-scFvD, pCT4Re-scFvD-intein, pCT4Re-scFvH, pCT4Re-scFvH-intein, and pCT4Re-scFv4S21, and pCT4Re-scFv4S21-intein. The pRS316-FLAG vector was created for protein secretion by inserting the constructs shown in Figure 3-1b into the pRS316-Gal vector [98] between the *GAL1-10* promoter and alpha factor terminator sequences to create unfused and intein-fused pRS316-FLAG vectors. The scFvs were sublconed into the pRS316-FLAG vectors to create pRS316-FLAG-4420, pRS316-FLAG-4420-intein, pRS316-FLAG-scFv2, pRS316-FLAG-scFv2-intein, pRS316-FLAG-GFP, pRS316-FLAG-GFP-intein, pRS316-FLAG-MR1, pRS316-FLAG-MR1-intein, and pRS316-FLAG-

2224, pRS316-FLAG-2224-intein.

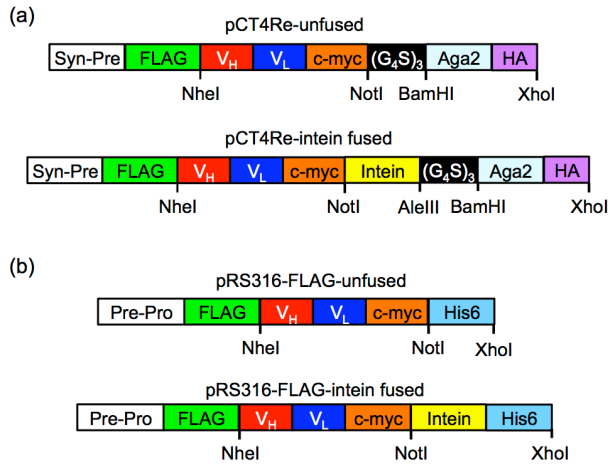

Figure 3-1: Surface display and secretion constructs
(a) In display construct pCT4Re, Aga2p is expressed at the carboxy-terminus to anchor the fusion protein to the yeast surface, while a FLAG epitope tag is expressed on the amino-terminus of the scFv or GFP to indicate full-length construct expression on the yeast surface. In the intein-containing display constructs, the Mxe GyrA intein is inserted between the carboxy-terminus of the scFv or GFP and the Aga2p surface anchor. (b) Secretion construct pRS316-FLAG is similar to the surface display construct, with a synthetic pre-pro leader sequence directing secretion and a six histidine epitope for purification.

3.2.2 Yeast growth, induction, and lysis

Yeast were transformed using the LiAc/ssDNA/PEG method [127]. For surface display strain EBY100, transformants were selected on tryptophan and uracil deficient SD-CAA agar plates (20.0 g/L dextrose, 6.7 g/L yeast nitrogen base, 5.0 g/L casamino acids, 10.19 g/L $Na_2HPO_4 . 7H_2O$, 8.56 g/L $NaH_2HPO_4 . H_2O$, 15 g/L agar). For secretion strain YVH10, transformants were selected on leucine and uracil deficient SD-2XSCAA + Trp agar plates (20 g/L dextrose, 6.7 g/L yeast nitrogenous base, 10.19 g/L $Na_2HPO_4 . 7H_2O$, 8.56 g/L $NaH_2HPO_4 . H_2O$, 15 g/L agar 190 mg/L Arg, 108 mg/L Met, 52 mg/L Tyr, 290 mg/L Ile, 440 mg/L Lys, 200 mg/L Phe, 1260 mg/L Glu, 400 mg/L Asp, 480

mg/L Val, 220 mg/L Thr, 130 mg/L Gly, and 40 mg/L Trp, lacking leucine and uracil).

EBY100 yeast were grown in SD-CAA medium (20.0 g/L dextrose, 6.7 g/L yeast nitrogen base, 5.0 g/L casamino acids, 10.19 g/L $Na_2HPO_4 . 7H_2O$, 8.56 g/L $NaH_2HPO_4 . H_2O$) until a culture density OD_{600nm}=1.0 was reached. Surface display was induced by replacing the media with an equivalent volume of SG-CAA (20 g/L galactose replacing dextrose) for 20 h at 20°C, 260 rpm. Yeast secretion strain YVH10 was grown in SD-2XSCAA + Trp (20 g/L dextrose, 6.7 g/L yeast nitrogenous base, 10.19 g/L $Na_2HPO_4 . 7H_2O$, 8.56 g/L $NaH_2HPO_4 . H_2O$, 190 mg/L Arg, 108 mg/L Met, 52 mg/L Tyr, 290 mg/L Ile, 440 mg/L Lys, 200 mg/L Phe, 1260 mg/L Glu, 400 mg/L Asp, 480 mg/L Val, 220 mg/L Thr, 130 mg/L Gly, and 40 mg/L Trp, lacking leucine and uracil) at 30°C, 260 rpm overnight. The following day, cultures were reset to an OD_{600nm}=0.1, and grown for 72 h at 30°C, 260 rpm. Yeast were induced by replacing the media with an equivalent volume of SG-2XSCAA + Trp (20 g/L galactose replacing dextrose) containing 0.1% w/v bovine serum albumin (BSA) and culturing the cells for 72 h at 20°C and 260 rpm.

To evaluate *in-vivo* autocleavage of the intein, yeast were lysed to analyze the intracellular protein contents (Supplemental Figure 3-6). Induced YVH10 (~$1x10^7$) were suspended in 100 µl TCA buffer (20 mM Tris, 50 mM ammonium acetate, 2 mM EDTA, pH 7.9) with 4 µl protease inhibitor (Roche) and 1 µl PMSF. Resuspended yeast were added to 100 µl 20% TCA and 100 µl glass beads, and the suspension was vortexed for 10 min. The supernatant was removed from the beads and centrifuged to precipitate a protein pellet. The pellet was dissolved in 200 µl TCA resuspension buffer (100 mM Tris, 3% SDS, 3 mM DTT, pH 11) and heated to 100°C for 5 min.

3.2.3 EGFR cell lines and creation of cell lysates

A431 (ATCC) and U87-EGFRvIII (kindly provided by Dr. Donald O'Rourke and Dr. Gurpreet S. Kapoor, University of Pennsylvania, Department of Neurosurgery) cell lines were maintained in Dulbecco's Modified Eagle Media (DMEM, Life Technologies) supplemented with 10% HyClone^{TM} Cosmic Calf Serum (Thermo–Fisher) and 1x antibiotic/antimycotic (PSA, Gibco) at 37°C and 5% CO_2. To prepare for lysis, cells were grown to ~90% confluence in 75 cm^2 tissue culture-treated T-flasks and washed three times with PBS. Cells were lysed by the addition of ice-cold 1 mL lysis buffer, consisting of 1% v/v Triton X-100 (Thermo–Fisher), 2 mM EDTA, and 1X cOmplete Protease Inhibitor Cocktail (Roche). Cells were scraped from the flask using a cell scraper at 4°C and collected into a microfuge tube. The lysed cells were rotated at 4°C for 15 min and centrifuged for 30 min to remove insoluble cell debris. The clarified lysates were then used to label yeast or antibody-conjugated beads as described below.

3.2.4 Intein Library Construction

Mutagenesis of the Mxe GyrA for the initial library creation was performed by error-prone PCR [157] of the pCT4Re-4420-intein construct containing intein using the nucleotide analogs 2′-deoxy-p-nucleoside-5′-triphosphate and 8-oxo-2′-deoxyguanosine-5′-triphosphate (TriLink Biotech) and primers (4420-intein-F 5'-CAGAACAAAAGCTTATTTCTGAAGAAGACTTGGCGGCCGCCGGCTGCATC-3') and (4420-intein-R 5'-GGTGGTGGTGGTTCTGGTGGTGGTGGTTCTGGTGGTGGTGGTTCTGGATC-3') that amplified the intein sequence but preserved the amino-terminal cysteine that is essential to protein splicing. The intein library was created by homologous

recombination in EBY100 using the mutagenized intein PCR product and the NotI/AleIII linearized pCT4Re-4420-intein acceptor vector (Figure 3-1a). The initial library size was determined to be $2.5x10^7$ clones by colony count. Twelve random yeast colonies were sequenced to determine an average nucleotide mutation rate of ~1.7%.

The second intein library was created by shuffling the mutations of clones 202-03, 202-08, 202-12, 202-13, 505-05, and 505-11 through assembly of degenerate oligonucleotides [158]. DNA oligonucleotides spanning the Mxe GyrA sequence were designed to contain the nucleotide base pair mutations at a ratio of 25:75 mutant: wild-type ratio. The intein gene was assembled from the oligonucleotides as previously described [159], and additional mutagenesis of the assembled gene was performed with error prone PCR. The library was created by homologous recombination as described above, and the initial library size was determined to be $3.2 x10^7$ clones by colony count. An average nucleotide mutation rate of 1.8% was determined by sequencing 22 of the yeast colonies.

3.2.5 Library Screening

The first intein library was screened via fluorescence activated cell sorting (FACS) in five rounds of enrichment. For the first round of FACS, $2x10^8$ yeast from the initial library were labeled to detect FLAG tag expression using the flow cytometry procedure described below (Supplemental Figure 3-7). Clones with the highest expression level (~5%) were selected using a Becton Dickinson FACSVantage SE sorter (University of Wisconsin Comprehensive Cancer Center). Using yeast from the previous sort, rounds 2-4 were completed in a similar manner (Supplemental Figures 3-8 and 3-9). For the fifth round, yeast clones exhibiting both high construct expression

and 4-4-20 activity were selected by labeling for the FLAG tag and binding to FITC-dextran (Supplemental Figure 3-10). From the second intein library, 1.5 x10^8 cells were labeled to detect FLAG tag expression and FITC-dextran binding, and clones with the highest expression level and binding (5%) were selected (Supplemental Figure 3-14). Four additional rounds of FACS were performed, each time enriching the pool from the previous sort for high expression and FITC-dextran binding (Supplemental Figures 3-15, 3-16, and 3-17).

Individual clones were isolated by plating the final library pools on selective media (SD-CAA) and selecting single colonies for characterization. Plasmids were recovered from the yeast with the ZymoPrep Yeast Plasmid Miniprep II Kit (Zymo Research), and clones were sequenced with the following primers: mxe4420seq_F (5'-TCTGTGAAAGGCAGATTCACCA-3') and mxe4420seq_R (5'-ACAAAGAGTACGGCGTCGATT-3'). Clones were re-transformed into parent strain EBY100 for subsequent analysis.

3.2.6 Flow cytometry

To determine surface display expression levels, the following anti-FLAG immunolabeling steps were performed at 4°C prior to flow cytometry analysis. Induced EBY100 yeast were incubated with an anti-FLAG rabbit polyclonal antibody (Sigma–Aldrich, diluted 1:500 in PBS containing 0.1% BSA, PBS-BSA) for 30 min and washed once with PBS-BSA. Secondary antibody labeling was performed by incubating with either anti-rabbit Alexa 488 (Life Technologies, diluted 1:500 PBS-BSA), anti-rabbit PE (Sigma–Aldrich, diluted 1:45 in PBS-BSA), or anti-rabbit allophycocyanin (APC) (Life Technologies, diluted 1:500 in PBS-BSA) for 30 min, followed by a final wash with PBS-

BSA. To evaluate 4-4-20 binding activity, yeast were incubated with 10 μM fluorescein isothiocyanate-functionalized dextran in PBS-BSA (FITC-dextran, Sigma–Aldrich) for 30 min at 4°C followed by washing once with PBS-BSA prior to flow cytometry analysis. Activity of surface displayed scFv2 and 2224 was evaluated by incubating yeast with purified human EGFR isolated from A431 cells by immunoaffinity chromatography[160] (4 μg/mL in PBS-BSA) for 1 h at 4°C, followed by washing once with PBS-BSA. Yeast were next incubated with anti-EGFR mouse antibody cocktail Ab-12 (Lab Vision Corporation, diluted 1:200 in PBS-BSA) for 30 min, washed once with PBS-BSA, and labeled with anti-mouse PE (Sigma–Aldrich, diluted 1:40 in PBS-BSA) for 30 minutes followed by a final wash with PBS-BSA. Binding of MR1 to EGFRvIII was evaluated by yeast display immunoprecipitation (YDIP) [161]. Yeast were incubated with undiluted U87-EGFRvIII lysates in PBS containing 1% v/v Triton-X-100 (PBS-TX) for 1 h at 4°C, followed by washing once with PBS-TX and anti-EGFR primary and secondary antibody labeling steps as performed for scFv2 and 2224. GFP activity was evaluated by measuring the GFP fluorescence of the yeast at 488 nm excitation. The yeast cell fluorescence was measured using a FACSCalibur flow cytometer (Becton Dickinson), and the geometric mean fluorescence intensities of the protein displaying populations were quantified with the FlowJo software package to determine relative display levels and activities.

3.2.7 Protein purification

Following YVH10 growth and induction at the 50 mL scale, the yeast supernatant containing the secreted proteins was separated from the yeast by centrifugation and dialyzed against Tris-buffered saline (TBS, 25 mM Tris, 150 mM NaCl, 2 mM KCl, pH

7.9). The purification column was loaded with 750 µl Ni-NTA agarose (Qiagen) and equilibrated with 10 mL bind buffer (TBS with 5mM imidazole) prior to loading the dialyzed yeast supernatant. The column was subsequently washed with 15 mL bind buffer followed by a wash with 3 mL wash buffer (TBS with 20 mM imidazole), and the proteins were eluted with 2 mL TBS containing 250 mM imidazole.

3.2.8 SDS-PAGE and Western blotting

Protein samples were reduced and denatured by boiling in LDS sample buffer (Life Technologies) containing 1 mM 2-mercaptoethanol for 10 min prior to resolution on 4-12% Bis-Tris gels (Life Technologies) Under these conditions, no additional intein cleavage above that of the 20 h MESNA reaction is observed. Proteins were subsequently transferred to a nitrocellulose membrane for Western blot analysis. Detection of FLAG tagged proteins was performed by probing the membranes with anti-FLAG M2 mouse monoclonal antibody (Sigma–Aldrich, diluted 1:3000) followed by anti-mouse HRP conjugate (Sigma–Aldrich, diluted 1:2000). To detect biotinylated proteins, membranes were probed with anti-biotin mouse monoclonal antibody Ab-2 clone BTN.4 (Lab Vision Corporation, diluted 1:500) followed by anti-mouse HRP conjugate. Membranes were developed using Clarity™ Western ECL Substrate (Bio-Rad) and imaged with the ChemiDoc XRS+ system (Bio-Rad). Unsaturated band intensities were measured with the Image Lab Software (Bio-Rad) to quantify the relative protein amounts.

3.2.9 Fluorescein Quench Assay and GFP Activity

The K_d of secreted 4-4-20 and 4-4-20-202-08 was calculated by fluorescein quenching as previously described [99, 162]. Yeast supernatants containing the soluble proteins were dialyzed against TBS prior to analysis. Fluorescein (Sigma–Aldrich) was added stepwise to 1 mL of the dialyzed supernatant, and the resulting fluorescence at 514 nm was monitored using a Fluoromax-3 Spectrofluorometer (Horiba) and an excitation wavelength of 492 nm. The fluorescence intensities were fit to an equilibrium binding model to determine the concentration and K_d of the 4-4-20 proteins.

Secreted GFP activity was determined by measuring the emission spectrum of purified samples at 488 nm excitation with the Fluoromax-3 Spectrofluorometer, and the area under the curve was computed. Anti-FLAG quantitative Western blotting was performed to determine relative GFP expression levels, and the fluorescence intensity was divided by expression level to calculate specific activity.

3.2.10 Intein-Mediated Release and EPL

The ability to release the scFvs and GFP from the display construct in an intein-dependent manner was also evaluated as previously described [145]. Briefly, yeast displaying the intein-linked constructs were incubated with 50 mM 2-mercapthoethanesulfonic acid (MESNA, Sigma–Aldrich) in TBS for 45 min at room temperature to release a mixture of scFvs and scFv-intein-Aga2p fusion proteins. The yeast were subsequently removed from the reaction mixture by centrifugation, and the supernatant containing MESNA and the released proteins was allowed to react for 20 h to complete release of the scFvs from intein. The released proteins were subjected to

anti-FLAG Western blot analysis. Expressed protein ligation (EPL) with a biotinylated cysteine peptide was also performed as previously described [145]. Following the 45 min reaction of the yeast with the MESNA solution, the released proteins were separated from the yeast by centrifugation and 1 mM Bio-P1 peptide was added (synthesized by the University of Wisconsin Biotechnology Center, Sequence: NH_2-CDPEK(Bt)DS-$CONH_2$). The combined release and EPL reaction was allowed to proceed for 20 h at room temperature, and the proteins were analyzed with an anti-biotin Western blot.

For release and functionalization of the secreted scFvs and GFP, 100 µl of 1 M MESNA was added to 900 µl of purified scFv- or GFP-intein (~5-300 mg fusion protein/L) and the reaction was allowed to proceed for 20 hours at room temperature prior to anti-FLAG Western blot analysis. To generate azide-functionalized proteins, cysteine azide (Anaspec) was added to a final concentration of 5 mM during a combined 20 h release and EPL reaction. The proteins were subsequently dialyzed with TBS to remove unreacted cysteine azides prior to performing the immobilization reactions.

3.2.11 Protein Immobilization via Strain-Promoted Click Chemistry

The following protein immobilization and incubation steps were performed at room temperature with gentle rotation. Dibenzocyclooctyne (DBCO)-fuctionalized agarose (10 µl, Click Chemistry Tools) was blocked for with 500 µl DBCO blocking buffer (PBS with 2% w/v BSA and 1% Tween-20) for 1 h. The blocking buffer was removed, and 200 µl of the azide-modified proteins were added to the beads for 2 h. The 2 h reaction time was employed based the findings presented in Supplemental

Figure 3-21, where >50% immobilization was achieved after just 1 h incubation. The beads were subsequently washed twice with PBS-BSA and once with DBCO blocking buffer. To evaluated 4-4-20 binding to fluorescein, the antibody-linked beads were incubated in 10 μM FITC-dextran in PBS-BSA for 30 min followed by washing three times with PBS-BSA. Activity of the EGFR scFv was assayed by incubating the antibody-linked agarose beads with 200 μl undiluted A431 cell lysates or U87-EGFRvIII cell lysates for 1 h. The beads were washed twice with PBS-TX and once with DBCO blocking buffer before incubation with 200 μl anti-EGFR antibody cocktail Ab-12 (1:200 dilution in DBCO blocking buffer) for 30 min. The antibody-linked beads were subsequently washed twice with PBS-BSA and once with DBCO blocking buffer, followed by incubating with 200 μl anti-mouse Alexa 488 antibody (1:500 dilution in DBCO blocking buffer) for 30 min. The beads were washed three times with PBS-BSA. Beads were imaged with an Olympus IX70 fluorescence microscope, and the fluorescence intensities of the beads at 509 nm were measured using a Tecan Infinite M1000 fluorescent microplate reader with an excitation wavelength of 488 nm.

3.3 Results

3.3.1 Intein library generation and screening

Evolution of the Mxe GyrA intein was performed with the primary screening criterion being increased yeast display of an scFv-intein fusion. The anti-fluorescein scFv (4-4-20) construct was employed as the fusion partner since intein fusion decreased yeast display by 40% compared with unfused 4-4-20 display [145], offering a convenient screening pressure of improved yeast display (Figures 3-1a and 3-2a). For the first round of directed evolution, random mutagenesis was selectively targeted to the

intein moiety, and upon recombination with unmutated 4-4-20, a library of ~$2.5x10^7$ 4-4-20-intein fusion mutants was generated. The library was enriched for clones with elevated full-length surface expression (FLAG epitope tag) through four rounds of fluorescence activated cell sorting (FACS), followed by one additional round of FACS that ensured retention of 4-4-20 binding activity by using fluorescein labeling in addition to FLAG epitope labeling (Figure 3-2a). A 1.7-fold increase in display and fluorescein binding compared to the wild-type intein was observed in this final sorted pool (Figure 3-2b, compare panels i and ii), and the display levels of the 4-4-20-intein fusion were restored to that of the unfused 4-4-20 protein (Figure 3-2b, panel iv).

Individual intein clones were next isolated and evaluated for display levels and intein activity. Since mutations to the Mxe GyrA intein could potentially inhibit intein activity [163], the clones were first screened for activity by examining 4-4-20 release from the 4-4-20-intein fusion construct by reaction with a sulfur nucleophile, MESNA. The wild-type intein catalyzes an N- to S- acyl shift at the amino-terminal cysteine of the intein, forming a thioester that is susceptible to a nucleophilic attack. Reaction with a nucleophile, such as MESNA, releases 4-4-20 from the intein and the yeast display construct while simultaneously appending a carboxy-terminal thioester onto 4-4-20 (Figure 3-3c) [145]. Because MESNA also reduces the disulfide bonds between Aga1p and Aga2p on the yeast surface (Figure 3-2a) [145], 4-4-20 release from the intein could not be measured inline with the screen by flow cytometry. Instead, intein activity was determined for each individual clone via anti-FLAG Western blotting (shown in Figure 3-2d for clone 202-08 and in Supplemental Figure 3-11 for all clones). Six mutated intein

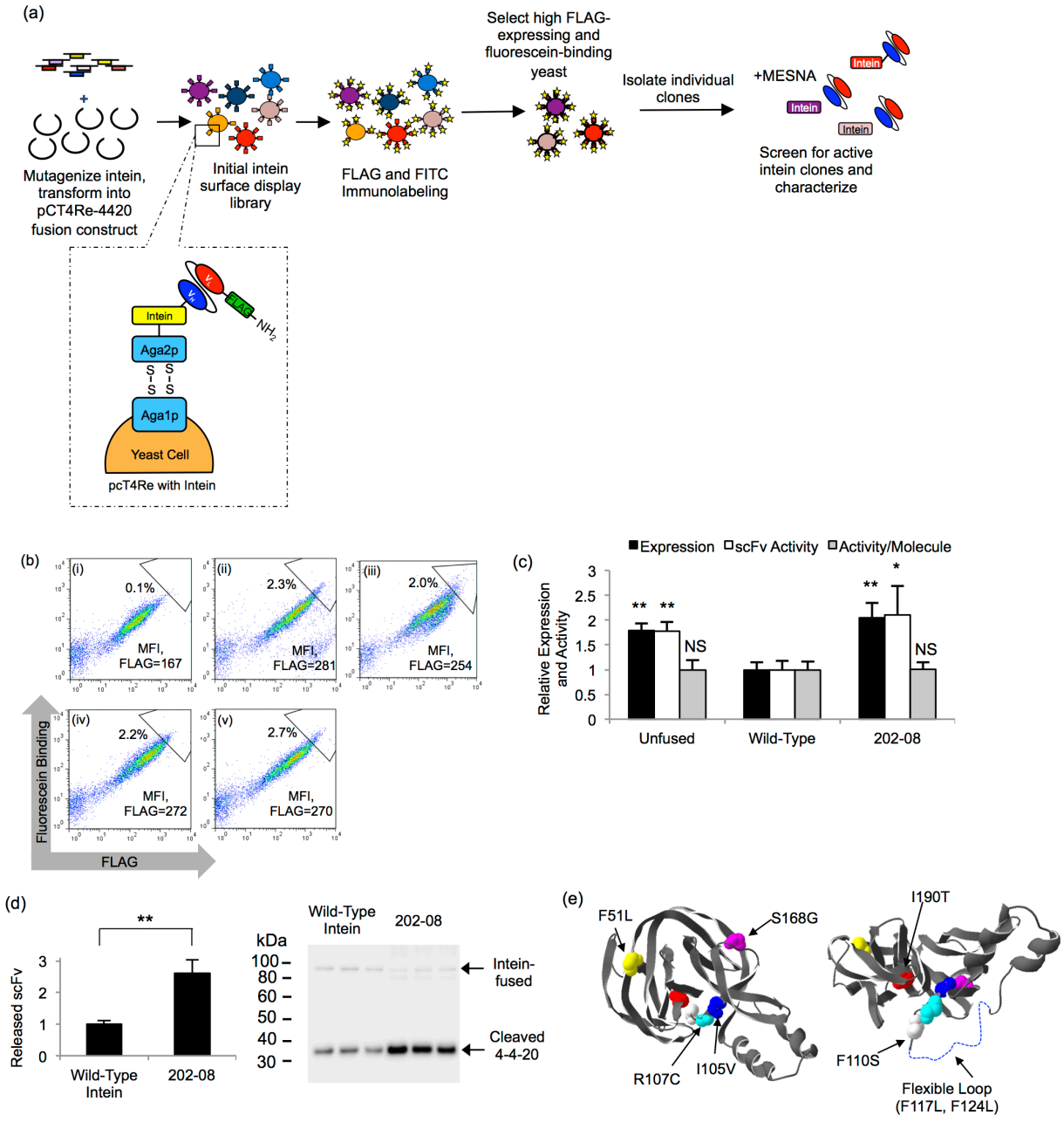

Figure 3-2: Directed evolution of the Mxe GyrA intein.
(a) For directed evolution round 1, the Mxe GyrA intein library was created by random mutagenesis and transformed into the pCT4Re-4420 construct. The library was screened in four rounds of enrichment for improved FLAG tag expression via FACS. A fifth round of enrichment selected for both improved FLAG tag expression and comensurate increases in binding to fluorescein. Individual clones were isolated and screened for intein activity by the addition of MESNA, which releases the scFv from the display construct when an active intein is present. For directed evolution round 2, the round 1 clones were shuffled and mutagenized prior to screening for increased display levels. (b) Flow cytometry dot plots depicting expression and binding activity of scFv-intein clones and pools on the yeast surface. Geometric mean flurescence intensity (MFI) of the FLAG signal for the displaying population shown as inset and

a sample sort gate is included to illustrate the enrichment. Panel i, wild-type intein fusion; panel ii, round 1 final selected pool; panel iii, round 2 final selected pool, panel iv, unfused 4-4-20 scFv; panel v, round 1 202-08 intein mutant (c) The geometric mean fluorescence of the positive population was quantified and normalized to the wild-type 4-4-20−intein contruct to compare the relative expression levels (FLAG) and activity (fluorescein binding) of the unfused 4-4-20 construct, wild-type intein construct, and the 202-08 intein mutant. Activity per molecule is expressed as the ratio of fluorescein binding to FLAG expression level. Plotted are the means ± S.D. from three independent yeast transformants. Statistically significant improvements over the wild-type intein construct were determined by an unpaired student's t-test (*, $p<0.05$; **, $p<0.01$; NS, non-significant) Data for other individual intein mutants are compiled in Table 3-1 and Supplementary Figure 3-11. (d) Quantitative anti-FLAG Western blotting was performed to determine the relative amount of 4-4-20 released from the yeast surface in the MESNA reaction. Plotted are means ± S.D. for three independent reactions originating from three independent yeast surface display transformants. Next to the bar graph are the triplicate Western blot data at the cleaved scFv size of ~30 kDa. The double asterisk represents a statistically significant increase in 4-4-20 release for clone 202-08 ($p<0.01$) as determined by an unpaired student's t-test. (e) The crystal structure of the Mxe GyrA intein (pdb ID: 1AM2 [164]) is shown with the mutations found in the 202-08 intein highlighted. A flexible loop missing from the crystal structure and contains two of the eight mutations present in 202-08. The structure on the right was rotated 90° to display the flexible loop, which is denoted by a dotted line, and surrounding mutations.

clones exhibited an increase in surface display over the wild-type intein and retained their cleavage activity (Table 3-1 and Supplemental Figure 3-11).Expression levels of all analyzed clones from Round 1 are given in Supplemental Table 3-2. In an attempt to further improve 4-4-20-intein fusion display levels, these six clones were shuffled and additionally mutated to create a library containing ~3.2×10^7 clones for a second round of directed evolution (see Materials and Methods for details and Supplemental Table 3-3). In the second round of evolution, the library was again screened for elevated display levels and fluorescein binding over five rounds of FACS. Characterization of the final pool demonstrated an increase in display levels compared to the wild-type intein, but display level was not significantly greater than that achieve through the first round of directed evolution (Figure 2b, iii), as also confirmed by evaluation of individual clones (Supplemental Figure 3-18a,c and Supplemental Table 3-4). Interestingly, while

several individual clones from Round 2 did exhibit expression levels comparable to that of 202-08, many of the clones had diminished protein splicing capabilities (Supplemental Figure 3-18b,d). Furthermore, these clones failed to improve upon the protein secretion level of 202-08 (discussed below).

Amino Acid	21	33	50	51	74	105	107	110	112	114	117	118	124	129	144	158	160	164	168	190	191	Fold Increase[a]	Statistical Significance[b]
Wild-Type	I	I	L	F	N	I	R	F	V	C	F	A	F	Y	H	D	R	A	S	I	T	1.0±.0	
202-03					D					R					R	G						1.4±.1	**
202-08				L		V	C	S			L		L						G	T		1.8±.2	**
202-12		T	P						A		C											1.5±.3	*
202-13	T			S						G		T					Q					1.3±.2	NS
505-05	T									R										V		1.3±.1	**
505-11														C				P			M	1.7±.1	**

Table 3-1: Intein mutations and surface display levels.
(a) Fold increase relative to the wild-type intein as fusions to 4-4-20, mean ± S.D from three independent yeast transformants. (b) Statistical analysis was perfomed by an unpaired student's t-test, with double asterisks representing $p < 0.01$, single asterisks representing $p < 0.05$, and NS designating that differences are not significant ($p > 0.05$).

3.3.2 Surface display characterization of 202-08 intein

Clone 202-08 from round 1 of directed evolution was selected for further characterization based upon its elevated display levels, retention of protein splicing activity, and its capability to also significantly elevate secretion of scFv-intein fusions (discussed below and compared with other clones in Supplemental Figures 3-12 and 3-19). The 202-08 intein contained eight amino acid mutations (Table 3-1, Figure 3-2e) and increased the surface display level of 4-4-20 1.8 fold compared to the wild-type intein fusion (Figure 3-2b, v), making its display level comparable to that of the unfused 4-4-20 protein (Figure 3-2c). Furthermore, the fluorescein binding per molecule of 4-4-20 was unchanged by fusion to 202-08 (Figure 3-2c). The retention of 202-08 catalytic activity was confirmed by examining the relative amount of 4-4-20 cleaved from the

yeast surface display construct in a MESNA release reaction. Quantitative Western blotting demonstrated a 2.6 fold increase in the amount of 4-4-20 released from yeast with clone 202-08 compared to the wild-type intein (Figure 3-2d), consistent with the increased surface display levels mediated by the 202-08 intein (Figure 3-2c).

Next, the generalizability of the 202-08 intein mutant was evaluated by testing effects on display and activity after its fusion to GFP and a cohort of 7 additional scFvs. The tested scFvs included three epidermal growth factor receptor (EGFR)-binding scFvs, scFv2 [126], MR1 [154], and 2224 [155, 156], and a panel of brain endothelial-binding scFvs, scFvA, scFvD, scFvH, and 4S21 [130] that collectively exhibit a range of unfused expression levels on the yeast surface (Figure 3-3a). The expression level of GFP was unchanged upon fusion to wild-type intein as previously reported [145], while scFv fusion to the wild-type intein generally decreased construct expression levels ~25-50%, regardless of unfused display efficiency (Figure 3-3a). The lone exception was 2224, where both the unfused and wild-type intein-fused forms exhibited similar, low display levels (Figure 3-3a). When each scFv or GFP was instead expressed as a fusion to the 202-08 intein, display was uniformly improved compared to the wild-type intein fusion reaching levels similar to or greater than that of the unfused protein (Figure 3a). Next, the activity of GFP- and EGFR-specific scFv-intein fusions was evaluated to ensure the 202-08 intein did not have deleterious effects on the specific activity of its fusion partner. Much like the case of 4-4-20, GFP fluorescence activity was not altered by fusion with the 202-08 intein (Figure 3-3b). Interestingly, compared with unfused scFv, fusion to 202-08 yielded small increases in per molecule EGFR binding for scFv2

and MR1, while 2224 exhibited more substantial 1.5-fold increases in binding to its EGFR ligand (Figure 3-3b).

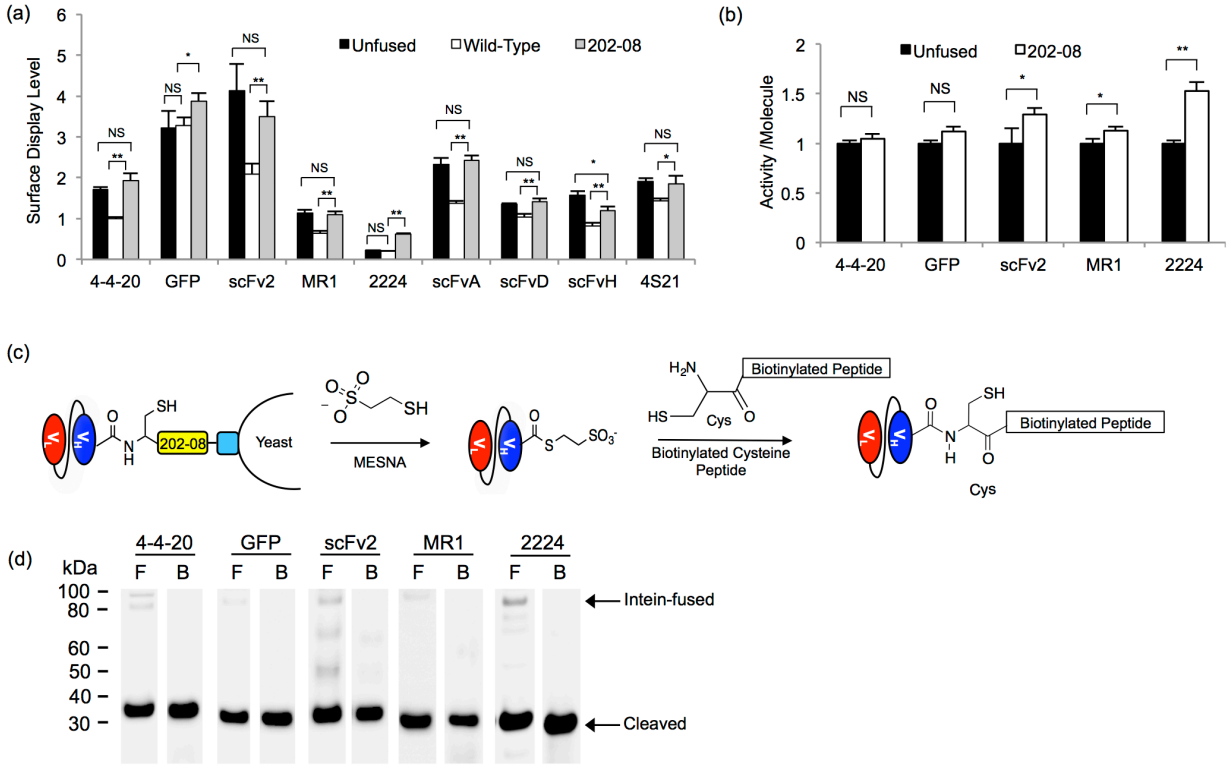

Figure 3-3: Analysis of surface displayed scFv- and GFP-202-08 fusions.
(a) Surface display levels of unfused, wild-type intein fused or 202-08 intein fused scFvs and GFP were analyzed by flow cytometry. The MFI of the FLAG-positive yeast populations was quantified and all were normalized to the 4-4-20 construct containing the wild-type intein. Reported are the means ± S.D. of three independent yeast transformants. Statistical analysis was performed by an unpaired student's t-test (*, $p < 0.05$; **, $p < 0.01$; NS, not significant $p > 0.05$). (b) ScFv and GFP per molecule activity was evaluated by detecting binding to the scFv antigens at saturating ligand concentrations or by measuring GFP fluorescence. Activity per molecule was determined by calculating the ratio of the geometric means for activity (binding or fluorescence) to FLAG expression levels and normalizing to the unfused construct lacking intein. Plotted are the means ± S.D. from three independent yeast transformants, with statistical significance determined by an unpaired student's t-test (*, $p < 0.05$; **, $p < 0.01$; NS, not significant $p > 0.05$) (c) For intein-mediated protein release, MESNA reacts to release the scFv or GFP from the display construct and append a carboxy-terminal thioester. For EPL functionalization, the carboxy-terminal thioester reacts with a biotinylated peptide containing an amino-terminal cysteine to covalently link the scFv or GFP to the biotin by an amide bond. (d) Products of the reaction depicted in panel c resolved and analyzed by Western blotting to detect

release of the scFv or GFP (~30 kDa) from the 202-08 intein construct using an anti-FLAG antibody (F) or biotin functionalization via EPL with an anti-biotin antibody (B). A small amount of uncleaved scFv-intein-Aga2p product can be seen in the anti-FLAG Western blot between ~80 kDa and 100 kDa due to the glycosylation of Aga2p.

3.3.3 Secretion of scFv-intein fusion proteins

Next, yeast secretion constructs were designed to flank scFv or GFP inserts with the FLAG epitope tag at the amino-terminus and a six histidine epitope tag at the carboxy-terminus to permit protein detection (before or after intein release) and purification, respectively (Figure 3-1b). Similar to the surface display experiments, secretion of unfused scFv or GFP was compared directly to the secretion of the same protein as a fusion to the amino-terminus of the wild-type or 202-08 intein (Figure 3-1b). Along with GFP, four scFvs (4-4-20 and the EGFR-binding scFvs, scFv2, MR1, and 2224) were examined in the protein secretion studies. When the scFvs were produced as fusions to wild-type intein, quantitative Western blotting analysis demonstrated substantial decreases in scFv secretion, ranging from 75% (MR1) to 99% (scFv2) reduction compared to the unfused scFv, while GFP expression did not decrease when fused to wild-type intein (Figure 3-4a). However, as observed with surface display, secreting the scFvs and GFP as fusions to the evolved 202-08 intein substantially improved the protein production compared to the wild-type intein fusion (Figure 3-4a). Expression of MR1 and 4-4-20 increased 3- and 10-fold, respectively, compared to the wild-type intein fusion to achieve secretion levels that were comparable to the unfused protein (Figure 3-4a). Fusion of 202-08 to scFv2 and 2224 increased secretion ~30-fold and ~3-fold over the wild-type intein fusions, respectively, although expression of these

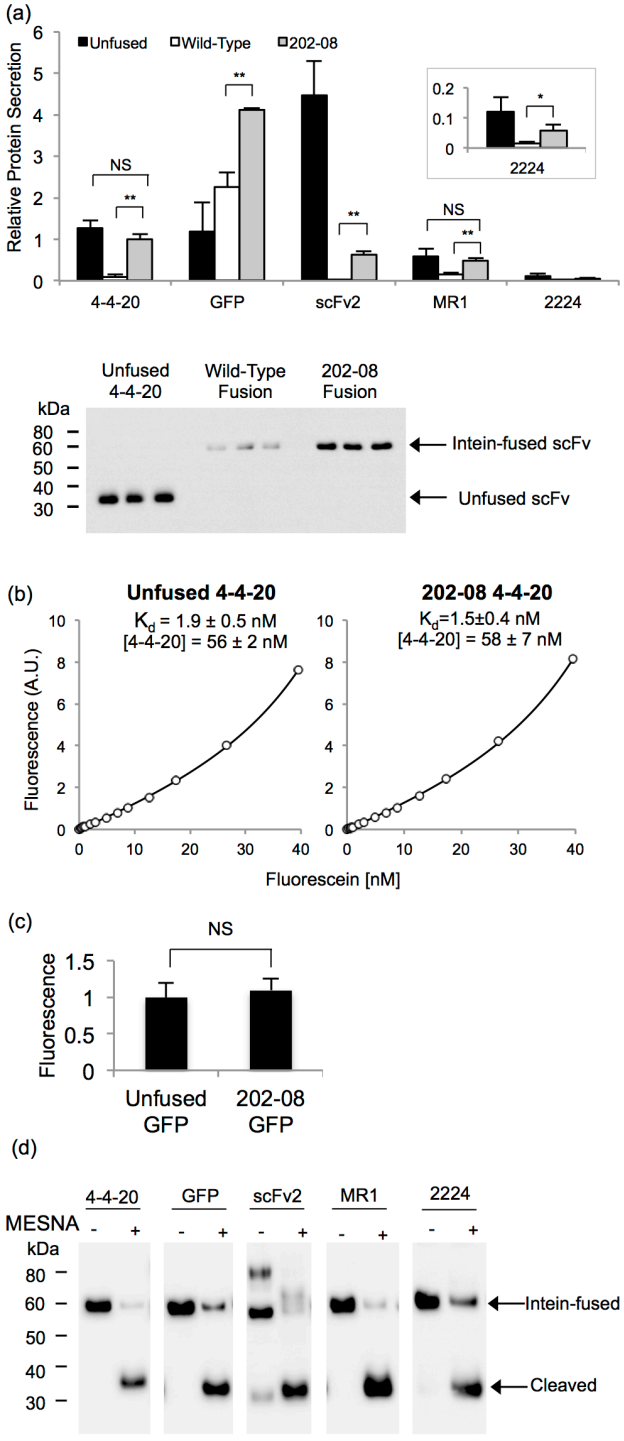

Figure 3-4: Secretion of scFv and GFP intein fusion proteins.
(a) Yeast supernatants containing scFv or GFP fused to the wild-type intein or 202-08 intein were subjected to anti-FLAG quantitative Western blotting and compared to the unfused target protein. Values are normalized to the level of the 4-4-20-202-08 fusion to determine relative amounts. The absolute secretion titer of the 4-4-20-202-08 fusion protein is 3.1 mg/L as

determined in panel b). Reported are the means ± S.D. from three independent yeast transformants. Statistical significance was determined by an unpaired student's t-test (*, $p < 0.05$; **, $p < 0.01$; NS, not significant $p > 0.05$). Western blot of supernatant samples used for the quantitation of relative 4-4-20 protein secretion is shown below the bar graph. (b) An equilibrium binding curve was generated by fluorescein quenching to compare the K_d of unfused 4-4-20 and 4-4-20 fused to 202-08. A sample curve for each of the proteins is shown, and the mean ± S.D for the fitted parameters of K_d and 4-4-20 concentration were obtained by fitting quench curves generated from supernatants resulting from three independent yeast transformants. From the molar concentrations of 4-4-20, the average mass concentration of the 4-4-20 component was calculated to be 1.6 mg/L of yeast culture for both the unfused and the intein-fused 4-4-20 (corresponding to 3.1 mg/L for the full 4-4-20-202-08 fusion protein) The K_d and 4-4-20 concentrations were statistically indistinguishable, as determined by an unpaired student's t-test ($p > 0.05$). (c) GFP activity was determined by calculating the ratio of fluorescence to FLAG expression levels and normalizing to the unfused construct lacking intein. The mean ± S.D results from three independent yeast tranformants. The fluorescence per molecule of unfused GFP and 202-08 fused GFP was statistically indistinguishable, as determined by an unpaired student's t-test (**, $p > 0.05$) (d) The catalytic activity of 202-08 was examined by reacting secreted and purified proteins with MESNA and evaluating cleaved yield after standard 20 h reaction. Anti-FLAG Western blotting demonstrates between 70% (2224) and 99% (MR1) release of the target protein from the 202-08 intein in the presence of MESNA.

scFvs was not fully restored to the unfused protein level (Figure 3-4a). Furthermore, even though the GFP fusion to the wild-type intein did not decrease secretion compared to the unfused GFP, expression when fused to 202-08 was modestly improved (~1.5 fold) over the wild-type intein (Figure 3-4a). Secretion analysis of other intein clones as 4-4-20 fusion proteins is presented in Supplemental Figures 3-12 (Round 1) and 3-19 (Round 2). While some of the clones exhibited improved secretion over the wild-type intein, clone 202-08 produced the greatest expression improvements.

Next, the activities of secreted scFv-intein fusion proteins were examined both from fusion partner and intein perspectives. First, 4-4-20 scFv and GFP activity was quantitatively evaluated using the secreted 4-4-20 and GFP intein fusion proteins (functionality of anti-EGFR scFvs evaluated as immobilized proteins below). The equilibrium binding affinity of 4-4-20 fused to 202-08 was measured in order to ensure

that the antibody component of the fusion protein was folded and functional. Monitoring the fluorescence quench upon binding of fluorescein to 4-4-20 allowed determination of the equilibrium dissociation constant, K_d, of the 4-4-20-202-08 fusion protein to be 1.5 ± 0.4 nM, making it statistically indistinguishable ($p > 0.05$) from the unfused 4-4-20 protein (1.9 ± 0.5 nM) (Figure 3-4b). The activity of GFP fused to 202-08 was assessed by measuring its fluorescence per molecule, and it was shown to be identical to that of the unfused GFP ($p > 0.05$) (Figure 3-4c). Next, the intein-mediated release of the scFv or GFP from the 202-08 intein was evaluated by reacting the secreted and purified scFv or GFP fusion proteins with MESNA. All four scFvs along with GFP were released from the intein with efficiencies ranging from 70-99%, thus demonstrating that the 202-08 intein component is active when produced as a soluble fusion protein (Figure 3-4d). Similar release efficiencies were observed for wild-type intein fusion proteins indicating that the engineered intein did not affect the cleaved scFv or GFP yields (Supplemental Figure 3-13).

3.3.4 Immobilization of scFv and GFP via strained cycloaddition reaction

Next, by employing EPL functionalization techniques [39, 145], the scFvs and GFP were chemically functionalized to enable covalent immobilization of the proteins onto surfaces. The secreted and purified scFv- and GFP- 202-08 intein fusion proteins were reacted with MESNA in the presence of cysteine azide, thereby releasing the scFv or GFP from the intein and installing a carboxy-terminal azide onto the protein (Figure 3-5a). The azide-modified scFvs and GFP were subsequently reacted with dibenzocyclooctyne (DBCO)-functionalized agarose beads to immobilize the proteins via strain-promoted azide–alkyne cycloaddition (SPAAC) (Figure 3-5a). In this way,

GFP-azide protein was immobilized on the beads and yielded roughly 40-fold more GFP fluorescence than beads reacted with the control thioester functionalized GFP, indicating specific SPAAC-mediated immobilization of active GFP protein (Figure 3-5b). Similarly, immobilization and activity of 4-4-20 was confirmed by specific fluorescein binding to beads loaded with 4-4-20-azide, but not EGFR-specific scFv2-azide (Figure 3-5c). Finally, beads reacted with azide-functionalized EGFR scFvs were shown to bind their antigens from whole cell lysates that contained either wild-type EGFR or mutant EGFR vIII. ScFv2 and scFv2224 recognize epitopes conserved on both wild-type [126, 155, 156] and vIII EGFR isoforms [155], while MR1 is a vIII-specific scFv [154]. Accordingly, if beads decorated with scFv2, 2224, or MR1 were incubated with cell lysates containing the EGFR vIII mutant, they all bound EGFR vIII as expected, while the anti-fluorescein 4-4-20 scFv exhibited negligible non-specific binding to the cell lysates (Figure 3-5d). When incubated with wild-type EGFR-containing A431 cell lysates, beads loaded with scFv2-azide and 2224-azide again exhibited a clear binding signal. In contrast, beads loaded with MR1 exhibited a marked, 85% reduction in A431-derived EGFR binding signal compared to that generated from EGFR vIII cell lysates, indicating a clear preference for MR1 binding to the EGFR vIII mutant (Figure 3-5d). Taken together, each of the scFvs retained antigen-specific binding activity after being produced as secreted protein-intein fusions, EPL reaction, and SPAAC immobilization.

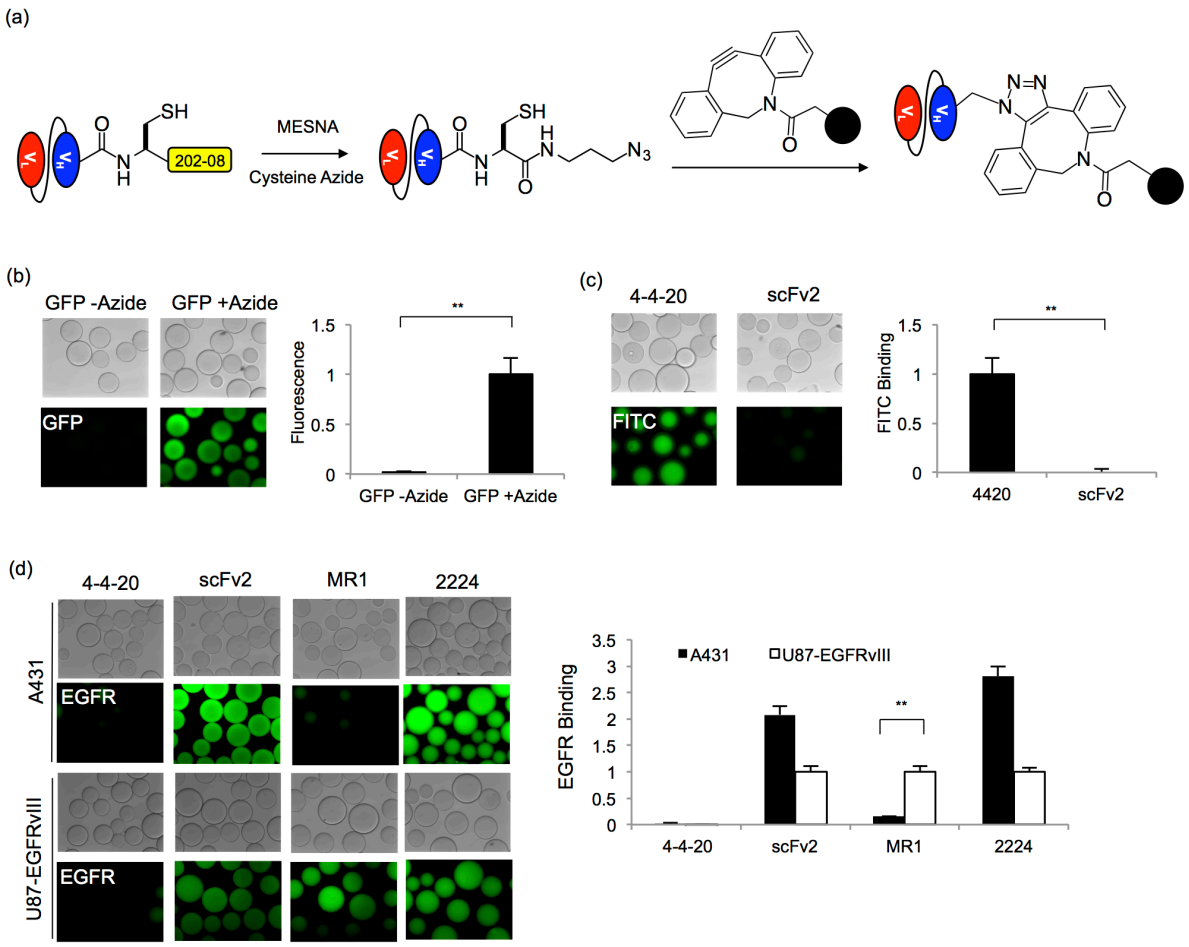

Figure 3-5: Strain-promoted click chemistry immobilization.
(a) Secreted and purified scFv and GFP proteins fused to the 202-08 intein were released with MESNA to form scFv- and GFP- thioesters. The carboxy-terminal thioesters were subsequently reacted with a cysteine azide via EPL to install an azido group onto the protein. To immobilize the proteins on surfaces, the scFv- and GFP-azide proteins were reacted with DBCO-functionalized agarose beads in a strain promoted click chemistry reaction. (b) Fluorescent microscope images of GFP fluorescence associated with beads reacted with GFP-azide or non-azido GFP (GFP-thioester). Relative protein immobilization was quantified by measuring total bead fluorescence and normalizing to the azide-GFP loaded beads. The mean ± S.D. of three independent immobilization reactions is plotted. Statistical significance was determined by an unpaired student's t-test (**, $p < 0.01$) (c) Binding of fluorescein to beads reacted with azide functionalized 4-4-20 was analyzed and compared to beads reacted azide-linked scFv2. FITC-dextran binding was quantified by measuring the fluorescence intensity of the beads, and the fluorescence was normalized to the 4-4-20-linked sample. Three independent immobilization reactions were carried out to obtain the mean ± S.D. values. An unpaired student's t-test was performed to determine statistical significance (**, $p < 0.01$) (d) Immobilized EGFR scFv activity was assessed by EGFR capture from cell lysates. Fluorescent microscopy images were employed to demonstrate EGFR capture and EGFR isoform specificity. A431 cells express wild-type EGFR while U87 cells are transfected to express the EGFR vIII isoform. ScFv activity was quantified by measuring the resulting fluorescence intensity of the beads, and the

fluorescence value was normalized to the signal originating from the U87-EGFRvIII lysate binding to the respective scFv. The fluorescence value for the negative control, 4-4-20, was normalized to the signal originating from the U87-EGFRvIII binding to MR1. The mean ± S.D. of three independent immobilization reactions is plotted. Statistical significance was determined by an unpaired student's t-test (**, $p < 0.01$)

3.4 Discussion

Producing antibodies as fusion partners to the Mxe GyrA intein enables site-specific, bioorthogonal chemical protein modification, thereby enabling antibody conjugation to desired small molecules, proteins, or surfaces. Through directed evolution, we have engineered the Mxe GyrA intein to increase the amount of scFv-intein fusion proteins displayed on the yeast surface by ~1.5- to 3- fold, thus increasing the amount of chemically functionalized protein obtained via intein-linked yeast surface display. Importantly, the engineered 202-08 intein clone was shown to be generalizable by increasing the surface display of GFP and eight different scFvs. Furthermore, we demonstrated that the engineered intein improves secretion of scFv-intein fusion proteins by ~3-30- fold over the wild-type intein. Finally, secreted scFvs could be directly modified via EPL, immobilized onto surfaces using SPAAC, and employed to bind their respective antigens.

While previous studies have employed rational design to improve Mxe GyrA production levels by reducing in vivo autocleavage [77, 81] or by reducing intein size [77] we instead employed directed evolution to achieve this goal. The surface display levels of scFv-intein fusions are generally 25-50% reduced compared to the unfused scFv, thus providing a screening pressure for improved intein clones. Although the screen employed intein fusion to the anti-fluorescein scFv, 4-4-20, intein clone 202-08

increased surface display of seven additional scFvs that exhibited a range of display levels as unfused proteins. For many different scFvs, 202-08 returned surface display of scFv-intein fusions back to unfused levels and this unfused display level appeared to be the ceiling for 4-4-20 expression, given the inability to achieve further expression increases in second round of directed evolution. However, the display levels of two of the tested proteins, GFP and 2224, fused to the 202-08 intein did exceed that of the respective unfused proteins, and the 2224 scFv had an improved EGFR specific binding capacity, indicating beneficial folding and processing effects of the intein fusion partner. These two proteins also did not demonstrate a decrease in expression upon fusion to the wild-type intein, and so the “chaperone-like” effects of the 202-08 may be limited to proteins that are better equipped to handle intein fusion. It has previously been reported that surface display levels often correlate with secretion levels [100, 110, 148, 149], and that modest elevation in surface display can lead to substantial increases in protein secretion [165]. Similarly, in this study, fairly modest display improvements produced by 202-08 resulted in substantial secretion improvements. For two of the scFvs, 4-4-20 and MR1, the 202-08 fusion increased expression 10- and 3-fold, respectively, to restore the secretion level to that of the unfused protein. Although unfused protein secretion levels were not restored for all of the tested scFvs, substantial increases in secretion were still obtained. As a result of 202-08 fusion, scFv production levels using the basal low-copy expression vector were estimated to range from 90 ug to 1.6 mg per liter of yeast culture for the antibodies tested here (6 mg/L for GFP), which is consistent with typical scFv yields in yeast [103], and greatly improves upon that for wild-type intein fusions (30 to 250 μg/L). Thus, much like the surface display levels, the 202-08 intein fusion

secretion levels tend to track reasonably well with those of the unfused proteins. These data suggest that the engineered intein should be generally compatible with fusion protein partners that are successfully produced in *Saccharomyces cerevisiae*.

Intein fusion proteins have traditionally been expressed in the cytoplasm of *E. coli*, where they are often produced as insoluble inclusion bodies, thus requiring protein solubilization and refolding in order to obtain active protein [47, 77, 80, 81, 87, 146]. In addition to requiring post-production processing to produce active intein-fusion proteins, the refolding process can result in thioester hydrolysis, thus preventing or substantially reducing subsequent EPL functionalization of the target protein [47, 87]. One possibility to circumvent refolding issues in bacteria would be targeting of fusion proteins to the periplasm, where the oxidizing environment enables the formation of disulfide bonds and can potentially provide advantages for protein folding. This approach was successful with a single-domain antibody (sdAb) fused to the Mxe GyrA intein [89], but has not yet been demonstrated for a broad panel of antibody fusion partners. In addition, since some antibodies are still expressed as unfolded aggregates in the periplasm [94, 166, 167], while others simply cannot be expressed [95, 167], periplasmic expression of antibody-intein fusions may have limitations. Thus, as an alternative, expressing scFv-intein fusion proteins in a eukaryotic organism such as yeast could be beneficial. Indeed, by employing the evolved 202-08 intein, a panel of active scFv- and GFP-intein fusion proteins could be displayed or secreted from yeast and directly functionalized via EPL without any solubilization or refolding steps. While we observed near complete release of the scFv or GFP with surface displayed intein fusion proteins, the secreted protein cleavage efficiencies ranged from 70-99%

depending upon the fusion partner. The evolved 202-08 intein did not appear to affect cleavage efficiency compared with the wild-type intein, and these cleavage efficiencies are consistent with those observed for bacterially produced proteins [38, 47, 77]. Furthermore, the release could possibly be enhanced by optimizing the carboxy-terminal residue of the target protein, which has previously been shown to impact the cleavage efficiency [38, 168]. Regardless, the small amount of uncleaved material is not chemically functionalized and would not impact many downstream applications like antibody immobilization, but the uncleaved material could be removed by depletion via histidine tag purification if desired.

The directed evolution process revealed that several different combinations of mutations led to improvements in scFv-intein surface display levels, and that no single mutation dominated either round of directed evolution (Table 3-1 and Supplemental Tables 3-2 and 3-4). Although Round 2 of directed did not produce higher expressing clones, it did, however, reveal enrichment of several residues that could be significant for improved surface display (Supplemental Table 3-4). When the enriched 202-08 mutations were combined, modest improvements in surface display were observed, indicating that the combination of the mutations found in 202-08 is essential to fully restore expression (Supplemental Figure 3-20). A large percentage of the mutations (44%) found in the Round 1 clones were within or in close proximity to the flexible loop of the Mxe GyrA intein that could not be resolved by crystallography (residues 112-129). Specifically, for 202-08, two of its eight mutations (F117L, F124L) fell within the flexible loop, while three other mutations occurred near the amino-terminus of the loop (I105V, R107C, F110S) (Figure 3-2c). Thus, it appears that modifications in and around the

flexible loop may be key to improving fusion protein expression. This finding is also supported by a recent study where a smaller Mxe GyrA intein was created by deleting residues 107-160 (including the flexible loop) and replacing the deletion with a short glycine-serine linker. This smaller intein variant led to a 1.2-fold increase in intein-peptide fusion production in *E. coli* [77].

The secreted, EPL-functionalized scFvs and GFP were shown to be compatible with strain-promoted click chemistry, thus demonstrating the utility of intein fusion protein production in yeast. A carboxy-terminal azide was installed via EPL, and using SPAAC, active scFv and GFP were site-specifically immobilized on beads decorated with a strained alkyne. Previously we had demonstrated the compatibility of yeast displayed scFv-intein fusions with one of the most widely used forms of click chemistry, copper(I)-catalyzed azide–alkyne cycloaddition (CuAAC) [145, 169]. CuAAC requires the addition of copper, a reducing reagent, and a stabilizing ligand. In contrast, SPAAC enables the direct immobilization of azide-conjugated proteins without a copper catalyst, reducing reagent, or stabilizing ligand. Not only does SPAAC simplify the conjugation process, but it also prevents issues associated the copper catalyst, such as protein precipitation [23, 31, 61] and toxicity [60, 63]. Thus, the ability to employ these scFvs in SPAAC reactions offers many potential applications such as the generation of antibody-drug conjugates [170, 171] and targeted nanoparticles [172, 173]. In conclusion, directed evolution of the Mxe GyrA intein has permitted the extension of EPL and click chemistry modification techniques to scFvs secreted from yeast, thereby providing a viable alternative to bacterial expression systems and a facile method to chemically functionalize antibodies and other proteins.

3.5 Supplemental Figures

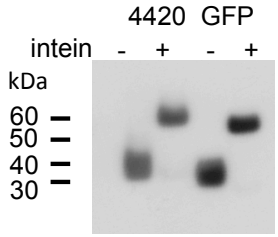

Figure 3-6: YVH10 yeast cell lysis
YVH10 expressing soluble 4-4-20 and GFP as either unfused or wild-type intein fusion proteins were lysed to evaluate *in vivo* autocleavage of the intein. The intracellular contents were analyzed with an anti-FLAG Western blot to demonstrate the intein fusion was intact, thus indicating that *in vivo* autocleavage is not responsible for the decrease in expression of the scFv-intein fusion protein.

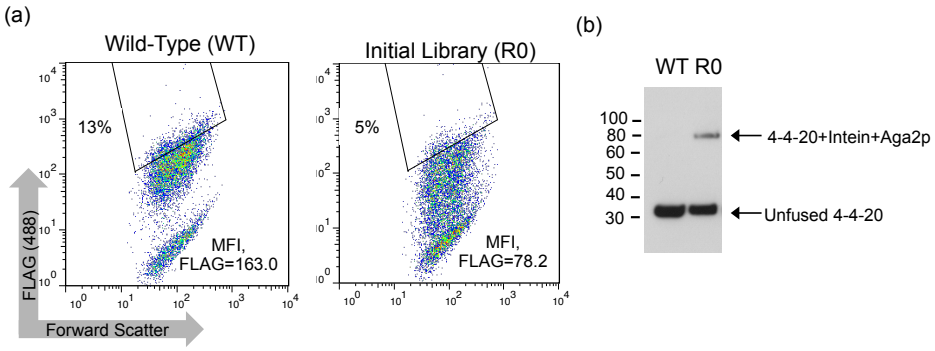

Figure 3-7: Analysis of initial library for directed evolution Round 1
(a) Flow cytometry dot plots compare the surface display level of wild-type intein and the initial intein library fused to 4-4-20. The initial library (R0) demonstrated a decrease in full-length construct expression (FLAG) compared to the wild-type intein (10,000 clones shown). (b) 4-4-20 was released from yeast displaying the wild-type intein construct or R0 library with MESNA. After deglycosylating the released proteins, an anti-FLAG Western blot demonstrated that a large portion of the R0 library contained active intein.

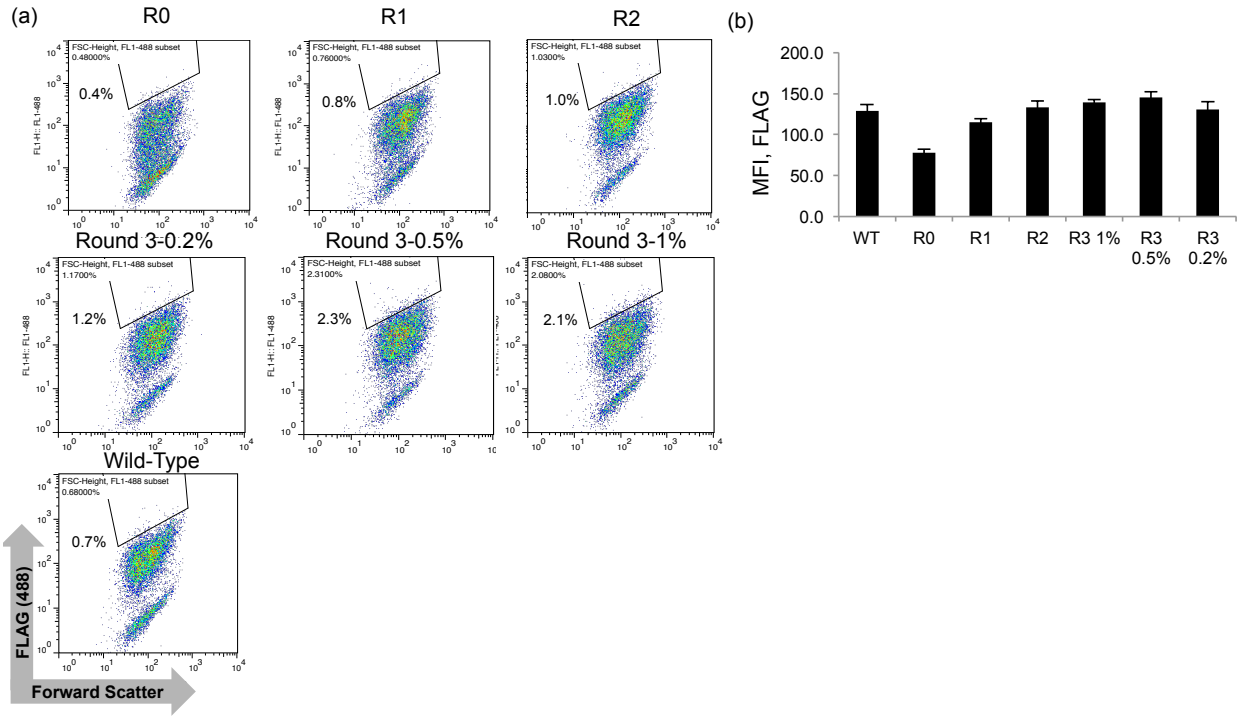

Figure 3-8: Direct evolution Round 1, FACS enrichment Rounds 1-3
(a) Flow cytometry dot plots illustrate an improvement in 4-4-20-intein construct expression over the first three rounds of FACS (10,000 events shown). An example sort gate is drawn to emphasize enrichment over the rounds. For the first three rounds of FACS, yeast were sorted for improved expression by labeling with Alexa 488. The Round 3 pools were obtained by applying more/less stringent sort gates, with the percentage representing the sort gate (i.e. 0.2% indicates the top 0.2% were selected). The Round 3-0.5% pool was continued to the next round (b) The geometric mean fluorescence from each pool was quantified to demonstrate an improvement in the average construct expression of the population. For wild-type intein, the mean ± SD for three independent yeast transformants are plotted, and for the yeast pools, the mean ± SD represents three independent labeling experiments of 10,000 clones.

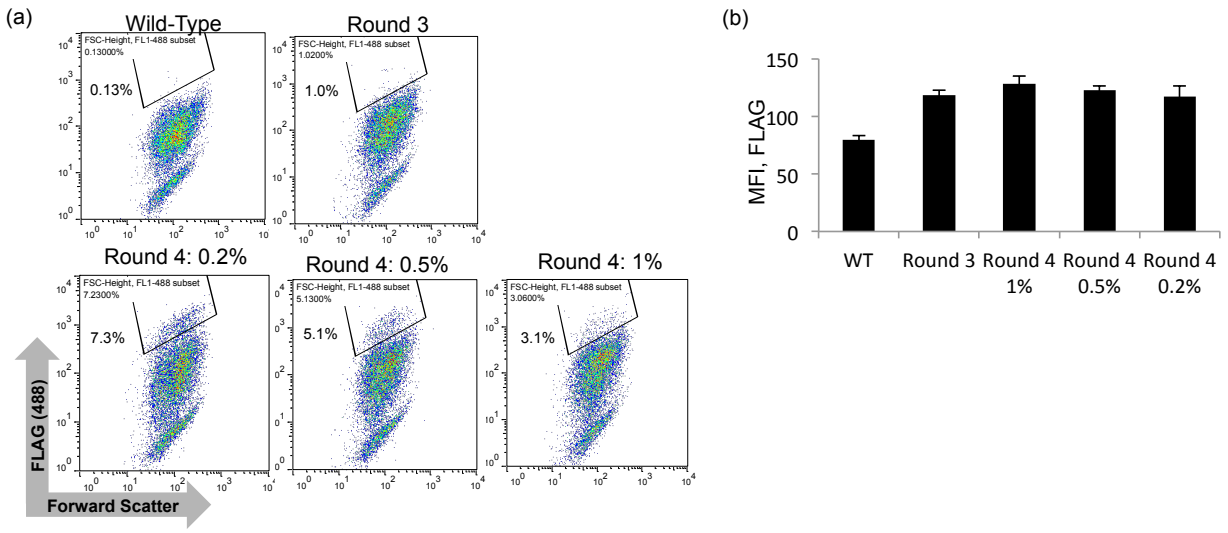

Figure 3-9: Direct evolution Round 1, FACS enrichment Round 4
(a) For round 4 of FACS, yeast were sorted for improved full-length construct expression by labeling with PE. Dot plots displaying 10,000 events represent an improvement in construct expression compared to the wild-type intein and round 3. An example sort gate is drawn to show enrichment of the population. The different pools from Round 4 were obtained by selecting the indicated top percentage of yeast. The Round 4-0.2% and Round 4-0.5% pools were continued to the next round of sorting. (b) The geometric mean fluorescence from each pool was quantified to demonstrate an improvement in the average number of constructs per yeast. The mean ± SD represents three independent yeast colonies for the wild-type construct, while the mean and ±SD for the pools represents three independent labeling experiments of 10,000 clones.

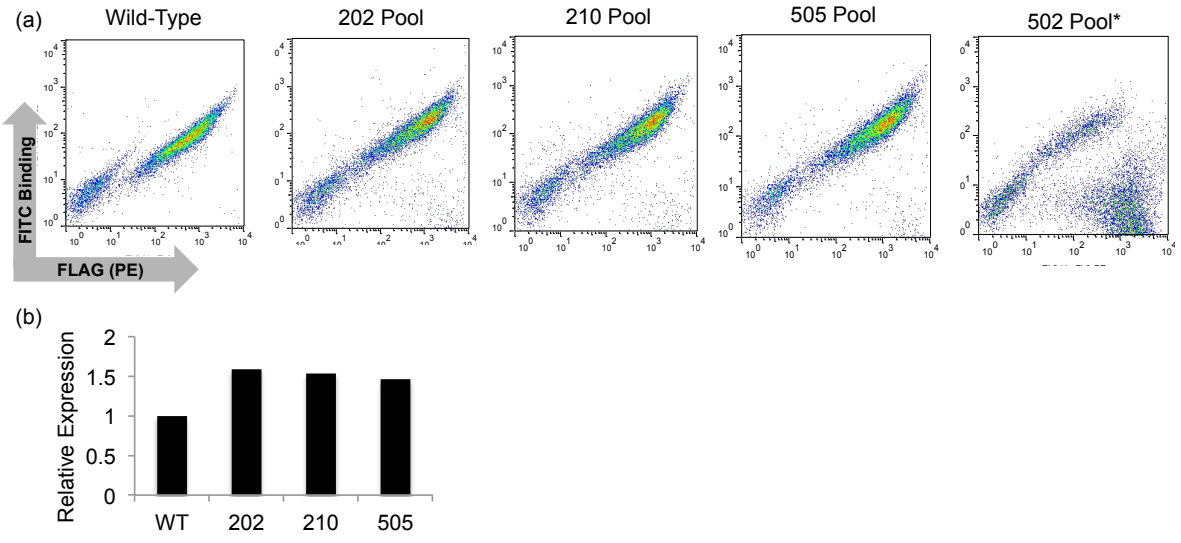

Figure 3-10: Direct evolution Round 1, FACS enrichment Round 5

(a) For FACS Round 5, yeast were selected both for high construct expression (PE) and 4-4-20 activity (FITC labeling), with the exception of the 502 pool, which was selected only based upon construct expression. The different pools were obtained by applying more/less stringent sort gates in Round 5. Dot plots displaying 10,000 events show an increase in expression and FITC binding over the wild-type intein for the 202, 210, and 505 pools, but the 502 pool demonstrated poor FITC binding, indicating that the dual label for 4-4-20 activity was critical for Round 5. (b) The geometric means of the pools (10,000 events) were quantified and normalized to the wild-type intein, thus demonstrating an ~1.5-1.7 fold improvement in construct expression.

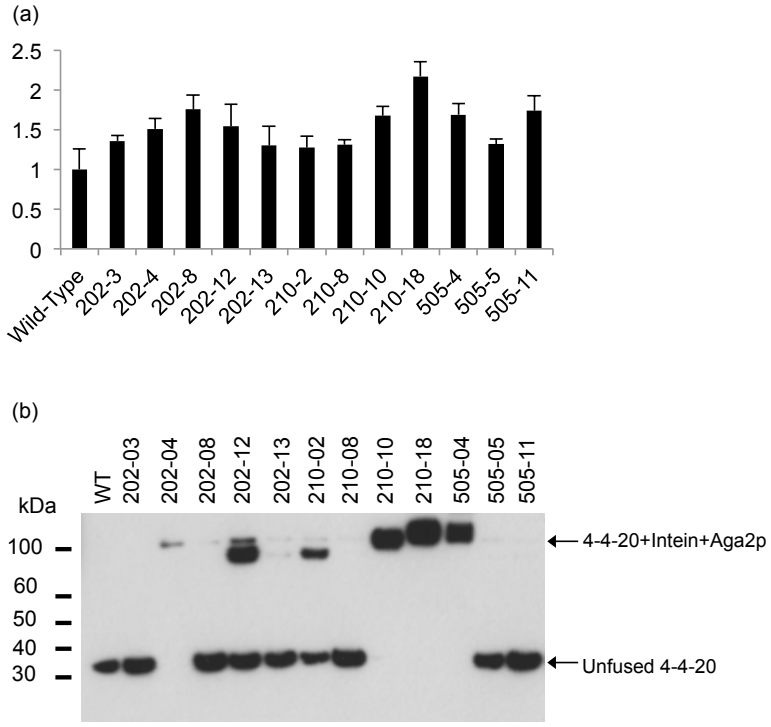

Figure 3-11: Surface displayed clones from directed evolution Round 1
(a) Twelve clones from the final pools demonstrated significant construct expression improvements compared to the wild-type intein. Using flow cytometry, the geometric mean fluorescence of the FLAG-positive populations was quantified and normalized to the wild-type intein, thus revealing a range of expression improvements. Plotted are the mean ±SD results from three independent yeast colonies. (b) Yeast displaying the intein fusion proteins were reacted with MESNA to release 4-4-20 from the display construct. Since Aga2p contains glycans that can make it difficult to detect on a Western blot, the release proteins were deglycosylated prior to analysis. Anti-FLAG Western blotting demonstrated that while some intein clones did not cleave the 4-4-20, several of the clones fully release 4-4-20 from the yeast display construct.

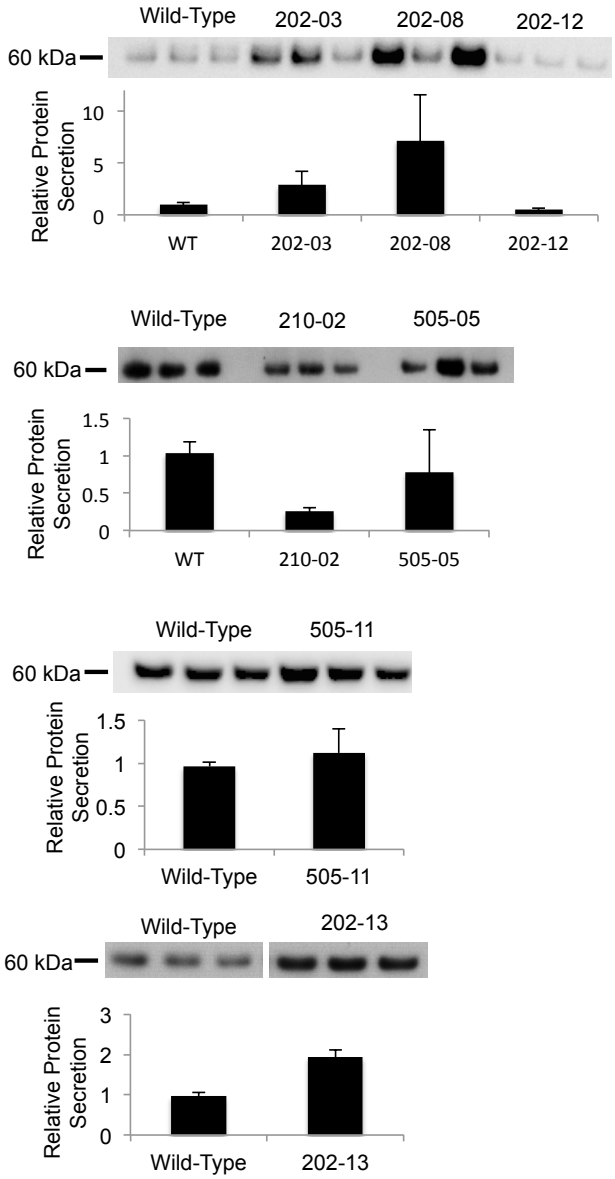

Figure 3-12: Secretion of directed evolution Round 1 clones
Anti-FLAG quantitative Western blots compare the protein secretion levels of 4-4-20 intein fusion proteins for seven intein clones. Relative secretion amounts are normalized to the wild-type intein construct, and the mean ±SD results from three independent yeast colonies. While some clones exhibit modest improvements in secretion (~2-3 fold), 202-08 exhibited nearly 10-fold improvement (experiments with more consistent 202-08 production levels appear elsewhere in the text).

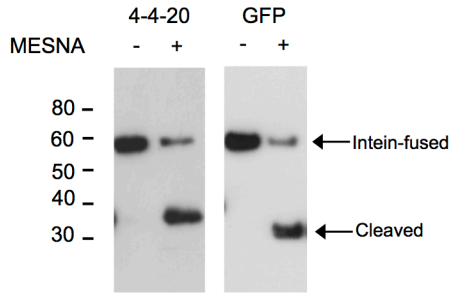

Figure 3-13: MESNA release of 4-4-20 and GFP with the wild-type intein.
The catalytic activity of the wild-type intein was examined by reacting secreted 4-4-20 and GFP with MESNA for 20 h. Anti-FLAG Western blotting demonstrates ~75% release for both 4-4-20 and GFP in the presence of MESNA.

		4	7	10	12	13	15	18	20	21	22	23	25	28	29	31	33	34	35	36	38	43	45	47	50	51	52	53	55	56	59	61	64	67	74	75	76	77	78	80
WT	#	G	L	L	E	G	S	I	D	I	V	P	A	N	S	N	I	D	L	K	L	N	V	A	L	F	H	S	E	H	Y	V	V	L	N	H	P	L	L	L
202-03	4																																		D					
202-04	34								G	T							T		P							S				Y			R					S	S
202-08	8																									L														
202-12	4																T								P														
202-13	5									T																S														
210-02	7																	G								L														
210-08	13										A																			Y										
210-10	33		P					T				L		D		D	T			R		D				L	R	F			C					R				S
210-18	55	E		P	G	S	P	V		P			T		G		T	N			P		T	V		S			G		A	A	P				S		
505-04	35							T	N					S									A							C				S		S	P		S
505-05	3									T																														
505-11	3																																							

		82	83	86	88	89	92	93	94	95	97	98	99	100	101	102	105	106	107	108	110	111	112	114	115	117	118	119	121	122	124	125	126	127	129	130	131	133	136	137	138
WT		D	V	V	T	L	K	L	I	D	I	K	P	G	D	Y	I	Q	R	S	F	S	V	C	G	F	A	R	K	P	F	A	P	T	Y	T	V	V	L	V	R
202-03																								R	A																	
202-04							E	P	T	S											S	N			T			R									A		P			
202-08																V		C			S					L				L											
202-12																							A		C																
202-13																								G		T															
210-02																								Y					G												
210-08																						G						C		S									A	H
210-10			A			P	E				T				G			R		N	S					S				S						A		P	M	
210-18				M	A		E		A		T	R	L	D		C			H						T	P			L	S			M	C	A			P	A	
505-04		N	A			P			V							H			H	G	L				R						T	S					A	S		C
505-05																									R																
505-11																															C										

		139	140	143	144	145	146	151	154	155	158	159	160	161	162	163	164	165	166	167	168	169	170	172	174	176	177	178	179	180	182	184	185	189	190	191	192	194	197	198	
WT		F	L	H	H	R	D	A	D	E	D	G	R	F	Y	Y	A	K	V	A	S	V	T	A	V	P	V	Y	S	L	T	T	A	F	I	T	N	F	H	A	
202-03					R						G																															
202-04		S		R					G					L		C				V		A		T			A		G	P		A				M	G		R			
202-08																					G														T							
202-12																																										
202-13													Q																													
210-02															C																			L		M						
210-08		S								G	A																		N			V			A						
210-10							G	V										E													A			T			R				
210-18		S	V			Q			K		E		S		C			E	A			A	I		L	A			P		V						P		T		
505-04		L						V	N						C	T	E	A			A			A			G			V	S			V							
505-05																																		V							
505-11																	P																		M							

Table 3-2: Full list of clonal mutations from directed evolution Round 1

.

Residue	21	33	50	51	74	105	107	110	112	114	117	118	124	129	144	158	160	164	168	190	191
Wild-type	I	I	L	F	N	I	R	F	V	C	F	A	F	Y	H	D	R	A	S	I	T
Shuffle	T	T	P	S/L	D	V	C	S	A	R/G	C/L	T	L	C	R	G	Q	P	G	V/T	M
% Mutated[a]	38%	27%	46%	35%	49%	19%	5%	32%	49%	49%	22%	27%	22%	49%	22%	11%	46%	30%	14%	8%	14%

Table 3-3: Sequence analysis of the shuffled intein library
(a) Presented is the occurrence of mutation (%) at each shuffled residue for the library.

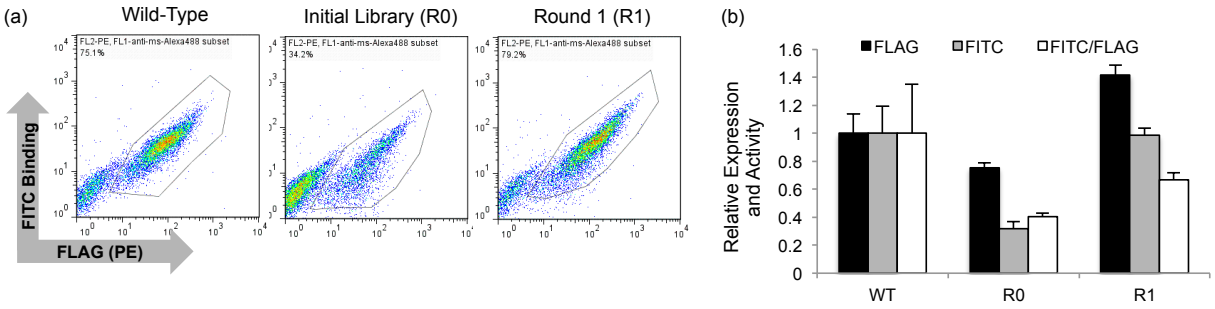

Figure 3-14: Directed evolution Round 2, FACS enrichment Round 1
(a) Flow cytometry analysis was performed to characterize the initial library (R0) and the Round 1 pool (R1). Dot plots represent full-length construct expression (FLAG) and 4-4-20 activity (FITC binding). The R1 pool was obtained by selecting for both high construct expression and 4-4-20 activity. (b) In the accompanying bar graph, the geometric mean fluorescence is quantified and normalized to the wild-type intein construct. Plotted are the mean ±SD from three independent yeast colonies for the wild-type intein, while the mean ±SD for R0 and R1 represents three independent labeling experiments of 10,000 clones. Both construct expression and 4-4-20 activity is diminished in the initial library (R0), but substantial improvements are obtained in the first round of FACS (R1) by selecting for clones with high FLAG expression and 4-4-20 activity.

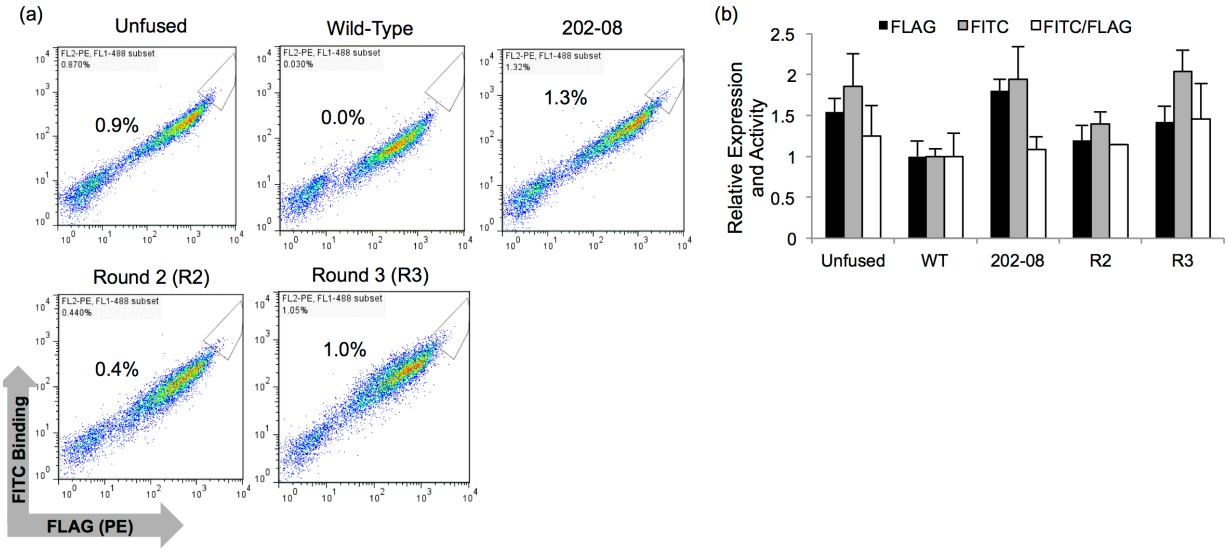

Figure 3-15: Directed evolution Round 2, FACS enrichment Rounds 2 and 3
(a) Flow cytometry dot plots represent construct expression and 4-4-20 activity for Round 2 (R2) and Round 3 (R3) of FACS (10,000 events shown). Round 2 (R2) and Round 3 (R3) were performed by selecting clones with high expression and 4-4-20 activity. These sorting pools are compared to the unfused, wild-type, and 202-08 constructs, and a sample sort gate is drawn to illustrate enrichment of expression and activity. (b) The geometric mean fluorescence intensity was quantified and normalized to the wild-type intein construct. The mean ±SD is presented in the bar graph and represents either three independent yeast colonies or three independent labeling experiments of 10,000 clones.

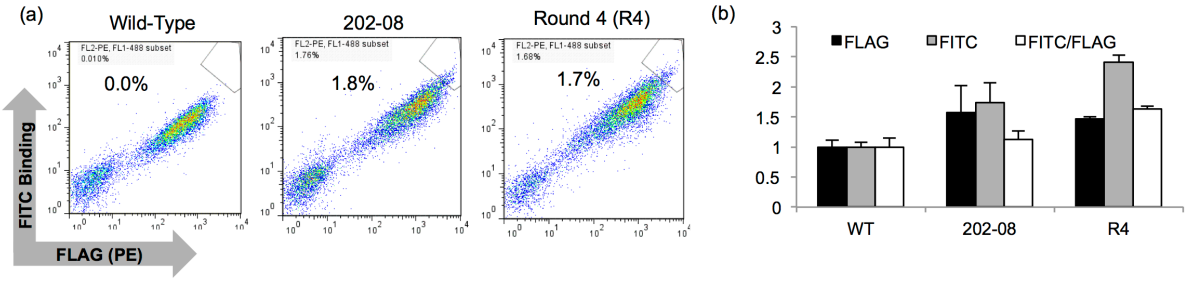

Figure 3-16: Directed evolution Round 2, FACS enrichment Round 4
(a) For FACS Round 4, yeast were sorted for high construct expression and 4-4-20 activity. Flow cytometry dot plots represent expression and activity for 10,000 events of the Round 4 (R4) selected pool. A sample sort gate is drawn to illustrate population differences between the wild-type intein construct and R4. (b) The geometric mean fluorescence was quantified and normalized to the wild-type intein construct. The mean ± SD represents three independent yeast colonies for the wild-type and 202-08 constructs, while the mean ±SD for the R4 pool represents three independent labeling experiments of 10,000 clones.

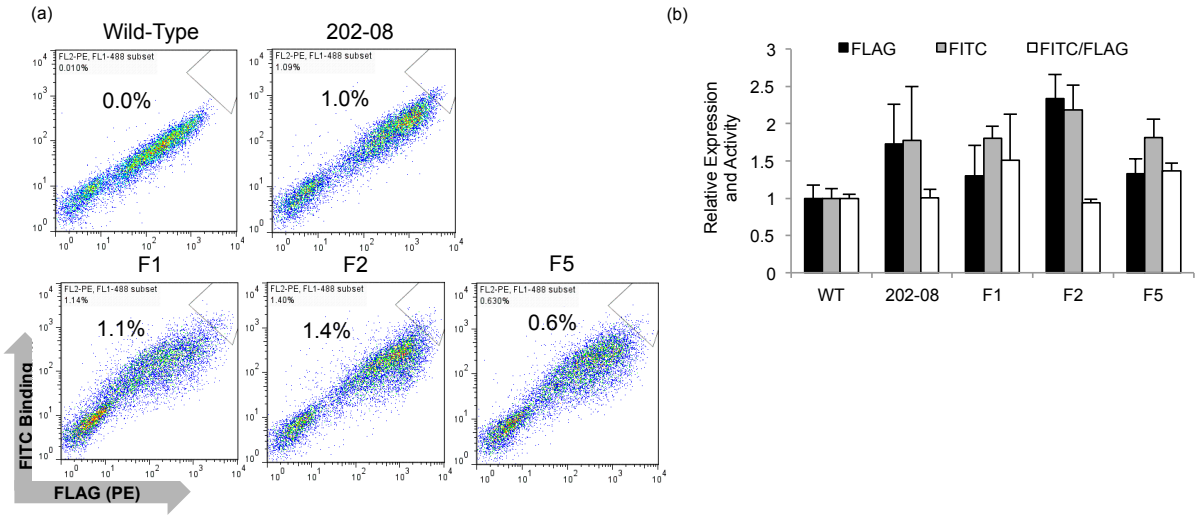

Figure 3-17: Directed evolution Round 2, FACS enrichment Round 5
(a) Flow cytometry dot plots represent construct expression and 4-4-20 activity for the final, Round 5 pools (F1, F2, F5). Screening was performed to select for high expression and 4-4-20 activity with varying degrees of gate stringency among the three pools. A sample sort gate shows improvement of the pools compared to the wild-type intein. (b) The geometric mean fluorescence was quantified and is displayed in the accompanying bar graph. For the wild-type and 202-08 intein constructs, the mean ± SD for three independent yeast transformants are plotted, and for the yeast pools, the mean ± SD represents three independent labeling experiments of 10,000 events. Although the final pools demonstrate an improvement over the wild-type intein, the expression means are similar to that of 202-08.

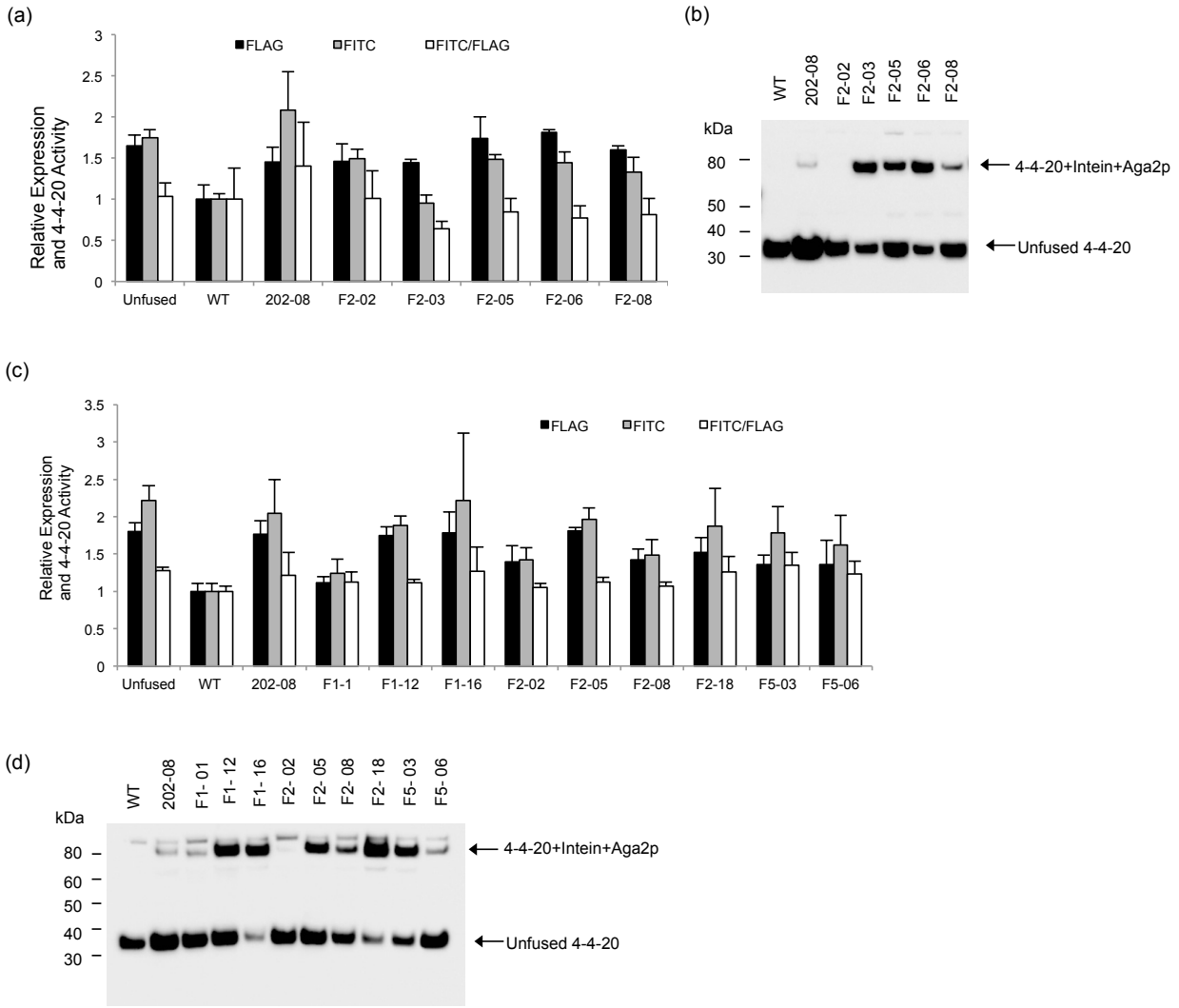

Figure 3-18: Surface displayed clones, directed evolution Round 2
(a) Construct expression and 4-4-20 activity for clones from the F2 pool were analyzed by measuring the geometric mean fluorescence with flow cytometry. Plotted in the graph are the mean ± SD for three independent yeast transformants. The clones were compared to the unfused 4-4-20, the wild-type intein fusion, and the 202-08 fusion constructs. Although the clones retained 4-4-20 activity and demonstrated expression improvements over the wild-type 4-4-20, their expression was near that of the unfused and 202-08 constructs. (b) Intein activity of the F2 clones was assessed by reacting yeast displaying intein fusion proteins with MESNA. Proteins were deglycosylated to remove Aga2p glycans prior to anti-FLAG Western blotting. Only F2-02 demonstrated complete release of 4-4-20 from the intein, while the remaining clones partially released 4-4-20. (c) Clones from the F1 and F5 pools were analyzed with flow cytometry as described in (a), and in addition to comparison with unfused 4-4-20, the wild-type intein fusion, and the 202-08 intein fusion, they were also compared to several of the F2 clones. Again, expression levels were improved over the wild-type intein, but the clones demonstrated similar expression levels to that of the unfused 4-4-20 or the 202-08 intein fusion. (d) Yeast displaying 4-4-20 intein fusion proteins were reacted with MESNA, and the released products

were deglycosylated and analyzed with anti-FLAG Western blotting. Only F1-01 and F2-02 completely release 4-4-20, while the remaining clones show varying degrees of intein activity.

Amino Acid	21	33	50	51	74	105	107	110	112	114	117	118	124	129	144	158	160	164	168	190	191	Fold Increase[a]	Statistical Significance[b]
WT	I	I	L	F	N	I	R	F	V	C	F	A	F	Y	H	D	R	A	S	I	T	1.0±.1	
F1-01									A	R		T		C	R							1.1±.1	NS
F1-12		T			D					R							Q					1.8±.1	**
F1-16				S					A				L	C							M	1.8±.3	**
F2-02									A	R		T			R				G			1.4±.2	NS
F2-05	T			S						G	L						Q					1.8±.2	**
F2-08				S				S	A	G		T					Q		G			1.4±.1	*
F2-18		T	P	L						H	L	T					Q					1.5±.2	*
F5-03				L	D			S		R	L		L									1.4±.1	*
F5-06							C	S		G		T		C	R	G	Q					1.4±.3	NS
Round 2 Fold Enrichment [c]	0.5	0.5	0.1	1.2	1.1	0.4	1.3	1.1	0.6	0.9	0.8	1.1	1.3	0.6	0.7	1.3	0.7	0.0	1.1	0.7	0.4		

Table 3-4: Intein mutations and surface display levels for directed evolution Round 2.
(a) Fold increase relative to the wild-type intein as fusions to 4-4-20, mean ± S.D from three independent yeast colonies. (b) Statistcal analysis was perfomed by an unpaired student's t-test, with double asterisks representing $p < 0.01$, single asterisks representing $p < 0.05$, and NS designating that differences are non-significant ($p > 0.05$). (c) The Round 2 fold enrichment which calculates the occurrence of mutation at each residue compared to the shuffled library (final pool/shuffled library).

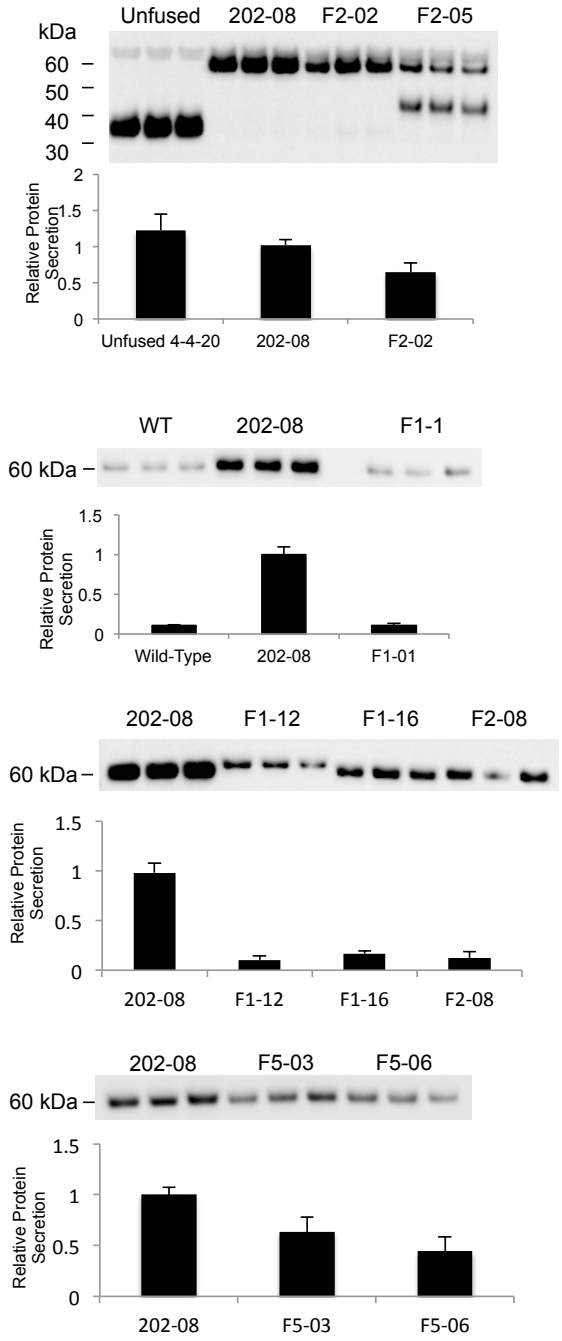

Figure 3-19: Secretion of directed evolution Round 2 clones
Anti-FLAG quantitative Western blots compare the protein secretion levels of the directed evolution 2 clones as 4-4-20 fusion proteins. The relative expression levels are normalized to the 202-08 intein construct, and the mean ±SD results from three independent yeast colonies. While some clones exhibited expression levels near that of 202-08 (F2-02, F5-03, F5-06), none exceeded 202-08 expression levels. Other clones, (F1-01, F2-12, F1-16, F2-08) had substantially reduced expression levels compared to 202-08, while F5-05 expression was not quantified because it appear to exhibit an odd autosplicing pattern.

(a)

Amino Acid	51	105	107	110	117	124	168	190
Wild-Type	F	I	R	F	F	F	S	I
202-08	L	V	C	S	L	L	G	T
4M	L		C	S		L		
5M	L		C	S		L	G	

(b)

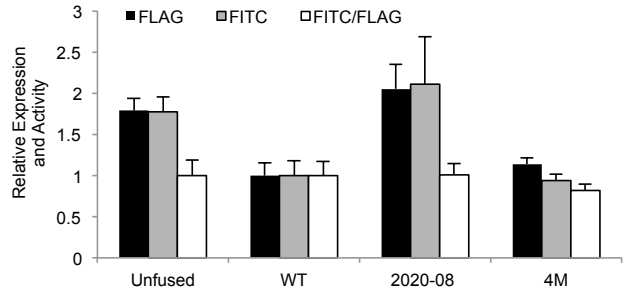

(c)

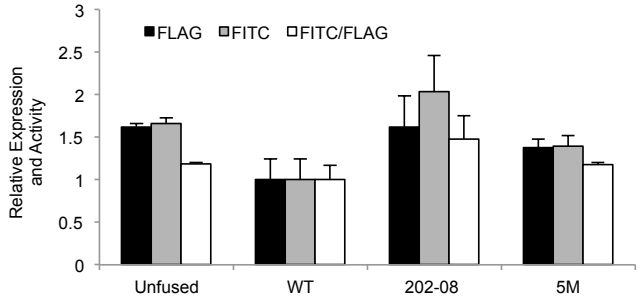

Figure 3-20: Analysis of enriched 202-08 residues
(a) 202-08 residues enriched in the directed evolution round 2 were combined to create two different mutants, 4M and 5M, and the mutations are listed in the table. 5M is identical to 4M, except that it contains one additional mutation (S168G). (b) Flow cytometry analysis of the 4M clone fused to 4-4-20 shows a modest improvement over the wild-type intein (~1.1-fold), but it does not attain the expression level of 202-08. (c) The 5M clone shows greater improvements over the wild-type intein (~1.3-fold), but, again, the expression level is less than that of 202-08. The relative expression and 4-4-20 activity levels are normalized to the wild-type intein, and plotter are the mean ±SD from three independent yeast colonies.

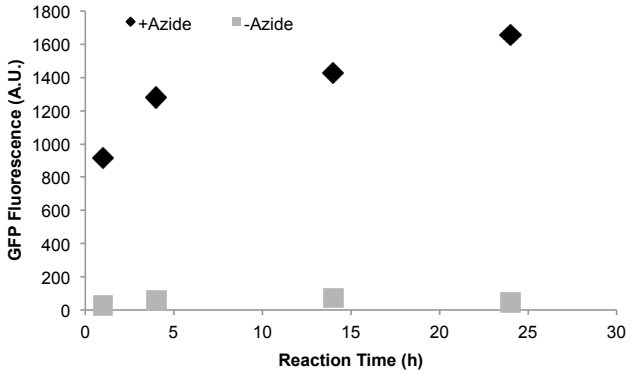

Figure 3-21: Time course reaction for GFP-azide immobilization.
(a) GFP-azide was reacted with DBCO agarose beads for 1, 4, 14, and 24 h, and GFP immobilization was measured by quantifying bead fluorescence at each time point. Although immobilization increased with reaction time, substantial GFP immobilization was observed after just 1 h (>50%), indicating that shorter reaction times are sufficient for the SPAAC-mediated immobilization. GFP-thioester was used as a non-alkyne control to demonstrate a low level of nonspecific GFP binding.

Chapter 4 – Characterization of EGFR-Specific Antibodies for Liquid Crystal Assay Development

In this chapter, we further characterize two of the anti-EGFR scFvs (scFv2 and MR1) that were introduced in the previous chapters. The goal of this work was to establish EGFR binding capabilities and specificities in order to employ the antibodies in a liquid crystal-based detection assay that is being developed by the Abbott group (Department of Chemical and Biological Engineering, University of Wisconsin-Madison). Since most of this work was completed prior to the acquisition of 2224, it does not include characterization of this antibody.

4.1 Introduction

The epidermal growth factor receptor (EGFR) is a transmembrane receptor tyrosine kinase that is known to be an important biomarker and predicative of disease state. While normally functioning EGFR regulates cellular responses such as cell division, proliferation, and differentiation [174, 175], over-activation of EGFR provides continuous signals for cell proliferation, angiogenesis, metastasis, and inhibition of apoptosis, and these signals can result in the transformation of cells from normal to cancerous [176]. This over-activation of EGFR can result from receptor overexpression or mutation, and, for cancer patients, these alterations have been shown to be indicative of a particularly poor prognosis, advanced disease progression, and resistance to

standard methods of treatment [177, 178]. Hence, EGFR is of high interest both as a therapeutic target and as a diagnostic biomarker.

Recognizing that EGFR alterations are implicated in some cancers, researchers have sought to inhibit EGFR function through targeted therapies to treat the disease. One common EGFR alteration is a deletion in the intracellular kinase domain at residues E746-A750, known as ΔELREA mutant (Figure 4-1) [179-185]. This mutation is most often found in non-small cell lung carcinomas (NSCLC), and patients with the ΔELREA mutant respond to tyrosine kinase inhibitor (TKI) drugs that block EGFR signaling [186-188]. Another mutant, EGFRvIII, contains a large deletion in the ligand binding domain of EGFR and an insertion of a glycine residue (Figure 4-1) [189, 190], and, along with the overexpression of wild-type EGFR, it is implicated in glioblastoma multiforme (GBM), an extremely aggressive brain tumor [191-193]. Clinical trials are currently underway to evaluate an EGFRvIII vaccine, CDX-110, which, thus far, has been shown to elicit an immune response against EGFRvIII by the patients [194].

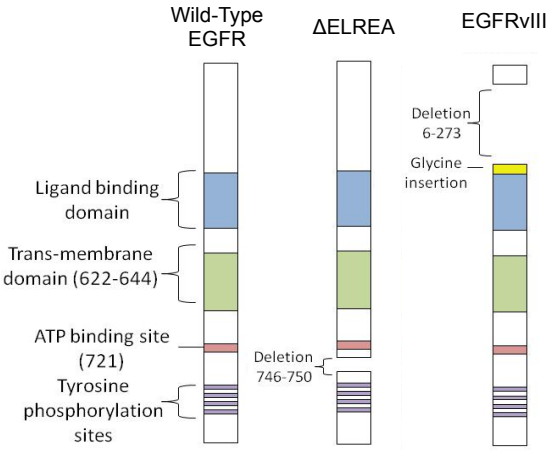

Figure 4-1: EGFR mutants
EGFR is a receptor tyrosine kinase that contains an extracellular ligand binding domain, a transmembrane domain, and an intracellular kinase domain with tyrosine phosphorylation sites.

The ΔELREA mutant has a 5-amino acid deletion in the intracellular domain near the ATP binding site that causes the receptor to become constituently active. The EGFRvIII mutant contains a large deletion in the extracellular domain and insertion of a glycine residue that causes ligand-independent phosphorylation of the intracellular kinase domain, thus constantly stimulating downstream signaling pathways.

While the current methods to detect the aforementioned EGFR mutants are DNA-based [195-197], it is recognized that antibody-based tools for protein analysis, such as antibody microarrays or other miniaturized biosensors, could construct better diagnostic methods by providing high-throughput detection capabilities and more direct readouts of disease state. DNA techniques currently employed to identify protein mutation and overexpression, such as sequencing and fluorescence *in situ* hybridization (FISH) [195-197], are laborious and time consuming, making it difficult to apply these methods for universal screening. Another disadvantage of DNA analysis is that is unable to detect post-translational modification of proteins, such as phosphorylation, that can be a critical signal of disease progression and therapeutic response [15]. Furthermore, DNA and mRNA levels often don't correlate to protein abundance [198, 199], which, particularly in the case of EGFR overexpression, can be a strong indicator of disease state [200, 201]. In contrast, antibodies are capable of recognizing different protein isoforms [202], mutations [203, 204], and post-translational modifications [205], and antibody-based assays have been employed to measure protein expression levels [206]. Therefore, it is thought that direct protein analysis through antibody-based assays could be the future of disease diagnostics [207, 208].

Recently, the Abbott group at UW-Madison has demonstrated that liquid crystals (LCs) are capable of reporting molecular-level events at surfaces, and they have shown promise to become highly sensitive detection devices of biomarkers [209, 210]. LCs are

able to detect the antibody-mediated capture of proteins and biomolecules at surfaces, thus providing a facile and sensitive readout of biomarker presence [210, 211]. The generation, characterization, and surface immobilization of binding molecules (i.e. antibodies) that can selectively identify these biomarkers from complex cell sources, therefore, is highly critical to developing LC protein assays.

We previously demonstrated that our intein-linked yeast display platform could be employed to express, chemically modify, and site-specifically immobilize single-chain antibodies (scFvs), thus generating detection surfaces decorated with scFvs capable of binding their antigenic targets (Chapter 2). These methods could potentially be combined with highly sensitive LC detection techniques to produce a biomarker detection assay. Here, we further characterize two yeast displayed EGFR-specific scFvs: scFv2, which binds the intracellular kinase domain of EGFR [126], and MR1, an EGFRvIII-mutant specific antibody [203]. While typical yeast display analysis requires antigens to be purified and soluble, we employ a recently developed technique called yeast display immunoprecipitation (YDIP) [161] in order to evaluate binding of the scFvs to EGFR present in whole cell lysates. Since an LC-based assay will require the ability of antibodies to bind antigen from complex cell samples containing sources of non-specific interactions, such as detergents, micelles, and other proteins, YDIP will permit preliminary scFv analysis and characterization regarding their applicability in an LC assay.

4.2 Materials and Methods

4.2.1 EGFR cell lines

The A431, U87-EGFRvIII, and B82L-ΔELREA cell lines were a generous gift from Greg Wiepz and the Bertics laboratory (UW Department of Biomolecular Chemistry). Cells were maintained in Dulbecco's Modified Eagle Media (DMEM, Life Technologies) supplemented with 10% Cosmic Calf Serum (Thermo–Fisher) and 1x antibiotic/antimycotic (PSA, Gibco) at 37°C and 5% CO_2. For the U87-EGFRvIII cells, the media was supplemented with 200 µg/mL G418 (Life Technologies) to maintain transfection of EGFRvIII. Methotrexate (ThermoFisher, 10 µM) was added to the B87L-ΔELREA media to maintain ΔELREA transfection. When indicated, EGFR phosphorylation was stimulated by washing the cells once with PBS and adding epidermal growth factor (EGF, 10 nM) in 10 mM HEPES buffer for 10 min at 37°C. EGF-stimulated cells were subsequently washed once with PBS and immediately used to create cell lysate.

4.2.3 Creation of cell lysate

Cells were grown to ~90% confluence in 75 cm^2 tissue culture-treated T-flasks and washed three times with PBS prior to lysis. To lyse the cells, 1 mL of ice-cold lysis buffer, consisting of 1% v/v Triton X-100 (Thermo–Fisher), 2 mM EDTA, and 1X cOmplete Protease Inhibitor Cocktail (Roche) was added to flask, and the cells were scraped from the flask with a cell scraper at 4°C. The lysate was collected in a 1.5 mL microfuge tube and was incubated at 4°C with gentle rotation for 15 min. The lysate was subsequently centrifuged for 30 min at 4°C to remove any insoluble cell debris. To

biotinylate the cell surface proteins, prior to lysis, cells were washed three times with PBS and incubated with 0.5 mg/mL sulfo-NHS-LC-Biotin (Pierce) in PBSCM (PBS plus 1 mM $CaCl_2$, 0.5 mM Mg_2SO_4) for 30 min with gentle rocking at room temperature. The cells were again washed three times with PBS and then lysed as described above.

4.2.4 Yeast Display Immunoprecipitation

EBY100 yeast were grown and surface display was induced as detailed in 2.2.2. For flow cytometry analysis, $2x10^6$ yeast were washed with 500 µl PBS-BSA and incubated with either 100 µl cell lysate or 100 µl human EGFR (4 µg/mL in PBS-BSA) for 1 h at 4°C with gentle rotation. Yeast were subsequently washed with 500 µl cell lysis buffer, and the following immunolabeling steps were performed at 4°C. To detect EGFR binding, yeast were incubated with anti-EGFR mouse antibody cocktail Ab-12 (Lab Vision Corporation, diluted 1:200 in PBS-BSA) for 30 min, followed by washing once with 500 µl PBS-BSA, and incubating with anti-mouse 488 (Life Technologies, diluted 1:500 in PBS-BSA) for 30 minutes. Yeast were washed one final time with 500 µl PBS-BSA before analysis. To detect binding of phosphorylated EGFR, yeast were incubated with either rabbit anti-EGFR pY1068 (Cell Signaling, diluted 1:400 in PBS) or anti-EGFR pY1173 (Invitrogen, diluted 1:400 in PBS) for 30 min, followed by washing once with 500 µl PBS-BSA. Yeast were subsequently labeled with anti-rabbit PE (Sigma–Aldrich, diluted 1:40 in PBS-BSA) and washed with 500 µl PBS-BSA prior to analysis. The fluorescence of the immunolabeled cells was measured using a FACSCalibur flow cytometer (Becton Dickinson).

For elution of EGFR from the yeast surface, $2x10^8$ induced yeast were divided into three tubes and incubated with 300 µl cell lysate for 1 h at 4°C with gentle rotation.

Yeast were washed three times by adding 500 µl lysis buffer, vortexing, and incubating at 4°C for ten minutes. Proteins were serially eluted from the yeast surface by the addition of 50 µl 0.2 M glycine-HCl solution (pH 2.0) buffer with a 10 min incubation per tube.

4.2.5 SDS-PAGE and Western blotting

Eluted protein samples were resolved on 8% w/v SDS-PAGE gels under reducing conditions, and the proteins were transferred to a nitrocellulose membrane for Western blot analysis. To detect the presence of EGFR, membranes were probed with anti-EGFR rabbit polyclonal antibody SC-03 (Santa Cruz biotech, 1:1000 dilution), followed by anti-rabbit HRP conjugate (Sigma–Aldrich, diluted 1:2000). The presence of biotinylated proteins was detected by probing the membranes with anti-biotin mouse monoclonal antibody Ab-2 clone BTN.4 (Lab Vision Corporation, diluted 1:500) followed by anti-mouse HRP conjugate (Sigma–Aldrich, diluted 1:2000). To detect phosphorylation of EGFR tyrosine residues, membranes were probed with either rabbit anti-EGFR pY1068 (diluted 1:1000) or anti-EGFR pY1173 (diluted 1:1000), followed by anti-rabbit HRP. Proteins were detected by developing the membranes with ECL reagents (GE Healthcare) followed by exposure to Hyperfilm (GE Healthcare).

4.2.6 Agarose bead immunolabeling

The scFvs were alkyne-functionalized and immobilized onto azide-conjugated agarose beads as described in Chapter 2. To 10 µl of beads, 200 µl of biotinylated A431 cell lysate was added for 2 h at room temperature with gentle rotation. Beads were subsequently washed three times with 500 µl lysis buffer and incubated with 200

µl anti-EGFR mouse antibody cocktail Ab-12 (1:500 dilution in PBSA) for 1 h at room temperature. After washing three times with 500 µl PBSA, beads were incubated with 200 µl anti-mouse Alexa 488 (diluted 1:500 in PBSA) with Alexa 594-conjugated streptavidin (diluted 1:500) for 1 h at room temperature. Beads were subsequently washed three final times with 500 µl PBSA and imaged with an Olympus IX70 fluorescence microscope. Bead fluorescence was quantified with a Tecan Infinite M1000 fluorescent microplate reader.

4.3 Results

4.3.1 Yeast display immunoprecipitation (YDIP) of wild-type EGFR

While traditional yeast display analysis requires purified, soluble antigen sources, yeast display immunoprecipitation (YDIP) permits the binding of surface displayed antibodies to antigen present in whole cell lysates (Figure 4-2a). A431 cells that express wild-type EGFR were solubilized with a non-ionic detergent, Triton X-100, to generate cell lysates. These lysates were incubated with yeast expressing either the negative control scFv, anti-fluorescein 4-4-20, or the EGFR antibody specific to kinase domain, scFv2 [126]. Since it was previously demonstrated that surface displayed scFv2 could bind purified, soluble EGFR [145], cell lysate binding was compared to that of the purified receptor. Using flow cytometry, it was demonstrated that yeast-displayed scFv2 captured EGFR from detergent-solubilized cell lysates in a similar manner to the purified receptor, while the negative control scFv, 4-4-20, did not appear to bind either purified EGFR or EGFR from cell lysates (Figure 4-2b). To further confirm this finding, the proteins were eluted from the yeast surface and analyzed with an anti-EGFR Western blot (Figure 4-2c). EGFR was present in eluants from yeast displaying scFv2

that had been incubated with either purified receptor or A431 lysate, while yeast displaying 4-4-20 did not elute EGFR in either case.

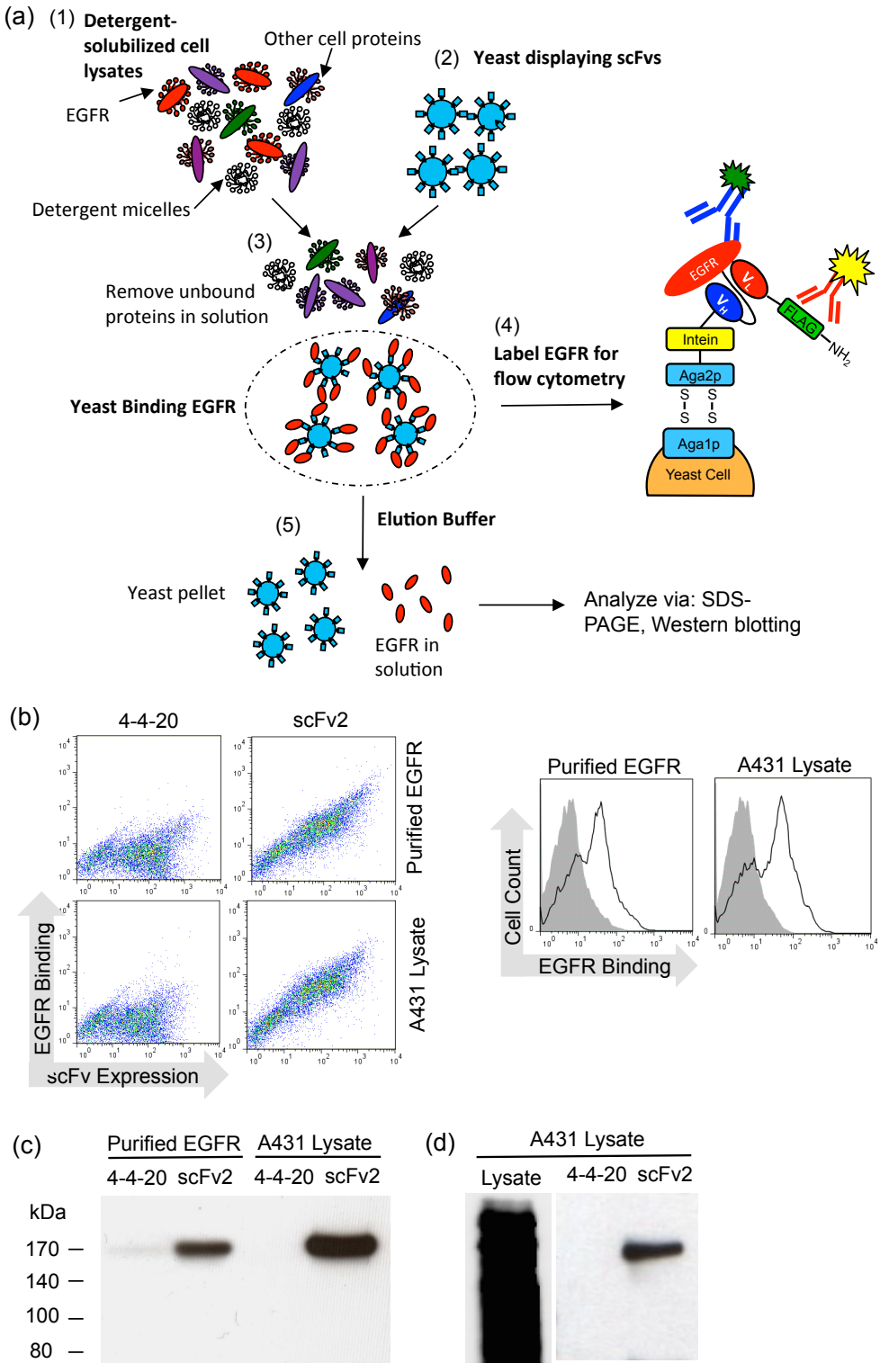

Figure 4-2: YDIP with surface displayed scFv2 and A431 cell lysates.
(a) A YDIP schematic details the analysis of scFv binding to EGFR present in whole cell lysates. (1) Detergent-solubilized cell lysates are incubated with (2) yeast displaying an EGFR-specific scFv. (3) After washing away the unbound proteins, the yeast can either (4) be analyzed for EGFR binding by flow cytometry, or (5) the proteins can be eluted from the yeast surface and analyzed by Western blotting. This schematic is adapted from Cho, Y.K., Chen, I., Wei X., Li, L., and Shusta E. V., (2009) *J. Immunol. Methods* [161] (b) Flow cytometry dot plots demonstrate that yeast displaying scFv2 could bind EGFR both from a purified source and from A431 lysates. Yeast displaying 4-4-20 were used as a negative control for EGFR binding. Histograms are also presented to emphasize differential binding between yeast displaying scFv2 (black line) and 4-4-20 (shaded). (c) Antigens isolated using YDIP were eluted from the yeast surface and analyzed with an anti-EGFR Western blot to confirm EGFR binding. ScFv2 eluted EGFR when yeast were incubated with either the purified receptor or A431 lysate, while 4-4-20 did not bind/elute EGFR. (d) Cell surface proteins were biotinylated prior to incubation with yeast displaying scFv2 or 4-4-20. Antigens were eluted from the yeast surface and analyzed with an anti-biotin Western blot, thus revealing a single band at ~170 kDa from scFv2 elution. Lysate that had not been incubated with yeast was also analyzed using anti-biotin Western blotting to illustrate the presence of multiple biotinylated proteins.

Next, since cell lysates contain sources of nonspecific interactions such as detergents, micelles, and other proteins, the effects of lysate presence on the specificity of scFv2 binding was analyzed. The A431 cell surface proteins were biotinylated prior to cell lysis in order to enable anti-biotin detection of A431 proteins. Yeast displaying scFv2 or 4-4-20 were incubated with the biotinylated lysate to permit antigen binding, and isolated proteins were subsequently eluted from the yeast surface with a low-pH glycine buffer (Figure 4-2a). Anti-biotin Western blot demonstrated that, while the cell lysate contained multiple biotinylation proteins, yeast displaying scFv2 only eluted one biotin-tagged protein, as demonstrated by a single band on the Western blot (Figure 4-2d). Since this band aligns with the anti-EGFR Western blot and its molecular weight corresponds to that of EGFR (~170 kDa), it can be presumed that the identity of this protein is EGFR.

4.3.2 Analysis of EGFRvIII binding from lysates

After demonstrating that YDIP could be employed to bind wild-type EGFR from lysates using scFv2, the ability to isolate the EGFRvIII mutant from cell lysates with surface displayed antibodies was evaluated. In addition to scFv2, an EGFRvIII-specific scFv, MR1 [203], was expressed in the yeast display construct and the specificity of its binding to EGFRvIII was analyzed. Using flow cytometry, it was demonstrated that yeast expressing either scFv2 or MR1 could bind EGFRvIII from U87-EGFRvIII cell lysates (Figure 4-3a). Although scFv2 appeared to bind more EGFRvIII than MR1, flow cytometry histograms highlight that MR1 binding is still greater than the negative control scFv, 4-4-20. The specificity of MR1 binding to the EGFRvIII mutant was evaluated by incubating yeast displaying MR1 with A431 lysates that only contain the wild-type receptor. While scFv2 demonstrated binding to EGFR from A431 lysates, MR1 binding was not any greater than the negative control, thus indicating that the antibody is specific to EGFRvIII (Figure 4-3a). These results were confirmed by eluting the proteins from the yeast surface and analyzing with anti-EGFR Western blots. Wild-type EGFR was only present in eluants from yeast displaying scFv2 that had been incubated with A431 lysates and not from MR1-displaying yeast (Figure 4-3b). When the antigens were eluted from yeast that had been incubated with U87-EGFRvIII lysates, both scFv2 and MR1 yeast eluted EGFR (Figure 4-3b).

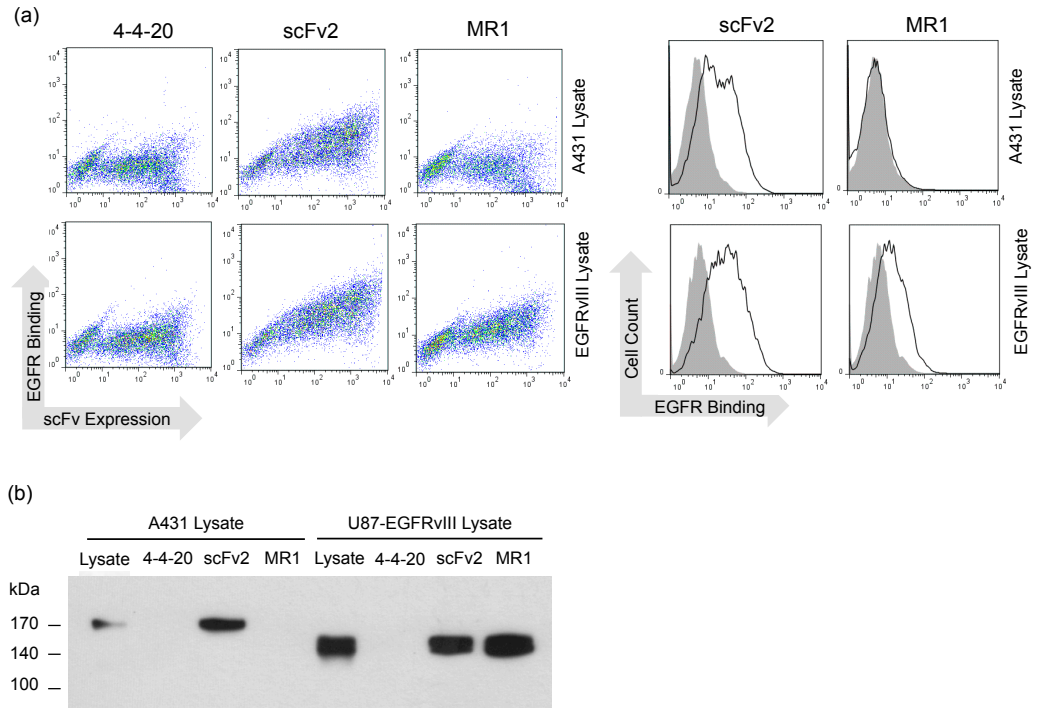

Figure 4-3: YDIP analysis with U87-EGFRvIII cell lysates.
(a) Flow cytometry dot plots demonstrate that yeast displaying MR1 do not bind wild-type EGFR from A431 lysates, but both scFv2 and MR1 are able to bind the EGFRvIII mutant from U87-EGFRvIII lysates. Histograms representing EGFR binding are also presented to emphasize differences in binding between MR1 or scFv2 (black line) and the 4-4-20 negative control (shaded). (b) Elution of EGFR from the yeast surface was analyzed with an anti-EGFR Western blot and compared to lysate samples. While EGFR has a molecular weight around 170 kDa, EGFRvIII is a smaller protein and appears around 140 kDa.

4.3.3 Analysis of scFv2 binding to the ΔELREA mutant

Since an scFv specific to the ΔELREA mutant has not been developed, scFv2 binding to ΔELREA was characterized in order evaluate its binding potential in a detection assay. Yeast displaying 4-4-20 or scFv2 were incubated with B82L-ΔELREA cell lysates and EGFR binding was compared to that of the A431 lysates. Flow cytometry analysis indicated a lack of EGFR capture by yeast displaying scFv2 when the B82L-ΔELREA lysates were used as an antigen source (Figure 4-4a). YDIP elution was performed to confirm the absence of binding to the ΔELREA mutant. Anti-EGFR

Western blot analysis demonstrated that, while EGFR was detected in the B82L-ΔELREA lysates, yeast displaying scFv2 were not able to capture and elute the ΔELREA mutant (Figure 4-4b).

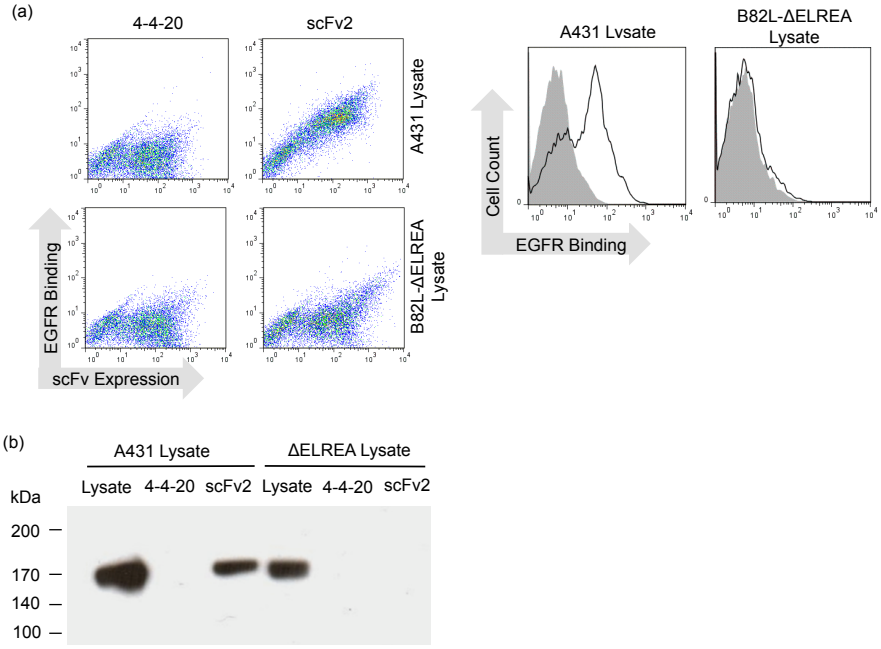

Figure 4-4: Characterization of scFv2 binding to the ΔELREA mutant
(a) Flow cytometry dot plots and histograms indicate an absence of scFv2 binding to the ΔELREA mutant. Binding of scFv2-displaying yeast to wild-type EGFR from A431 was used as a positive control. (b) An anti-EGFR Western blot demonstrates that, although EGFR is present in B82L-ΔELREA lysate samples, the ΔELREA mutant is not eluted from yeast surface displayed scFv2. A431 lysates were used as a positive control in the elution experiment.

4.3.4 YDIP detection of phosphorylated EGFR

Phosphorylation of EGFR's tyrosine kinase domain is an important indicator of EGFR activity and is correlated to disease state and prognosis [212]. It has previously been demonstrated that YDIP can be employed to identify protein interactions such as adaptin AP2 association [213], but it has yet to be established that post-translational modifications such as phosphorylation can also be detected. Furthermore, since scFv2

binds the intracellular domain of EGFR and was selected against a non-phosphorylated EGFR target [126], YDIP analysis could determine if EGFR phosphorylation impacts scFv2 binding. Prior to creation of the cell lysate, A431 cells were stimulated with EGF to promote phosphorylation of the intracellular tyrosine kinase residues. Using two phospho-specific EGFR antibodies, anti-pY1068 and anti-pY1173 that recognize phosphorylated tyrosine residues 1068 and 1173 respectively, binding of scFv2 to phosphorylated EGFR was demonstrated via flow cytometry (Figure 4-5a). Phosphorylation of these residues was not detected in the absence of EGF stimulation or when EGF-stimulated cell lysates were incubated with yeast displaying 4-4-20. Additionally, YDIP elution followed by anti-pY1068 and anti-pY1173 Western blotting confirmed the binding of phosphorylated EGFR to scFv2, and it demonstrated that, while phosphorylation of non-EGF stimulated lysate was undetectable by flow cytometry, basal phosphorylation was observed with anti-pY1068 Western blotting.

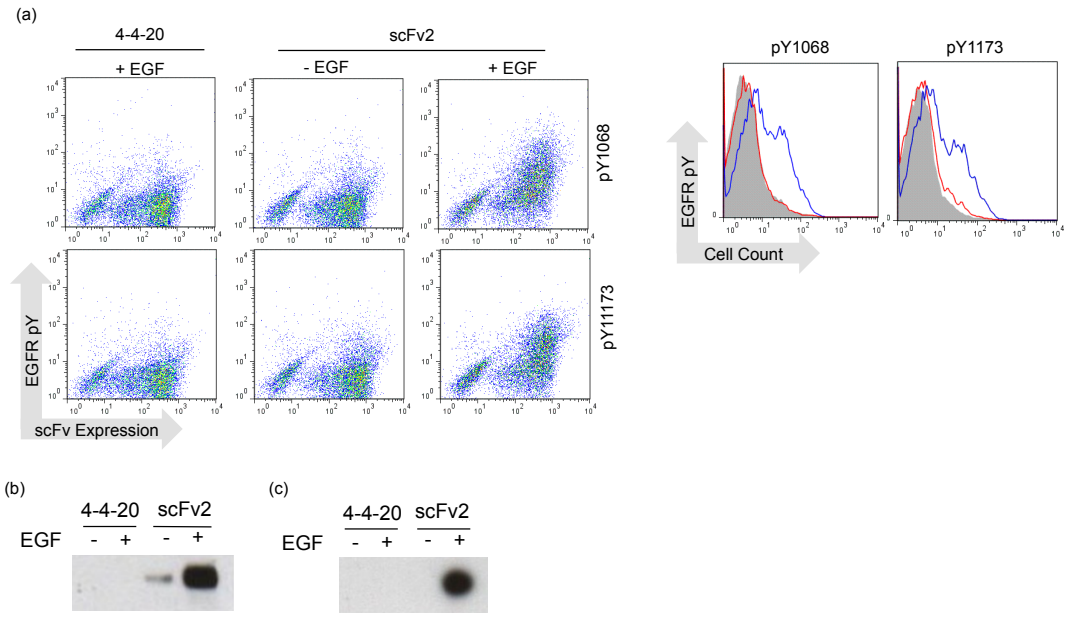

Figure 4-5: Analysis of EGFR phosphorylation via YDIP
(a) Using two phospho-specific EGFR antibodies, anti-pY1068 and anti-pY1173, flow cytometry dot plots demonstrate binding of yeast displaying scFv2 to phosphorylated EGFR. The binding of phosphorylated EGFR was shown to be specific to yeast displaying scFv2 that were incubated with EGF-stimulated cell lysate. Histograms emphasize the difference in phosphorylated protein binding between scFv2 +EGF lysates (blue line), scFv2 -EGF lysates (red line), and 4-4-20 +EGF lysates (shaded grey) (b) YDIP antigen elution and anti-pY1068 Western blotting also demonstrates isolation of phosphorylated EGFR by scFv2, with some basal phosphorylation observed for the non-EGF stimulated condition. (c) Likewise, an anti-pY1173 Western blot demonstrates elution of EGFR from yeast displaying scFv2 that were incubated with EGF-stimulated lysate.

4.3.5 EGFR capture with CuAAC-immobilized scFv2

After demonstrating that the yeast displayed antibodies could be employed to capture EGFR from cell lysates, the ability to capture EGFR from lysate sources using scFv2-decorated surfaces was analyzed to further determine its applicability in a detection assay. As described previously (Chapter 2, [145]), yeast displaying scFv2-intein fusion proteins were reacted with MESNA followed by cysteine alkyne to install a carboxy-terminal alkyne onto the antibody (Figure 4-6a). This alkyne was employed in a copper(I)-catalyzed azide–alkyne cycloaddition (CuAAC) reaction to immobilize scFv2 on azide-decorated agarose beads. Whereas previously, purified EGFR was used as an antigen source (Chapter 2), here, biotinylated A431 lysates were incubated with the beads, and EGFR capture was assessed with by immunofluorescence labeling. By detecting the presence of EGFR on the beads, it was demonstrated that only surfaces loaded with alkyne-conjugated scFv2 could bind EGFR from cell lysates, whereas beads loaded with alkyne-conjugated 4-4-20 or scFv-thioester did not capture EGFR (Figure 4-6b). EGFR binding selectivity was quantified and shown to be greater than 25:1 for beads loaded with alkyne-conjugated scFv2 compared to the alkyne-conjugated 4-4-20 or non-alkyne scFv2 (Figure 4-6c). Furthermore, the use of biotinylated lysate

provided a measure of non-specific adsorption of A431 proteins to the beads, and it also enabled detection of captured proteins without the use of an antigen-specific antibody. Detection of biotinylated proteins indicated lysate binding selectivity to be approximately 5:1 for the alkyne-conjugated scFv2 compared to the alkyne-conjugated 4-4-20, while this selectivity was greater than 30:1 for beads loaded with non-alkyne scFv2 (Figure 4-6c). It should be noted that no optimization was performed with the blocking or washing steps to prevent non-specific binding.

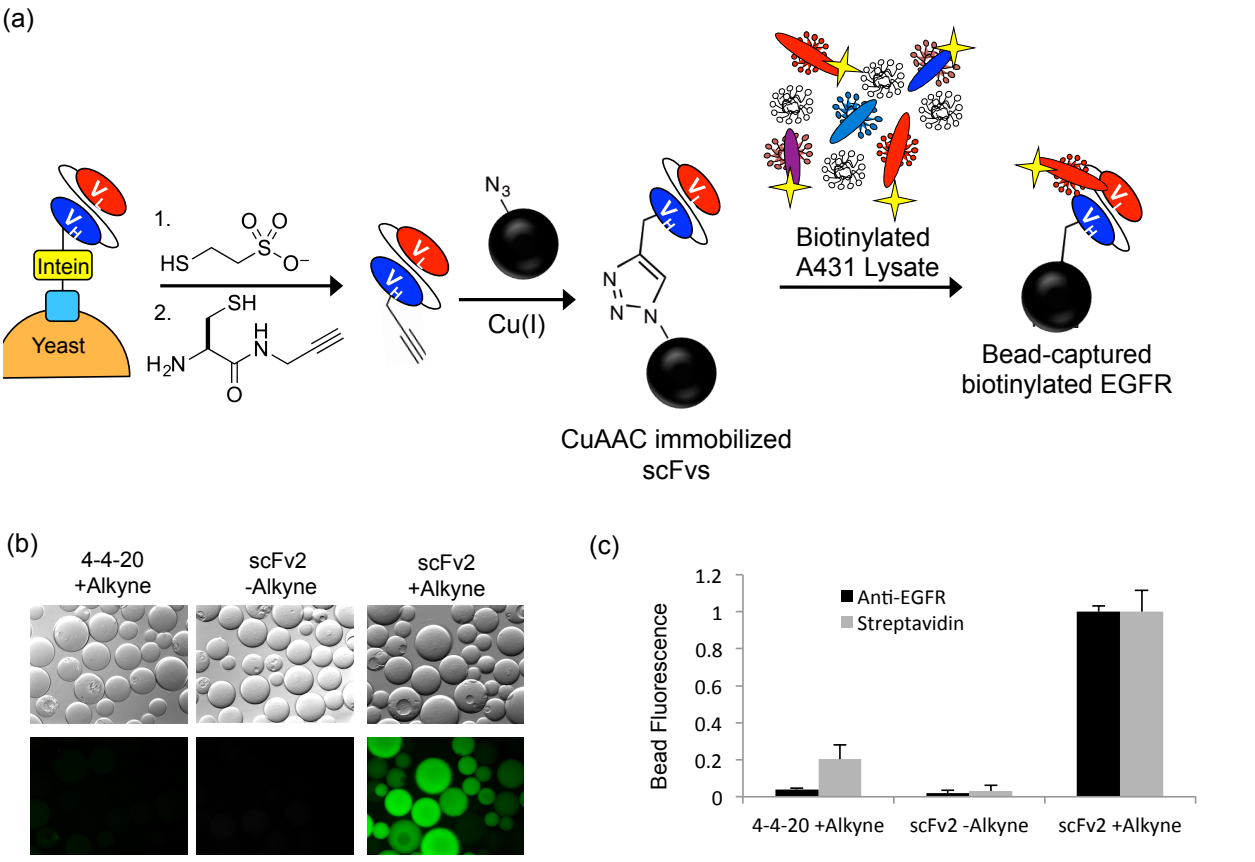

Figure 4-6: Immobilized scFv2 capture of EGFR from lysates
(a) As previously described [145], scFv2 was displayed as a fusion to intein on the yeast surface, released from the construct via MESNA, and alkyne modified at its carboxy-terminus through EPL reaction with a cysteine alkyne. A CuAAC reaction was performed to site-specifically immobilize the alkyne-conjugated scFv2 onto agarose beads, and incubation with biotinylated A431 lysate enabled bead capture of biotinylated EGFR. (b) Immunofluorescence

labeling with an anti-EGFR antibody detects capture of EGFR only by beads loaded with alkyne-conjugated scFv2. (c) EGFR capture is quantified by measuring total bead fluorescence with anti-EGFR or streptavidin labeling, and the values are normalized to alkyne-conjugated scFv2. Plotted are the mean ± SD of measurements from three independent bead immobilization reactions.

4.4 Discussion and Future Directions

Working towards an EGFR assay with LC detection capabilities, in this study, we have further characterized two EGFR scFvs and assessed their ability to engage antigens from complex, cell-based sources using YDIP. An scFv that recognizes the kinase domain of EGFR, scFv2, was shown to bind both wild-type EGFR and EGFRvIII from cell lysates, but was unable to bind the ΔELREA mutant. MR1 demonstrated specificity to the EGFRvIII mutant present in cell lysates, as we were unable to detect binding to wild-type EGFR from A431 cell lysates. This antibody should prove particularly useful in a detection assay due to its specificity and the fact that there is no commercially available antibody to the EGFRvIII mutant.

The absence of scFv2 binding to ΔELREA provides insight into scFv2's specific antigen recognition epitope and makes it a unique binding molecule for a detection assay. The ΔELREA mutation is a small, 5 amino acid deletion in the large kinase domain of EGFR (resides 746-750, Figure 4-1). Since scFv2 was selected against the entire intracellular region (residues 645-1186), its inability to bind ΔELREA indicates that residues 746-750 are critical for scFv2 to engage EGFR. This suggests that either scFv2 directly binds these residues, and/or the ΔELREA mutant produces a conformational change in the kinase domain that disrupts scFv2 binding. Nevertheless, this binding specificity makes scFv2 useful as a detection reagent because, in an assay, binding to scFv2 would indicate that the EGFR isoform in the sample is not ΔELREA.

Since scFvs that recognize the extracellular domain, such as 2224 (Chapter 3), engage EGFR away from the ΔELREA mutation site, they would likely be able to bind the mutant. In the future, these antibodies could be evaluated via YDIP using the described procedures and integrated into an EGFR assay.

Combining these antibodies with the chemical modification techniques presented in Chapters 2 and 3 permits the generation of binding surfaces that could be employed in an LC assay. Although here we demonstrated that CuAAC-immobilized scFv2 could bind EGFR from cell lysates, other chemical functionalities, such as catalyst-free click groups (Chapters 3 or 5) or biotin (Chapter 2), could be installed in order to employ different immobilization chemistries based on the desired application. For example, these antibodies could easily be integrated into a recently established LC-assay that enabled detection of EGFR-containing microvesicles shed from A431 cells [210]. Tan, Abbott, and colleagues immobilized a biotinylated, EGFR-specific IgG on the surface of streptavidin microbeads, and they were able to capture EGFR-containing microvesicles using the beads. Subsequently, the microvesicles were extracted from the beads, and the addition of LCs enabled quantitative detection of the microvesicles using flow cytometry (Figure 4-7). Using the intein-linked modification strategies described in Chapter 2, scFv2 and MR1 could easily be biotinylated, immobilized on the streptavidin beads, and employed to capture EGFR or EGFRvIII-containing microvesicles. Indeed, preliminary data from Tan indicated specific capture of wild-type and EGFRvIII vesicles with scFv2 and MR1, thus warranting further investigation into this assay.

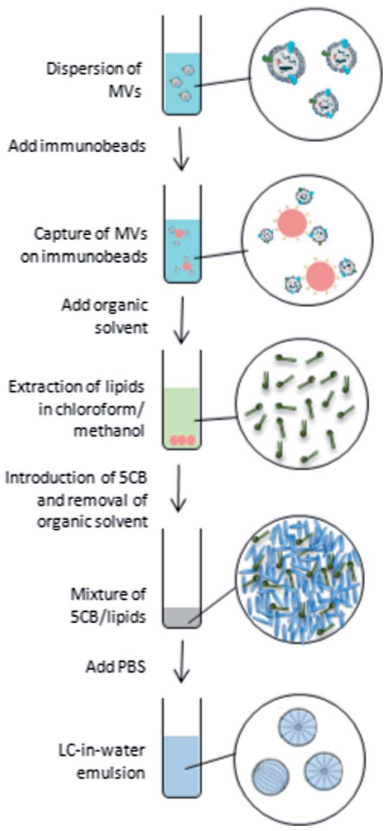

Figure 4-7: LC detection of EGFR microvesicles.
A schematic of the experimental procedures for LC detection of EGFR microvesicles was detailed by Tan et.al. [210]. Microvesicles are incubated with beads decorated with an anti-EGFR antibody. After allowing binding, the microvesicle lipids are extracted with organic solvents, LCs are added, and the organic solvent is replace with an aqueous buffer. An LC-in-water emulsion is obtained, and the presence of lipids produces an ordering transition of the LCs that is detectable by flow cytometry. Using this procedure, as few as 10^6 microvesicles could be detected, making it more sensitive than current techniques to detect microvesicles.

Finally, the techniques described here expand upon the utility of YDIP. Yongku Cho demonstrated in his work that YDIP could be employed to isolate antibodies that bind receptors associated with adaptin AP2 [213]. Since interaction with AP2 signals clathrin mediated endocytosis, YDIP could enable the identification of antibodies that target cellular specific pathways. Here, we demonstrated that YDIP could also identify antibody binding to phosphorylated proteins, and, since protein phosphorylation is associated with signal transduction pathways [214], these techniques could be

employed to identify antibodies that recognize proteins involved with this pathway. Furthermore, by combining YDIP with intein-linked yeast display, we can permit the generation of antibody-decorated detection surfaces that are able to immunoprecipitate antigen from whole cell lysate. While YDIP enables elution of captured proteins from the yeast surface, some elution methods also coextract yeast proteins, thus producing high yeast background [161]. Releasing, functionalizing, and immobilizing antibodies via intein-linked yeast display methods, therefore, would eliminate the need to elute from the yeast surface, and instead, potentially allow for a cleaner antigen extraction via antibody-decorated beads.

To conclude, by combining YDIP with intein-linked yeast display, we permitted the characterization of biomarker-specific scFvs while subsequently enabling the facile transition of the antibodies into downstream functional assays. In the future, the methods and analysis detailed here could prove particularly useful to generate a highly sensitive EGFR biomarker assay.

Chapter 5 : Rapid Tetrazine Click Ligations: Development of a Bispecific Antibody Platform

In this chapter, we begin to develop a clicked bispecific antibody platform that enables facile combinatorial screening of bispecific antibodies. While in Chapters 2-4 we employed intein-linked yeast display to generate antibodies with "clickable" groups, here we attempt to conjugate two antibodies using click chemistry. To complete this goal, it is discovered that we must employ the use of faster, more reactive chemistries such as the tetrazine click ligation. This chapter was done in collaboration with Nicholas McGrath, Kalie Mix, and Prof. Ronald Raines (Department of Chemistry and Department of Biochemistry, University of Wisconsin-Madison), who synthesized the tetrazine and styrene reagents and performed the NMR rate study.

5.1 Introduction

The development of monoclonal antibody (mAb) therapeutics has provided a new class of targeted drugs that show great promise to address and treat difficult diseases [215]. However limitations in mAb drugs, such as efficacy and specificity, have led to the emergence of a new generation of antibody therapeutics: bispecific antibodies (bAbs) [216]. While mAbs engage only one antigenic target, bAbs engage two targets simultaneously, thus enhancing the therapeutic efficacy of the antibody via improved cell-specific targeting and increased receptor avidity [216-218]. In addition to the 11 bAbs in clinical trials as of 2013, numerous other bAbs are being explored to treat

diseases such as cancer, tuberculosis, hepatitis B, and severe acute respiratory syndrome (SARS) [216].

Despite the potential of bAb therapeutics, the development of bAbs is highly cost prohibitive. Currently, mAbs are developed individually, and subsequent to full characterization and testing of each mAb, the two binding domains are combined in a bAb platform, which also must be characterized and tested, thus, making the effort to develop one bAb double or triple that of a mAb [219]. In addition, this development strategy does not permit the combinatorial pairing of binding domains in order to find the most efficacious pairs from a large pool of mAbs, and so, the best combinations of antibodies may be missed. Thus, there is a need for high-throughput methods to screen bAb combinations in order to identify optimum pairings and enable the development of highly effective bAb therapeutics.

One platform that could enable combinatorial screening of antibodies is yeast surface display. While yeast display has previously been employed to identify novel antibodies from large libraries [108, 109, 130] or to enhance antibody properties such as affinity, stability, and specificity [105, 111-113, 131, 132], in Chapters 2-4, we developed and characterized a yeast display platform that permits the chemical modification of antibodies with click chemistry compatible groups. These chemical groups could be employed to chemically conjugate two yeast displayed single chain antibody (scFvs) clones directly from a screen, thus creating a “clicked” bispecific antibody (CliBAb) (Figure 5-1). This could enable downstream analysis of combinatorial pairs of bispecific antibodies without subcloning, reformatting, and soluble expression that are necessary with currently available techniques to generate bispecific antibodies.

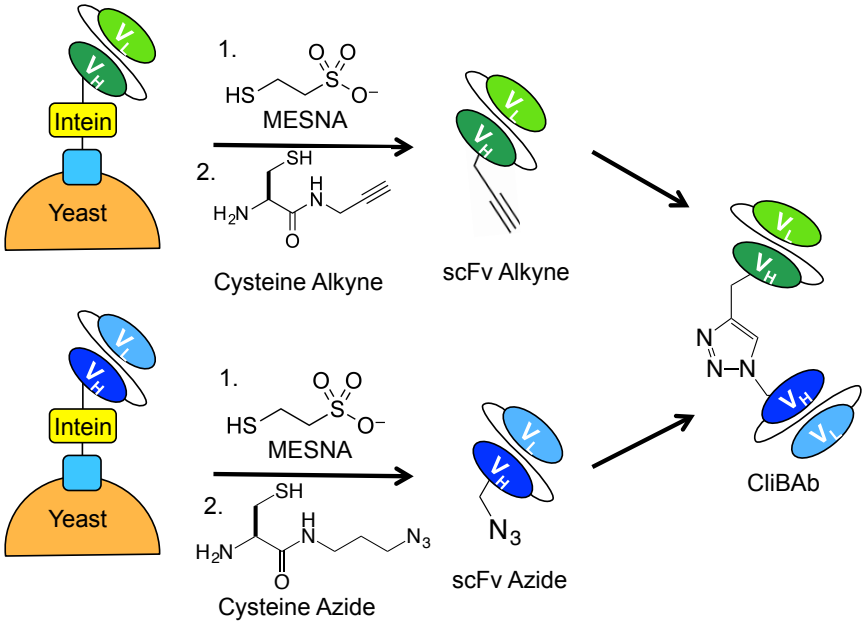

Figure 5-1: Schematic of CliBAb platform using CuAAC
As detailed in Chapter 2, azide and alkyne functionalities can be site-specifically installed on the carboxy-terminus of scFvs using intein-linked yeast display. With copper(I)-catalyzed azide–alkyne cycloaddition (CuAAC) the two scFvs could be chemically conjugated to create a clicked bispecific antibody (CliBAb). Since intein-linked yeast display enables a variety of chemical handles to be installed onto an antibody, alternative chemistries could be employed to generate CliBAbs.

While it has been demonstrated that intein-linked yeast display is compatible with copper(I)-catalyzed azide–alkyne cycloaddition (CuAAC) [145], CuAAC may not be ideally suited for the CliBAb platform. Efficient CuAAC conjugation requires the optimization of the copper, stabilizing ligand, and reducing reagent concentrations [220], which can vary widely based upon the system [221]. Furthermore, reported pseudo-second order rate constants for CuAAC reactions tend to range from 10^{-3} to 10^{0} $M^{-1}S^{-1}$, and, since scFv concentrations produced by intein-linked yeast display are around 1 μM, the time to obtain 50% clicked bispecific antibody product ($t_{1/2}$) could range from 11

days to 32 years. However, the intein-linked yeast display platform provides the ability to install a variety of chemical handles onto scFvs, and so alternative chemistries could be employed to enhance the CliBAb platform. In strain-promoted azide–alkyne cycloaddition (SPAAC), the terminal alkyne group is replace with a more reactive strained alkyne, such as a dibenzocyclooctyne (DBCO), to permit the reaction with an azide in the absence of a Cu(I) catalyst. Although this simplifies the conjugation by eliminating the addition of a catalyst, SPAAC reaction rates are not greatly improved compared to CuAAC [220], thus warranting the use of faster, catalyst-free chemistries.

Recently, bioorthogonal tetrazine-click ligations have emerged as a new class of rapid, catalyst-free chemistries and a viable alternative to the slower, Cu(I)-catalyzed or strain-promoted cycloadditions. Cycloaddition of tetrazines and dienophiles have demonstrated second order reaction rate constants of up to $2.7x10^5$ $M^{-1}S^{-1}$ [70], which would enable 50% yield of bispecific antibody product in less than 4 seconds. Therefore, these tetrazine-click ligations could allow for more efficient generation of CliBAbs.

In this study, we explore the generation of bispecific antibodies using the described chemistries and employ intein-linked yeast display to install click groups with fast reaction rates. We envision that the integration of these fast-reacting click groups will facilitate the development of a high-throughput CliBAb platform which can permit the combinatorial pairing of antibody clones obtained in a yeast surface display screen.

5.2 Materials and Methods

5.2.1 CuAAC reactions

Azide and alkyne functionalized 4-4-20 were generated as previously described [145], and proteins were dialyzed with PBS to remove excess azide and alkyne reagents prior to CuAAC reaction. For reaction with the homobifunctional PEG azide reagent, the following was added to 200 µl of 4-4-20 alkyne: 5 µl of 4 mM $CuSO_4$ in water, 10 µl of 1.6 mM TBTA ligand in 80% v/v tert-butanol, 5 µl of 100 mM sodium ascorbate in water, and 10 µl 100mM polyoxyethylene bis(azide) (Sigma–Aldrich). The reaction was carried out for 1 h at room temperature prior to Western blot analysis. The azide and alkyne functionalized 4-4-20 were reacted by combining 100 µl 4-4-20 azide and 100 µl 4-4-20 alkyne with 5 µl of 4 mM $CuSO_4$ in water, 10 µl of 1.6 mM TBTA ligand in 80% v/v tert-butanol, 5 µl of 100 mM sodium ascorbate in water. The reaction was allowed to proceed for 20 h at room temperature prior to anti-FLAG Western blotting.

5.2.2 SPAAC reactions

DBCO-PEG4-DBCO (Click Chemistry Tools) was dissolved to a final concentration of 10 mM in DBSO. The reagent was serially diluted from 1 mM to 1 nM in PBS. To 22.5 µl aliquots of azide-conjugated 4-4-20, 2.5 µl of each dilution was added to generate final concentrations ranging from 100 µM to 100 pM. The reaction was allowed to proceed for 20 h at room temperature, and the products were analyzed with anti-FLAG Western blotting.

5.2.3 Tetrazine click reagents

The tetrazine and styrene reagents were synthesized by Kalie Mix (Supplemental Figure 5-9). Intein-linked yeast display was employed to release and conjugate 4-4-20 to the click groups as previously described for azide and alkyne functionalization [145], except the cysteine styrene and cysteine tetrazine were used as the amino-terminal cysteine reagents. After a 20 h EPL reaction, the proteins were dialyzed with PBS to remove the excess cysteine. Biotin tetrazine was serially diluted from 50 mM to 50 μM in PBS containing 5% tert-butanol (Sigma–Aldrich). To 20 μl styrene-conjugated 4-4-20, 5 μl of each dilution was added to generate final biotin tetrazine concentrations ranging from 10 μM to 10 mM. The reaction was incubated overnight at room temperature prior to anti-biotin Western blotting. To detect 4-4-20 tetrazine conjugation, styrene biotin was dissolved to a final concentration of 50 mM in PBS with 5% tert-butanol, and 5 μl of the biotin styrene was added to 20 μl tetrazine conjugated 4-4-20. The reaction was allowed to proceed overnight prior to anti-biotin Western blotting.

5.2.4 GFP immobilization

Azide-functionalized agarose beads were generated as previously described [145], and agarose beads were functionalized with tetrazine in a similar manner. NHS-activated agarose beads (250 μl, Thermo-Fisher) were washed three times with PBS and resuspended in in 1 mL PBS containing 100 mM (4-(1,2,4,5-Tetrazin-3-yl)phenyl)methanamine hydrochloride (Sigma–Aldrich). The mixture was incubated for 2 h at room temperature with gentle rotation. Unreacted NHS groups were quenched by rotating the beads with 1 M Tris buffer (pH 7) for 2 h at room temperature. The beads were subsequently washed 3 times in PBS-BSA and resuspended in PBS-BSA.

CuAAC immobilization of alkyne-conjugated GFP onto azide agarose beads was performed as previously described [145], and reactions were stopped after 1, 4, and 20 h by removing the protein solutions and washing the beads three times with PBS-BSA. To immobilize GFP via SPAAC, tetrazine agarose beads (10 µl) were incubated with 100 µl GFP-styrene with gentle rotation for 1, 4, or 20 h. Reactions were stopped by removing the protein solutions and washing three times with PBS-BSA. The agarose beads were subsequently imaged with an Olympus IX70 fluorescence microscope, and bead-associated fluorescence was quantified with a Tecan Infinite M1000 fluorescent microplate reader.

5.3 Results

5.3.1 CuAAC antibody conjugation

As an initial attempt to created clicked bispecific antibodies, the traditional, Cu(I)-catalyzed click chemistry was employed. Using intein-linked yeast display techniques previously detailed [145], the anti-fluorescein single chain antibody, 4-4-20, was chemically modified with a carboxy-terminal azide or alkyne group. The efficiency of the alkyne insertion was tested by reacting 4-4-20 alkyne with a homobifunctional PEGylated azide reagent in excess (Figure 5-2a, i). Since this reagent has a molecular weight of 5 kDa, conjugation to the scFv was apparent by a shift in the molecular weight of the scFv with anti-FLAG Western blotting (Figure 5-2b, lane i). Over 90% of the scFv-alkyne was conjugated to the PEG-azide reagent, indicating that the expressed protein ligation (EPL) reaction was able to efficiently install the alkyne group and that more than 90% of the scFv is capable of reacting with an azide-conjugated molecule. Next, CuAAC was employed to react azide-conjugated scFvs and alkyne-conjugated

scFvs in an effort to conjugate the two molecules (Figure 5-2a, ii). However, anti-FLAG Western blotting did not detect any scFv conjugation, indicating that the CuAAC reaction of these molecules was unsuccessful (Figure 5-2b, lane ii).

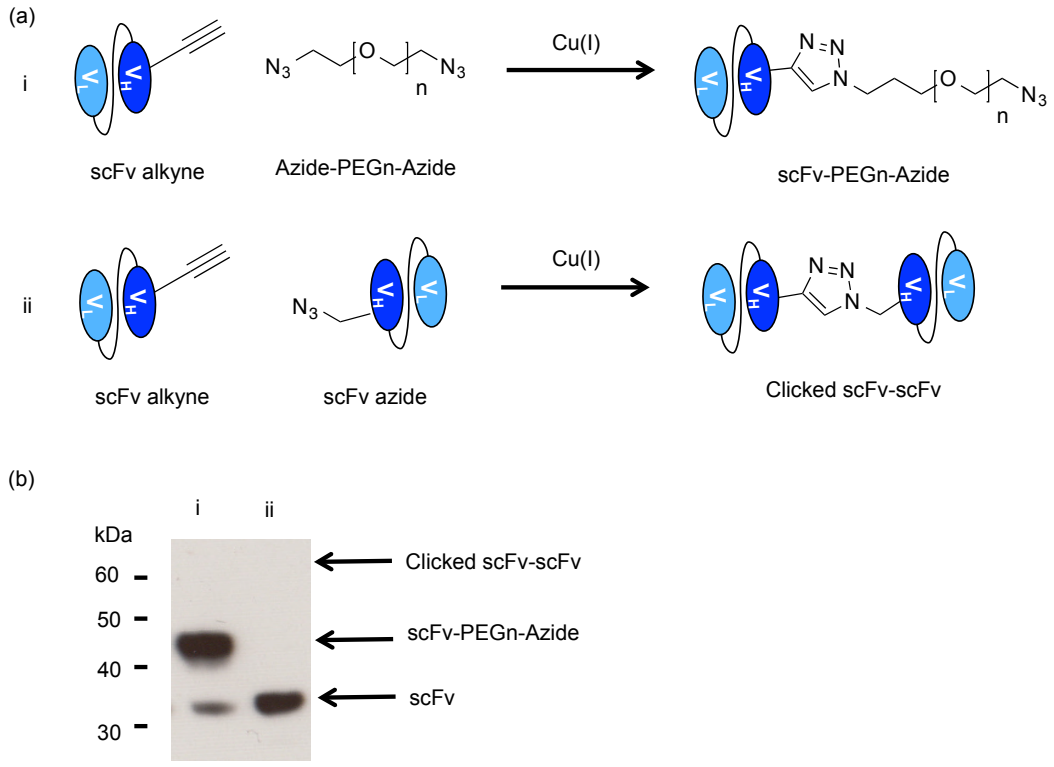

Figure 5-2: CuAAC reaction of scFv-alkynes and scFv-azides
(a) Using CuAAC, alkyne conjugated scFvs were reacted with azide targets. Panel i: a homobifunctional PEG azide reagent was reacted in excess with the scFv-alkyne to conjugate the antibody to the PEG linker. Panel ii: In an effort to conjugate two scFvs, azide-and alkyne-linked scFvs were reacted under the presence of Cu(I). (b) Anti-FLAG Western blotting evaluates the CuAAC reactions by detecting molecular weight shifts of the scFv. Lane i: The apparent molecular weight of the scFv (~32 kDa) increases to ~45 kDa, indicating that it reacted with the PEGylated azide reagent (5 kDa). Although this shift is slightly greater than expected, PEG often travels incorrectly on SDS-PAGE gels, making its apparent molecular weight greater [222]. Densitometry analysis indicated that >90% of the scFv is conjugated to the PEG reagent. Lane ii: Reaction of the scFv-alkyne and scFv-azide does not produce a change in the molecular weight of the antibodies, indicating that the conjugation was unsuccessful.

5.3.2 Antibody conjugation with a homobifunctional strained alkyne

After demonstrating that CuAAC likely is not compatible with the CliBAb platform, strain promoted azide–alkyne cycloaddition (SPAAC) was used to assess scFv conjugation with catalyst-free click chemistry. Since a cysteine-linked strained alkyne was not readily available, SPAAC was performed with a homobifunctional dibenzocyclooctyne (DBCO) reagent that contains two DBCO functional groups separated by a PEG linker (Figure 5-3a). By reacting this reagent with azide-functionalized scFvs, a mixture scFv-DBCO and scFv homodimers should be obtained, with the ratio of conjugated products depending on the concentration of the DBCO reagent (Figure 5-3a). To assess the effects of DBCO concentration on product formation, the concentration of the DBCO reagent was titrated from 100 μM down to 100 pM in reactions with azide-modified scFvs, and the conjugated products were detected with anti-FLAG Western blotting (Figure 5-3b). ScFv homodimers (~65 kDa) were formed when DBCO concentrations ranged from 10 nM to 100 μM, with the greatest yield of homodimers from 100 nm to 100 μM (Figure 5-3b). Additionally, since the DBCO reagent has a molecular weight of ~1 kDa, scFv-DBCO formation (~33 kDa) was detectable between concentrations of 10-100 μM. Below 10 nM, homodimer formation or conjugation to the DBCO reagent was not detectable.

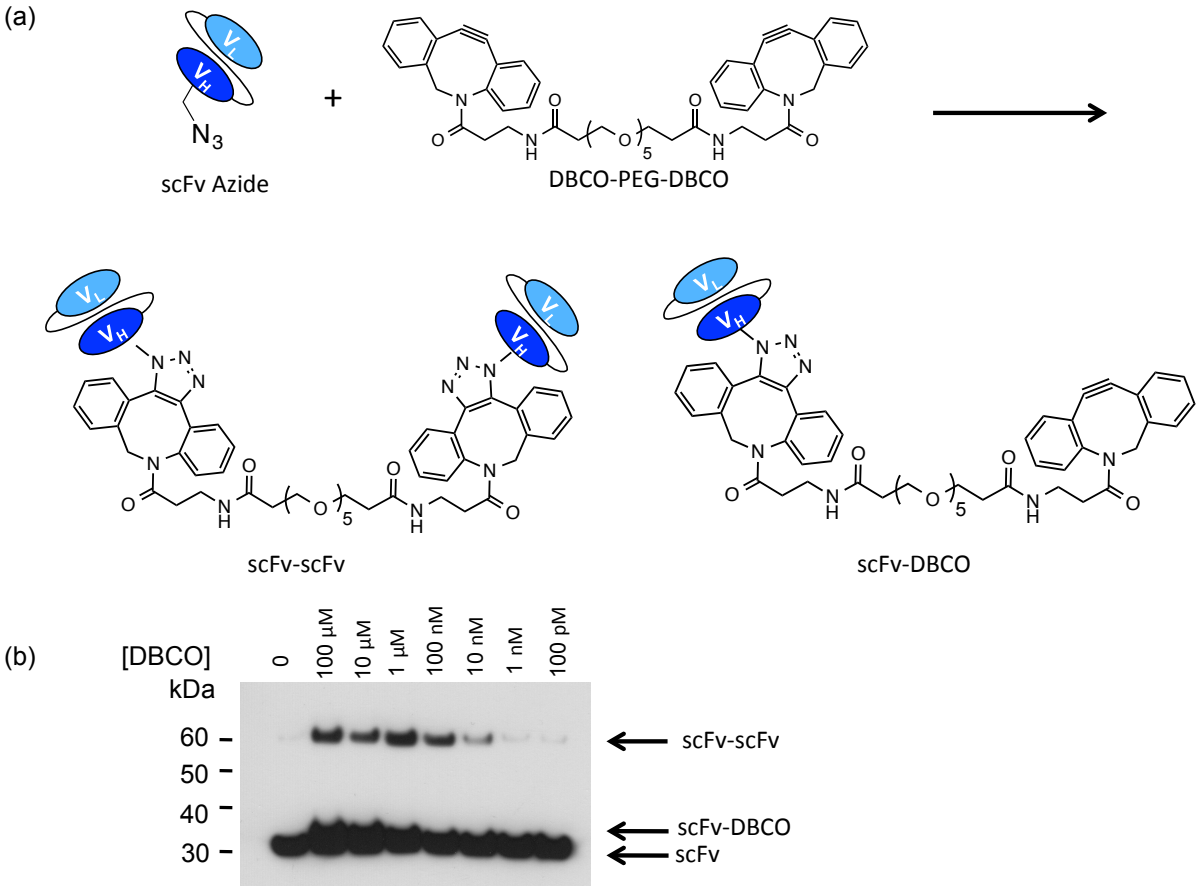

Figure 5-3: Homobifunctional DBCO titration with azide-conjugated scFvs
(a) Azide-conjugated scFvs react with the homobifunctional DBCO reagent, DBCO-PEG-DBCO, in a strain-promoted click reaction to form a mixture of scFv-DBCO and scFv homodimers. (b) Titrating the concentration of DBCO in reactions with azide-conjugated 4-4-20 reveals different ratios of product formation based upon DBCO concentration. An anti-FLAG Western blot shows a small increase in the molecular weight of the scFv when reacted with DBCO at concentrations of 1-100 µM, indicating that the scFv is conjugated to the DBCO reagent. Between 10 nM and 100 µM, formation of the scFv homodimer is detectable by the presence of scFv at ~65 kDa. At 1 nM and 100 pM, formation of homodimers or conjugation to the DBCO reagent is not detectable.

5.3.3 Tetrazine and dienophile modification with EPL

While scFv homodimer formation was detected using SPAAC, the conjugation was still inefficient (<10%), and, furthermore, this method does not guarantee the formation of bispecific antibodies since both scFvs would be azide conjugated.

Therefore, it is clear that faster chemistries, such as tetrazine-click ligations, must be employed to attain efficient CliBAb formation. By using EPL to site-specifically modify scFvs with tetrazines and dienophiles, two scFvs could be rapidly conjugated to form the desired CliBAb combination. To first test the ability to chemically modify scFvs with dienophiles, a cysteine functionalized with a styrene group was synthesized (Figure 5-4a). Although the typical dienophile used for tetrazine-click ligations is *trans*-cyclooctene (TCO), here, a styrene dienophile was initially employed because of its high stability and simple chemical synthesis. By reacting scFv-thioesters with the cysteine styrene, the scFvs can be modified at the carboxy-terminus with styrene group in an EPL reaction (Figure 5-4b). To detect the presence and the reactivity of the newly appended styrene functionality, a biotinylated tetrazine (Figure 5-4a) was reacted with the scFv to install a biotin group (Figure 5-4b). A range of biotin tetrazine concentrations (10 μM to 10 mM) was employed to assess the reactivity at low concentrations of reagents, as would be necessary for CliBAb formation. Anti-biotin Western blotting detected reaction of the scFv-styrene and the biotin tetrazine when the tetrazine was present at 10 mM, while the non-styrene control, an scFv-thioester, did not react with the tetrazine (Figure 5-4c). However, as the biotin tetrazine concentration was decreased to 1 mM and 100 μM, the extent of scFv biotinylation decreased, indicating that the biotin tetrazine was not fully reacting with the scFv-styrene. When the biotin tetrazine was present at 10 μM, no scFv biotinylation was detected, suggesting that the concentration was too low for a reaction to occur. Although click reactions at low concentrations of reagents were unsuccessful, 4-4-20 was still capable of styrene modification using intein linked yeast display techniques.

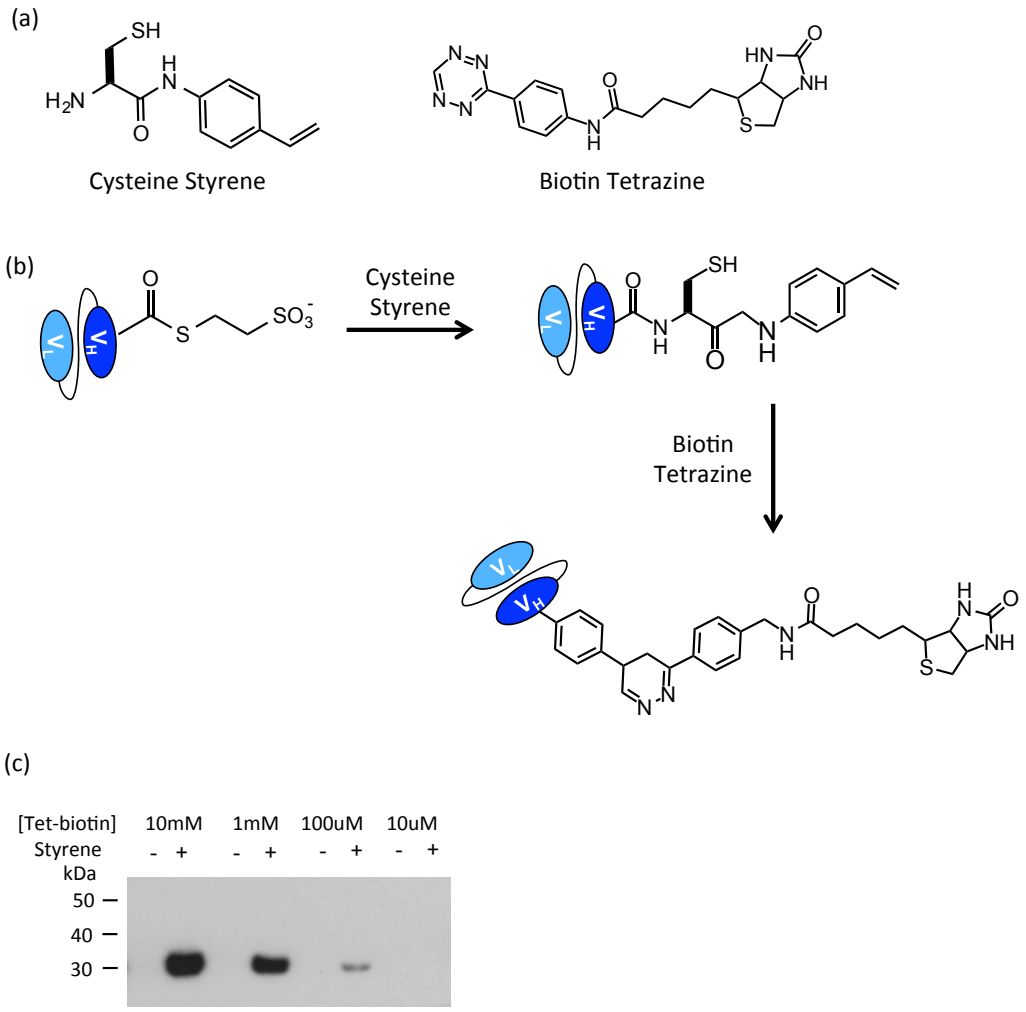

Figure 5-4: Styrene functionalization of scFvs
(a) Cysteine styrene was used to chemically modify 4-4-20, while biotin tetrazine was employed to detect the presence and reactivity of the styrene group. (b) Thioester scFvs were generated via intein-linked yeast display as previously described [145], and the scFvs were reacted with cysteine styrene using EPL to functionalize 4-4-20 with a carboxy-terminal styrene. Biotin tetrazine was subsequently reacted with the styrene-conjugated 4-4-20 to link the scFv and biotin in a click reaction. (c) Anti-biotin Western blotting detected the presence of biotinylated scFvs when scFv-styrene was reacted with biotin tetrazine. 4-4-20-thioester proteins were used as non-styrene controls to demonstrate reaction specificity. Although scFv biotinylation is detected when biotin tetrazine concentrations ranged from 100 μM to 10 mM, decreasing the concentration of biotin tetrazine reagent substantially decreased the extent of reaction. When 10 μM of biotin tetrazine is used, clicked products are not detectable.

The ability to install a tetrazine group onto the scFvs was next assessed by EPL reaction of 4-4-20-thioester with cysteine tetrazine (Figure 5-5a,b). Tetrazine

functionalization was evaluated by reacting the proteins with a biotinylated styrene (Figure 5-5a,b) and detecting the products with anti-biotin Western blotting. While the negative control, 4-4-20-thioester, did not react with the biotin styrene target, biotinylation of the tetrazine modified 4-4-20 was detected following the click reaction, thus indicating that the tetrazine was successfully installed onto the scFv and that its functionality is retained (Figure 5-5c).

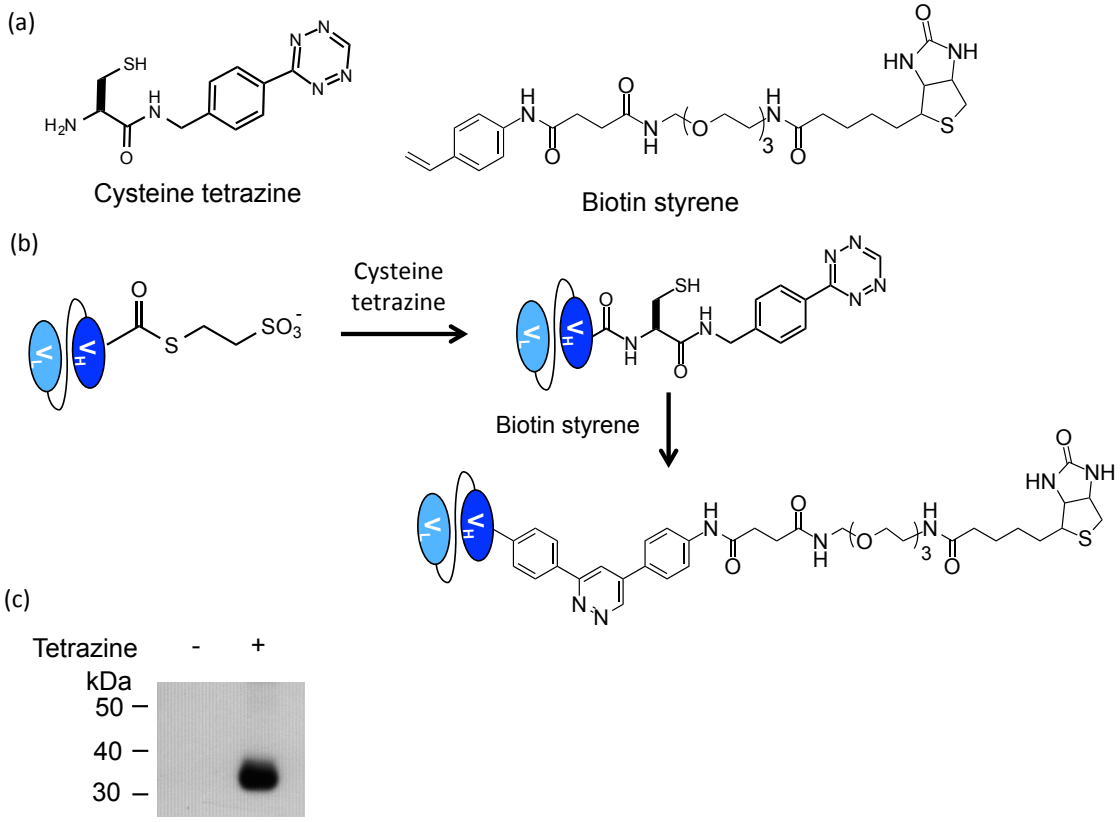

Figure 5-5: Tetrazine functionalization of scFvs
(a) Cysteine tetrazine permitted the EPL-mediated chemical modification of scFvs with a tetrazine group, while biotin styrene was employed to detect the presence and reactivity of the tetrazine functionality. (b) An scFv-thioester reacts with cysteine tetrazine to install a carboxy-terminus tetrazine. The tetrazine is subsequently reacted with biotin styrene, thereby appending a biotin onto the scFv via click reaction. (c) Anti-biotin Western blotting of the click reaction demonstrates specific biotinylation of the 4-4-20-tetrazine, thereby indicating that the EPL reaction appended a functional tetrazine on the carboxy-terminus of the scFv. As a negative control, scFv-thioesters were reacted with biotin styrene.

Next, the CuAAC and tetrazine-click reactions were compared by immobilizing proteins on functionalized beads with the different chemistries. Green fluorescent protein (GFP) was functionalized with an alkyne or styrene group using EPL, and the proteins were reacted with agarose beads containing the complementary clickable group (Figure 5-6a). GFP bead fluorescence was measured at 1, 4, and 20 h of reaction, thus demonstrating that while bead fluorescence for both chemistries was similar at 1 h, styrene-conjugated GFP was immobilized in greater amounts at 4 and 20 h compared to CuAAC (Figure 5-6b). Allowing the immobilization reaction to proceed for 20 h produced ~6-fold more immobilized GFP-tetrazine compared to the 1 h reaction.

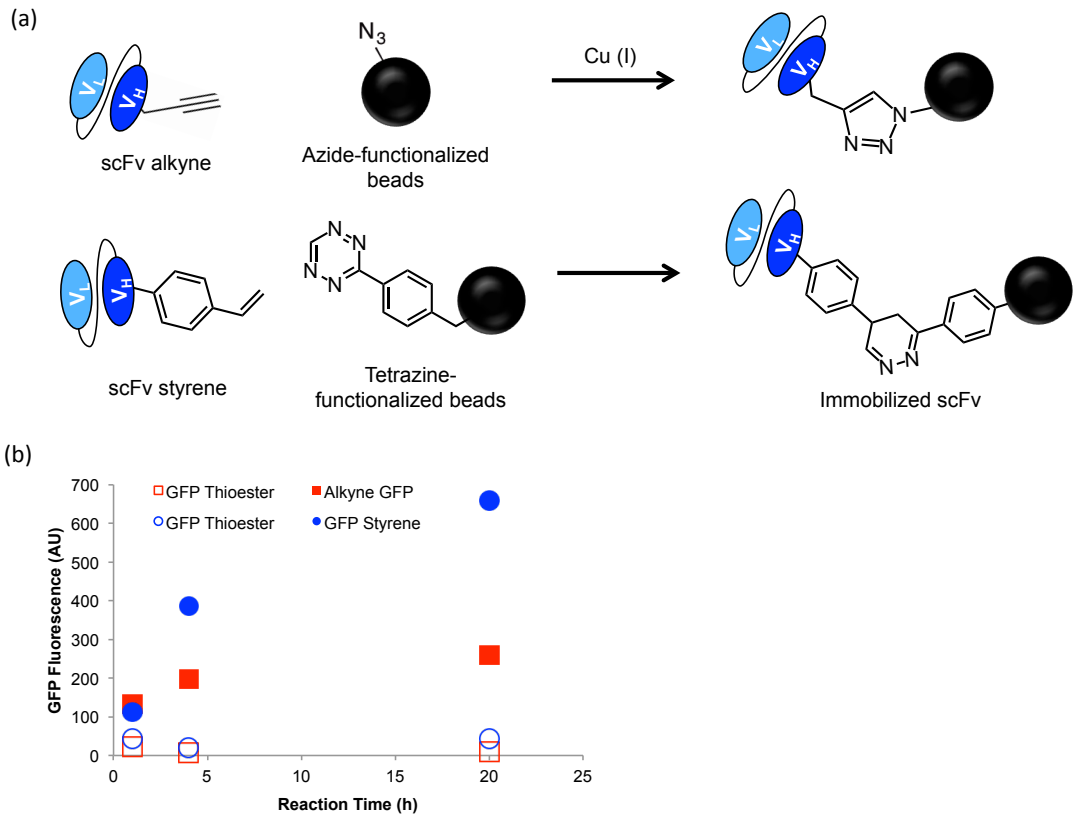

Figure 5-6: Comparison of CuAAC and tetrazine-click immobilization
(a) Alkyne-conjugated proteins react with azide-functionalized agarose beads in the presence of Cu(I) to covalently immobilize the protein on the beads via CuAAC. Styrene-conjugated

proteins are immobilized on tetrazine-loaded agarose beads in a catalyst-free click reaction. The schematic shows the immobilization of scFvs, but for this experiment, GFP was immobilized to provide a simple reaction readout using GFP fluorescence. (b) Bead fluorescence was measured at 1, 4, and 20 h, Red markers represent azide-functionalized agarose beads, while blue markers represent tetrazine-functionalized agarose beads. GFP-thioester was used as a negative control for both the CuAAC and tetrazine-click reactions. The tetrazine-click reaction enabled greater GFP immobilization at 4 and 20 h, but similar amounts were immobilized at 1 h.

5.3.4 Tetrazine-styrene reaction rate analysis

Finally, after failing detect appreciable clicked product when scFv-styrene was reacted with 10 μM biotin tetrazine (Figure 5-4c), the rate constant of the tetrazine-styrene click reaction was measured to determine if its reaction rate was comparable to

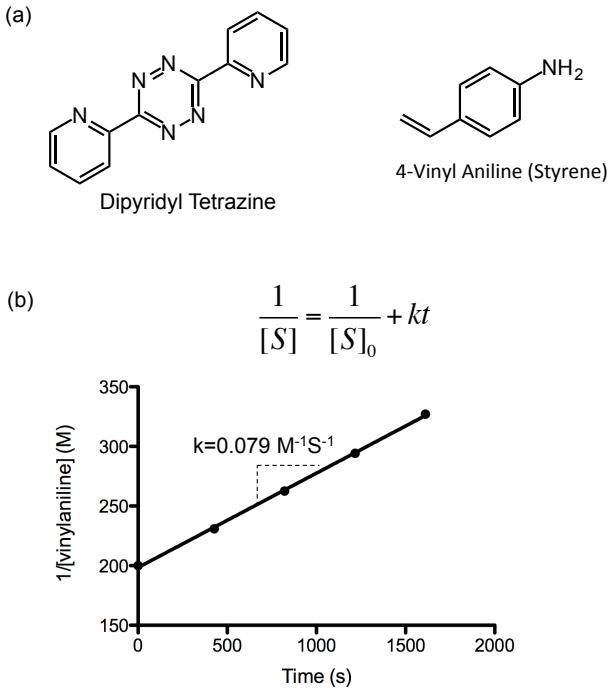

Figure 5-7: Tetrazine-styrene reaction rate analysis
(a) Dipyridyl tetrazine and 4-vinyl aniline (styrene) were reacted to determine the rate constant for the click ligation. (b) Using NMR, the disappearance of styrene was monitored, and the rate constant (k) was determined to be 0.079 $M^{-1}S^{-1}$ by fitting the second order rate law equation. [S]=concentration of styrene, $[S]_0$=initial concentration of styrene, k=second order rate constant, t=time. NMR analysis was performed by Kalie Mix.

the traditionally used TCO dienophile. Dipyridyl tetrazine and 4-vinyl aniline were employed in the rate study because they are chemically similar to the cysteine reagents but more readily available in greater concentrations (Figure 5-7a). The tetrazine and styrene were combined in equimolar ratios, and their reaction was monitored by measuring the disappearance of styrene with ^{1}H NMR. By fitting a second-order rate law equation, the rate constant was determined to be 0.079 $M^{-1}S^{-1}$ (Figure 5-7b) making the rate considerably slower TCO reaction rates [70].

5.4 Discussion and Future Directions

In this study, we examined several forms of click chemistry to determine their utility in our clicked bispecific antibody platform. While we demonstrated that CuAAC is likely not compatible with the platform due to its slow reaction rate, we were able to covalently conjugate two azide-functionalized scFvs using a bifunctional strained alkyne reagent in a SPAAC reaction. However, the yield of clicked products was low, and because both scFvs would need to be azide-modified to react, this method would likely produce a mixture of homodimer and heterodimer antibody combinations. Moving towards faster chemistries, intein-linked yeast display was employed to install dienophile and tetrazine clickable groups that are capable of reacting via catalyst-free click chemistry. While we initially employed styrene as the dienophile functional group because of its high stability and simple chemical synthesis, disappointingly, the styrene-conjugated scFvs were unable to react with a tetrazine target at low concentrations. Accordingly, the rate constant of the tetrazine-styrene click ligation was determined to be 0.079 $M^{-1}S^{-1}$, which is several orders of magnitude below the reported values for other dienophiles [70].

Despite the failure of scFv-styrenes to react with tetrazine at low concentrations, here, we established that intein-linked yeast display could be employed to site-specifically install tetrazine and dienophile groups onto scFvs. Moving forward, other dienophile functionalities can be explored to produce fast reaction rates with tetrazine. One proven dienophile is TCO, which has been previously employed in tetrazine-click reactions to conjugate proteins to fluorophores [69, 71, 72], nanoparticles [73], radioisotopes [70, 73, 74], and surfaces [223]. Since tetrazine-TCO reaction rate constants have been reported to be high as $2.7x10^5$ $M^{-1}S^{-1}$ [70], integrating TCO into the CliBAb platform should allow the rapid conjugation of bispecific antibody pairs.

A final consideration in the immediate future of CliBAb platform development is the effect of steric interference upon the ability to join two scFvs. Here, styrene and tetrazine groups were directly appended to the carboxy-terminus of scFvs with very little spacer between the protein and chemical modification. Protein folding may affect the accessibility of these groups and limit their availability to react. Therefore, one remedy to alleviate steric issues would be to synthesize cysteine reagents containing PEG spacers in order to distance the chemical functional groups from the protein and increase their accessibility. In this study, we observed formation of scFv homodimers when a homobifunctional DBCO reagent containing a PEG linker was employed to conjugate the proteins, thus suggesting that a PEG spacer could be key for scFv conjugation. Therefore, we propose a modified CliBAb platform where surface displayed scFvs are modified with tetrazine and TCO chemical groups containing PEG linkers, thus reducing steric effects and providing efficient conjugation reactions (Figure 5-8).

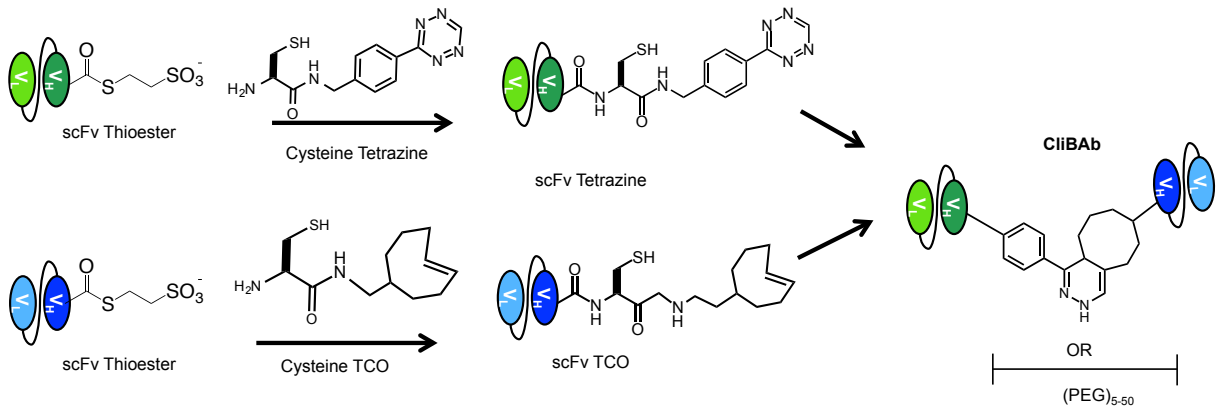

Figure 5-8: Modified CliBAb platform with tetrazine-TCO click
In the new proposed CliBAb platform, proteins will be chemically modified by reacting scFv thioesters with cysteine tetrazine and cysteine TCO. Subsequently, scFv-tetrazine will be combined with scFv-TCO, and the click reaction will enable the formation of a bispecific antibody. PEG linkers can be chemically inserted to help the spatial separation of the scFvs.

In summary, we envision that this clicked bispecific antibody platform will enable the combinatorial pairing of lead antibodies, thus facilitating downstream evaluation of bispecific antibody pairs from a protein engineering platform. While we have yet to demonstrate efficient conjugation of bispecific pairs, this study, along with the previous chapters, lays the foundation for platform development and provides a clear direction for continuing research.

5.5 Supplemental Figures

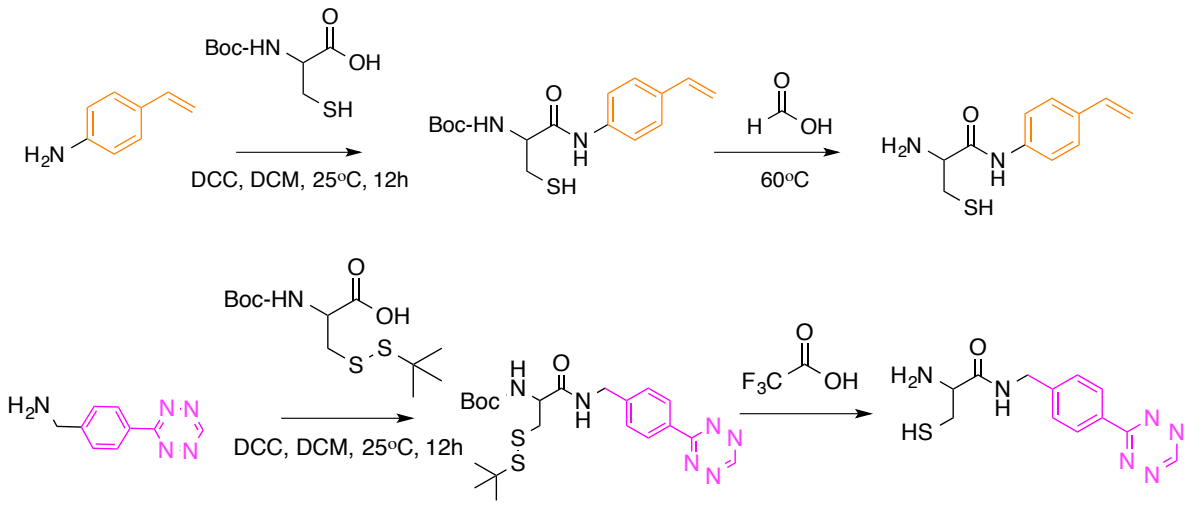

Figure 5-9: Chemical synthesis routes for the cysteine tetrazine and styrene
Cysteine tetrazine and cysteine styrene were synthesized by Kalie Mix.

REFERENCES

1. Alley, S.C., Okeley, N.M., and Senter, P.D., *Antibody–drug conjugates: targeted drug delivery for cancer.* Current Opinion in Chemical Biology, 2010. **14**(4): p. 529-537.
2. Mullard, A., *Maturing antibody-drug conjugate pipeline hits 30.* Nature Reviews Drug Discovery, 2013. **12**(5): p. 329-332.
3. Zolot, R.S., Basu, S., and Million, R.P., *Antibody–drug conjugates.* Nature Reviews Drug Discovery, 2013. **12**(4): p. 259-260.
4. Chapman, A.P., *PEGylated antibodies and antibody fragments for improved therapy: a review.* Advanced drug delivery reviews, 2002. **54**(4): p. 531-545.
5. Alconcel, S.N., Baas, A.S., and Maynard, H.D., *FDA-approved poly (ethylene glycol)–protein conjugate drugs.* Polymer Chemistry, 2011. **2**(7): p. 1442-1448.
6. Fishburn, C.S., *The pharmacology of PEGylation: Balancing PD with PK to generate novel therapeutics.* Journal of Pharmaceutical Sciences, 2008. **97**(10): p. 4167-4183.
7. Zalipsky, S., *Functionalized Poly(ethylene glycols) for Preparation of Biologically Relevant Conjugates.* Bioconjugate Chemistry, 1995. **6**(2): p. 150-165.
8. Rusmini, F., Zhong, Z., and Feijen, J., *Protein Immobilization Strategies for Protein Biochips.* Biomacromolecules, 2007. **8**(6): p. 1775-1789.
9. Silzel, J.W., Cercek, B., Dodson, C., Tsay, T., and Obremski, R.J., *Mass-sensing, multianalyte microarray immunoassay with imaging detection.* Clinical chemistry, 1998. **44**(9): p. 2036-2043.
10. Olle, E.W., Sreekumar, A., Warner, R.L., McClintock, S.D., Chinnaiyan, A.M., Bleavins, M.R., Anderson, T.D., and Johnson, K.J., *Development of an internally controlled antibody microarray.* Molecular & Cellular Proteomics, 2005. **4**(11): p. 1664-1672.
11. Arrabito, G., Reisewitz, S., Dehmelt, L., Bastiaens, P.I., Pignataro, B., Schroeder, H., and Niemeyer, C.M., *Biochips for Cell Biology by Combined Dip-Pen Nanolithography and DNA-Directed Protein Immobilization.* Small, 2013. **9**(24): p. 4243-4249.
12. Hernandez, K. and Fernandez-Lafuente, R., *Control of protein immobilization: Coupling immobilization and site-directed mutagenesis to improve biocatalyst or biosensor performance.* Enzyme and Microbial Technology, 2011. **48**(2): p. 107-122.
13. Williams, R.A. and Blanch, H.W., *Covalent immobilization of protein monolayers for biosensor applications.* Biosensors and Bioelectronics, 1994. **9**(2): p. 159-167.
14. Chen, R.J., Zhang, Y., Wang, D., and Dai, H., *Noncovalent sidewall functionalization of single-walled carbon nanotubes for protein immobilization.* Journal of the American Chemical Society, 2001. **123**(16): p. 3838-3839.
15. Brennan, D.J., O'Connor, D.P., Rexhepaj, E., Ponten, F., and Gallagher, W.M., *Antibody-based proteomics: fast-tracking molecular diagnostics in oncology.* Nature Reviews Cancer, 2010. **10**(9): p. 605-617.

16. El-Sayed, I.H., Huang, X., and El-Sayed, M.A., *Surface plasmon resonance scattering and absorption of anti-EGFR antibody conjugated gold nanoparticles in cancer diagnostics: applications in oral cancer.* Nano letters, 2005. **5**(5): p. 829-834.
17. Stuchinskaya, T., Moreno, M., Cook, M.J., Edwards, D.R., and Russell, D.A., *Targeted photodynamic therapy of breast cancer cells using antibody–phthalocyanine–gold nanoparticle conjugates.* Photochemical & Photobiological Sciences, 2011. **10**(5): p. 822-831.
18. Doppalapudi, V.R., Huang, J., Liu, D., Jin, P., Liu, B., Li, L., Desharnais, J., Hagen, C., Levin, N.J., and Shields, M.J., *Chemical generation of bispecific antibodies.* Proceedings of the National Academy of Sciences, 2010. **107**(52): p. 22611-22616.
19. Kalkhof, S. and Sinz, A., *Chances and pitfalls of chemical cross-linking with amine-reactive N-hydroxysuccinimide esters.* Analytical and bioanalytical chemistry, 2008. **392**(1-2): p. 305-312.
20. Vishwanath, S.K., Watson, C.R., Huang, W., Bachas, L.G., and Bhattacharyya, D., *Kinetic Studies of Site-Specifically and Randomly Immobilized Alkaline Phosphatase on Functionalized Membranes.* Journal of Chemical Technology & Biotechnology, 1997. **68**(3): p. 294-302.
21. Viswanath, S., Wang, J., Bachas, L., Butterfield, D., and Bhattacharyya, D., *Site-directed and random immobilization of subtilisin on functionalized membranes: activity determination in aqueous and organic media.* Biotechnology and bioengineering, 1998. **60**(5): p. 608-616.
22. Peluso, P., Wilson, D.S., Do, D., Tran, H., Venkatasubbaiah, M., Quincy, D., Heidecker, B., Poindexter, K., Tolani, N., Phelan, M., Witte, K., Jung, L.S., Wagner, P., and Nock, S., *Optimizing antibody immobilization strategies for the construction of protein microarrays.* Analytical Biochemistry, 2003. **312**(2): p. 113-124.
23. Kalia, J. and Raines, R.T., *Advances in bioconjugation.* Current organic chemistry, 2010. **14**(2): p. 138.
24. Han, H.S., Yang, S.L., Yeh, H.Y., Lin, J.C., Wu, H.L., and Shi, G.Y., *Studies of a novel human thrombomodulin immobilized substrate: surface characterization and anticoagulation activity evaluation.* Journal of Biomaterials Science, Polymer Edition, 2001. **12**(10): p. 1075-1089.
25. Kochendoerfer, G.G., *Site-specific polymer modification of therapeutic proteins.* Current opinion in chemical biology, 2005. **9**(6): p. 555-560.
26. Cha, T., Guo, A., and Zhu, X.Y., *Enzymatic activity on a chip: the critical role of protein orientation.* Proteomics, 2005. **5**(2): p. 416-419.
27. Cazalis, C.S., Haller, C.A., Sease-Cargo, L., and Chaikof, E.L., *C-terminal site-specific PEGylation of a truncated thrombomodulin mutant with retention of full bioactivity.* Bioconjugate chemistry, 2004. **15**(5): p. 1005-1009.
28. Franco, E.J., Hofstetter, H., and Hofstetter, O., *A comparative evaluation of random and site-specific immobilization techniques for the preparation of antibody-based chiral stationary phases.* Journal of Separation Science, 2006. **29**(10): p. 1458-1469.

29. Jung, Y., Jeong, J., and Chung, B., *Recent advances in immobilization methods of antibodies on solid supports.* The Analyst, 2008. **133**(6): p. 697-701.
30. Sletten, E.M. and Bertozzi, C.R., *Bioorthogonal chemistry: fishing for selectivity in a sea of functionality.* Angewandte Chemie International Edition, 2009. **48**(38): p. 6974-6998.
31. Kalia, J. and Raines, R.T., *Reactivity of Intein Thioesters: Appending a Functional Group to a Protein.* ChemBioChem, 2006. **7**(9): p. 1375-1383.
32. Noren, C.J., Anthony-Cahill, S.J., Griffith, M.C., and Schultz, P.G., *A general method for site-specific incorporation of unnatural amino acids into proteins.* Science, 1989. **244**(4901): p. 182-188.
33. Xie, J. and Schultz, P.G., *Adding amino acids to the genetic repertoire.* Current opinion in chemical biology, 2005. **9**(6): p. 548-554.
34. de Graaf, A.J., Kooijman, M., Hennink, W.E., and Mastrobattista, E., *Nonnatural Amino Acids for Site-Specific Protein Conjugation.* Bioconjugate Chemistry, 2009. **20**(7): p. 1281-1295.
35. Muir, T.W., *Semisynthesis of proteins by expressed protein ligation.* Annual review of biochemistry, 2003. **72**(1): p. 249-289.
36. Muir, T.W., Sondhi, D., and Cole, P.A., *Expressed protein ligation: A general method for protein engineering.* Proceedings of the National Academy of Sciences, 1998. **95**(12): p. 6705-6710.
37. Telenti, A., Southworth, M., Alcaide, F., Daugelat, S., Jacobs, W.R., and Perler, F.B., *The Mycobacterium xenopi GyrA protein splicing element: characterization of a minimal intein.* Journal of bacteriology, 1997. **179**(20): p. 6378-6382.
38. Evans, T.C., Benner, J., and Xu, M.-Q., *Semisynthesis of cytotoxic proteins using a modified protein splicing element.* Protein Science, 1998. **7**(11): p. 2256-2264.
39. Lin, P.C., Ueng, S.H., Tseng, M.C., Ko, J.L., Huang, K.T., Yu, S.C., Adak, A.K., Chen, Y.J., and Lin, C.C., *Site-Specific Protein Modification through CuI-Catalyzed 1,2,3-Triazole Formation and Its Implementation in Protein Microarray Fabrication.* Angewandte Chemie, 2006. **118**(26): p. 4392-4396.
40. Steinhagen, M., Holland-Nell, K., Meldal, M., and Beck-Sickinger, A.G., *Simultaneous "One Pot" Expressed Protein Ligation and Cu^{I}-Catalyzed Azide/Alkyne Cycloaddition for Protein Immobilization.* ChemBioChem, 2011. **12**(16): p. 2426-2430.
41. Elias, D.R., Cheng, Z., and Tsourkas, A., *An Intein-Mediated Site-Specific Click Conjugation Strategy for Improved Tumor Targeting of Nanoparticle Systems.* Small, 2010. **6**(21): p. 2460-2468.
42. Sun, X.L., Stabler, C.L., Cazalis, C.S., and Chaikof, E.L., *Carbohydrate and protein immobilization onto solid surfaces by sequential Diels-Alder and azide-alkyne cycloadditions.* Bioconjugate chemistry, 2006. **17**(1): p. 52-57.
43. Kim, Y.-P., Daniel, W.L., Xia, Z., Xie, H., Mirkin, C.A., and Rao, J., *Bioluminescent nanosensors for protease detection based upon gold nanoparticle–luciferase conjugates.* Chem. Commun., 2010. **46**(1): p. 76-78.
44. Lesaicherre, M.L., Lue, R.Y.P., Chen, G.Y.J., Zhu, Q., and Yao, S.Q., *Intein-Mediated Biotinylation of Proteins and Its Application in a Protein Microarray.* Journal of the American Chemical Society, 2002. **124**(30): p. 8768-8769.

45. Mohlmann, S.B., Peter; Greven, Simone; Harrenga, Axel;, *Site-specific modification of ED-B-targeting antibody using intein-fusion technology.* BMC Biotechnology, 2011. **11**(1): p. 76-85.
46. Gao, W., Liu, W., Christensen, T., Zalutsky, M.R., and Chilkoti, A., *In situ growth of a PEG-like polymer from the C terminus of an intein fusion protein improves pharmacokinetics and tumor accumulation.* Proceedings of the National Academy of Sciences, 2010. **107**(38): p. 16432-16437.
47. Sydor, J.R., Mariano, M., Sideris, S., and Nock, S., *Establishment of Intein-Mediated Protein Ligation under Denaturing Conditions: C-Terminal Labeling of a Single-Chain Antibody for Biochip Screening.* Bioconjugate Chemistry, 2002. **13**(4): p. 707-712.
48. Wood, R.J., Pascoe, D.D., Brown, Z.K., Medlicott, E.M., Kriek, M., Neylon, C., and Roach, P.L., *Optimized Conjugation of a Fluorescent Label to Proteins via Intein-Mediated Activation and Ligation.* Bioconjugate Chemistry, 2004. **15**(2): p. 366-372.
49. Tolbert, T.J. and Wong, C.H., *Intein-Mediated Synthesis of Proteins Containing Carbohydrates and Other Molecular Probes.* Journal of the American Chemical Society, 2000. **122**(23): p. 5421-5428.
50. Camarero, J.A., Kwon, Y., and Coleman, M.A., *Chemoselective Attachment of Biologically Active Proteins to Surfaces by Expressed Protein Ligation and Its Application for "Protein Chip" Fabrication.* Journal of the American Chemical Society, 2004. **126**(45): p. 14730-14731.
51. Kalia, J., Abbott, N.L., and Raines, R.T., *General Method for Site-Specific Protein Immobilization by Staudinger Ligation.* Bioconjugate Chemistry, 2007. **18**(4): p. 1064-1069.
52. Gupta, S.S., Kuzelka, J., Singh, P., Lewis, W.G., Manchester, M., and Finn, M., *Accelerated bioorthogonal conjugation: a practical method for the ligation of diverse functional molecules to a polyvalent virus scaffold.* Bioconjugate Chemistry, 2005. **16**(6): p. 1572-1579.
53. Lutz, J.-F. and Zarafshani, Z., *Efficient construction of therapeutics, bioconjugates, biomaterials and bioactive surfaces using azide–alkyne "click" chemistry.* Advanced drug delivery reviews, 2008. **60**(9): p. 958-970.
54. Kolb, H.C., Finn, M., and Sharpless, K.B., *Click chemistry: diverse chemical function from a few good reactions.* Angewandte Chemie International Edition, 2001. **40**(11): p. 2004-2021.
55. Deiters, A., Cropp, T.A., Summerer, D., Mukherji, M., and Schultz, P.G., *Site-specific PEGylation of proteins containing unnatural amino acids.* Bioorganic & Medicinal Chemistry Letters, 2004. **14**(23): p. 5743-5745.
56. Peschke, B., Zundel, M., Bak, S., Clausen, T.R., Blume, N., Pedersen, A., Zaragoza, F., and Madsen, K., *C-Terminally PEGylated hGH-derivatives.* Bioorganic & Medicinal Chemistry, 2007. **15**(13): p. 4382-4395.
57. Hong, V., Presolski, S.I., Ma, C., and Finn, M., *Analysis and Optimization of Copper‐Catalyzed Azide‐Alkyne Cycloaddition for Bioconjugation.* Angewandte Chemie International Edition, 2009. **48**(52): p. 9879-9883.

58. Gauchet, C., Labadie, G.R., and Poulter, C.D., *Regio-and chemoselective covalent immobilization of proteins through unnatural amino acids.* Journal of the American Chemical Society, 2006. **128**(29): p. 9274-9275.
59. Gaetke, L.M. and Chow, C.K., *Copper toxicity, oxidative stress, and antioxidant nutrients.* Toxicology, 2003. **189**(1): p. 147-163.
60. Hong, V., Steinmetz, N.F., Manchester, M., and Finn, M.G., *Labeling Live Cells by Copper-Catalyzed Alkyne−Azide Click Chemistry.* Bioconjugate Chemistry, 2010. **21**(10): p. 1912-1916.
61. Speers, A.E., Adam, G.C., and Cravatt, B.F., *Activity-based protein profiling in vivo using a copper (I)-catalyzed azide-alkyne [3+ 2] cycloaddition.* Journal of the American Chemical Society, 2003. **125**(16): p. 4686-4687.
62. Wang, Q., Chan, T.R., Hilgraf, R., Fokin, V.V., Sharpless, K.B., and Finn, M., *Bioconjugation by copper (I)-catalyzed azide-alkyne [3+ 2] cycloaddition.* Journal of the American Chemical Society, 2003. **125**(11): p. 3192-3193.
63. Agard, N.J., Prescher, J.A., and Bertozzi, C.R., *A Strain-Promoted [3 + 2] Azide−Alkyne Cycloaddition for Covalent Modification of Biomolecules in Living Systems.* Journal of the American Chemical Society, 2004. **126**(46): p. 15046-15047.
64. Chang, P.V., Prescher, J.A., Sletten, E.M., Baskin, J.M., Miller, I.A., Agard, N.J., Lo, A., and Bertozzi, C.R., *Copper-free click chemistry in living animals.* Proceedings of the National Academy of Sciences, 2010. **107**(5): p. 1821-1826.
65. Baskin, J.M., Prescher, J.A., Laughlin, S.T., Agard, N.J., Chang, P.V., Miller, I.A., Lo, A., Codelli, J.A., and Bertozzi, C.R., *Copper-free click chemistry for dynamic in vivo imaging.* Proceedings of the National Academy of Sciences, 2007. **104**(43): p. 16793-16797.
66. Marks, I.S., Kang, J.S., Jones, B.T., Landmark, K.J., Cleland, A.J., and Taton, T.A., *Strain-promoted "click" chemistry for terminal labeling of DNA.* Bioconjugate chemistry, 2011. **22**(7): p. 1259-1263.
67. Campbell‐Verduyn, L.S., Mirfeizi, L., Schoonen, A.K., Dierckx, R.A., Elsinga, P.H., and Feringa, B.L., *Strain‐Promoted Copper‐Free "Click" Chemistry for 18F Radiolabeling of Bombesin.* Angewandte Chemie International Edition, 2011. **50**(47): p. 11117-11120.
68. Codelli, J.A., Baskin, J.M., Agard, N.J., and Bertozzi, C.R., *Second-generation difluorinated cyclooctynes for copper-free click chemistry.* Journal of the American Chemical Society, 2008. **130**(34): p. 11486-11493.
69. Karver, M.R., Weissleder, R., and Hilderbrand, S.A., *Bioorthogonal Reaction Pairs Enable Simultaneous, Selective, Multi‐Target Imaging.* Angewandte Chemie International Edition, 2012. **51**(4): p. 920-922.
70. Rossin, R., van den Bosch, S.M., ten Hoeve, W., Carvelli, M., Versteegen, R.M., Lub, J., and Robillard, M.S., *Highly Reactive trans-Cyclooctene Tags with Improved Stability for Diels–Alder Chemistry in Living Systems.* Bioconjugate Chemistry, 2013. **24**(7): p. 1210-1217.
71. Devaraj, N.K., Upadhyay, R., Haun, J.B., Hilderbrand, S.A., and Weissleder, R., *Fast and sensitive pretargeted labeling of cancer cells through a tetrazine/trans‐cyclooctene cycloaddition.* Angewandte Chemie International Edition, 2009. **48**(38): p. 7013-7016.

72. Karver, M.R., Weissleder, R., and Hilderbrand, S.A., *Synthesis and evaluation of a series of 1, 2, 4, 5-tetrazines for bioorthogonal conjugation.* Bioconjugate chemistry, 2011. **22**(11): p. 2263-2270.
73. Selvaraj, R., Liu, S., Hassink, M., Huang, C.-w., Yap, L.-p., Park, R., Fox, J.M., Li, Z., and Conti, P.S., *Tetrazine-trans-cyclooctene ligation for the rapid construction of integrin αvβ3 targeted PET tracer based on a cyclic RGD peptide.* Bioorganic & Medicinal Chemistry Letters, 2011. **21**(17): p. 5011-5014.
74. Liu, S., Hassink, M., Selvaraj, R., Yap, L.-P., Park, R., Wang, H., Chen, X., Fox, J.M., Li, Z., and Conti, P.S., *Efficient 18F labeling of cysteine containing peptides and proteins using the tetrazine-trans-cyclooctene ligation.* Molecular imaging, 2013. **12**(2): p. 121.
75. Lang, K., Davis, L., Wallace, S., Mahesh, M., Cox, D.J., Blackman, M.L., Fox, J.M., and Chin, J.W., *Genetic encoding of bicyclononynes and trans-cyclooctenes for site-specific protein labeling in vitro and in live mammalian cells via rapid fluorogenic Diels–Alder reactions.* Journal of the American Chemical Society, 2012. **134**(25): p. 10317-10320.
76. Verma, R., Boleti, E., and George, A.J.T., *Antibody engineering: Comparison of bacterial, yeast, insect and mammalian expression systems.* Journal of Immunological Methods, 1998. **216**(1–2): p. 165-181.
77. Albertsen, L., Shaw, A.C., Norrild, J.C., and Strømgaard, K., *Recombinant production of peptide C-terminal α-amides using an engineered intein.* Bioconjugate chemistry, 2013. **24**(11): p. 1883-1894.
78. Machova, Z., Mühle, C., Krauss, U., Tréhin, R., Koch, A., Merkle, H.P., and Beck-Sickinger, A.G., *Cellular Internalization of Enhanced Green Fluorescent Protein Ligated to a Human Calcitonin-Based Carrier Peptide.* ChemBioChem, 2002. **3**(7): p. 672-677.
79. Mathys, S., Evans Jr, T.C., Chute, I.C., Wu, H., Chong, S., Benner, J., Liu, X.-Q., and Xu, M.-Q., *Characterization of a self-splicing mini-intein and its conversion into autocatalytic N- and C-terminal cleavage elements: facile production of protein building blocks for protein ligation.* Gene, 1999. **231**(1–2): p. 1-13.
80. Guo, C., Li, Z., Shi, Y., Xu, M., Wise, J.G., Trommer, W.E., and Yuan, J., *Intein-mediated fusion expression, high efficient refolding, and one-step purification of gelonin toxin.* Protein Expression and Purification, 2004. **37**(2): p. 361-367.
81. Cui, C., Zhao, W., Chen, J., Wang, J., and Li, Q., *Elimination of in vivo cleavage between target protein and intein in the intein-mediated protein purification systems.* Protein expression and purification, 2006. **50**(1): p. 74-81.
82. Shah, N.H., Eryilmaz, E., Cowburn, D., and Muir, T.W., *Naturally Split Inteins Assemble through a "Capture and Collapse" Mechanism.* Journal of the American Chemical Society, 2013. **135**(49): p. 18673-18681.
83. Lilie, H., Schwarz, E., and Rudolph, R., *Advances in refolding of proteins produced in E. coli.* Current opinion in biotechnology, 1998. **9**(5): p. 497.
84. Singh, S.M. and Panda, A.K., *Solubilization and refolding of bacterial inclusion body proteins.* Journal of bioscience and bioengineering, 2005. **99**(4): p. 303-310.

85. Kurucz, I., Titus, J.A., Jost, C.R., and Segal, D.M., *Correct disulfide pairing and efficient refolding of detergent-solubilized single-chain Fv proteins from bacterial inclusion bodies.* Molecular Immunology, 1995. **32**(17–18): p. 1443-1452.
86. Arnold, U., Hinderaker, M.P., Köditz, J., Golbik, R., Ulbrich-Hofmann, R., and Raines, R.T., *Protein Prosthesis: A Nonnatural Residue Accelerates Folding and Increases Stability.* Journal of the American Chemical Society, 2003. **125**(25): p. 7500-7501.
87. Bastings, M.M.C., Van Baal, I., Meijer, E., and Merkx, M., *One-step refolding and purification of disulfide-containing proteins with a C-terminal MESNA thioester.* BMC Biotechnology, 2008. **8**(1): p. 76.
88. Wülfing, C. and Plückthun, A., *Protein folding in the periplasm of Escherichia coli.* Molecular microbiology, 1994. **12**(5): p. 685-692.
89. Reulen, S.W., van Baal, I., Raats, J.M., and Merkx, M., *Efficient, chemoselective synthesis of immunomicelles using single-domain antibodies with a C-terminal thioester.* BMC biotechnology, 2009. **9**(1): p. 66.
90. Wu, W.Y., Miller, K.D., Coolbaugh, M., and Wood, D.W., *Intein-mediated one-step purification of Escherichia coli secreted human antibody fragments.* Protein expression and purification, 2011. **76**(2): p. 221-228.
91. Deschuyteneer, G.v., Garcia, S.p., Michiels, B., Baudoux, B., Degand, H., Morsomme, P., and Soumillion, P., *Intein-Mediated Cyclization of Randomized Peptides in the Periplasm of Escherichia coli and Their Extracellular Secretion.* ACS Chemical Biology, 2010. **5**(7): p. 691-700.
92. Guo, J.-Q., Li, Q.-M., Zhou, J.-Y., Zhang, G.-P., Yang, Y.-Y., Xing, G.-X., Zhao, D., You, S.-Y., and Zhang, C.-Y., *Efficient recovery of the functional IP10-scFv fusion protein from inclusion bodies with an on-column refolding system.* Protein Expression and Purification, 2006. **45**(1): p. 168-174.
93. Kipriyanov, S.M., Little, M., Kropshofer, H., Breitling, F., Gotter, S., and Dübel, S., *Affinity enhancement of a recombinant antibody: formation of complexes with multiple valency by a single-chain Fv fragment–core streptavidin fusion.* Protein Engineering, 1996. **9**(2): p. 203-211.
94. Kipriyanov, S.M., Moldenhauer, G., and Little, M., *High level production of soluble single chain antibodies in small-scale Escherichia coli cultures.* Journal of Immunological Methods, 1997. **200**(1–2): p. 69-77.
95. Tsumoto, K., Ogasahara, K., Ueda, Y., Watanabe, K., Yutani, K., and Kumagai, I., *Role of Tyr residues in the contact region of anti-lysozyme monoclonal antibody HyHEL10 for antigen binding.* Journal of Biological Chemistry, 1995. **270**(31): p. 18551-18557.
96. Buckholz, R.G. and Gleeson, M.A., *Yeast systems for the commercial production of heterologous proteins.* Nature Biotechnology, 1991. **9**(11): p. 1067-1072.
97. Romanos, M.A., Scorer, C.A., and Clare, J.J., *Foreign gene expression in yeast: a review.* Yeast, 1992. **8**(6): p. 423-488.
98. Hackel, B.J., Huang, D., Bubolz, J.C., Wang, X.X., and Shusta, E.V., *Production of soluble and active transferrin receptor-targeting single-chain antibody using Saccharomyces cerevisiae.* Pharmaceutical research, 2006. **23**(4): p. 790-797.

99. Shusta, E.V., Raines, R.T., Plückthun, A., and Wittrup, K.D., *Increasing the secretory capacity of Saccharomyces cerevisiae for production of single-chain antibody fragments.* Nature biotechnology, 1998. **16**(8): p. 773-777.
100. Wentz, A.E. and Shusta, E.V., *Enhanced Secretion of Heterologous Proteins from Yeast by Overexpression of Ribosomal Subunit RPP0.* Biotechnology Progress, 2008. **24**(3): p. 748-756.
101. Huang, D. and Shusta, E.V., *Secretion and Surface Display of Green Fluorescent Protein Using the Yeast Saccharomyces cerevisiae.* Biotechnology Progress, 2005. **21**(2): p. 349-357.
102. Chao, G., Cochran, J.R., and Dane Wittrup, K., *Fine epitope mapping of anti-epidermal growth factor receptor antibodies through random mutagenesis and yeast surface display.* Journal of molecular biology, 2004. **342**(2): p. 539-550.
103. Huang, D. and Shusta, E.V., *A yeast platform for the production of single-chain antibody-green fluorescent protein fusions.* Applied and environmental microbiology, 2006. **72**(12): p. 7748-7759.
104. Hackel, B.J., Kapila, A., and Dane Wittrup, K., *Picomolar affinity fibronectin domains engineered utilizing loop length diversity, recursive mutagenesis, and loop shuffling.* Journal of molecular biology, 2008. **381**(5): p. 1238-1252.
105. Boder, E.T. and Wittrup, K.D., *Yeast surface display for screening combinatorial polypeptide libraries.* Nature biotechnology, 1997. **15**(6): p. 553-557.
106. Pepper, L.R., Cho, Y.K., Boder, E.T., and Shusta, E.V., *A decade of yeast surface display technology: where are we now?* Combinatorial chemistry & high throughput screening, 2008. **11**(2): p. 127.
107. Chao, G., Lau, W.L., Hackel, B.J., Sazinsky, S.L., Lippow, S.M., and Wittrup, K.D., *Isolating and engineering human antibodies using yeast surface display.* Nature protocols, 2006. **1**(2): p. 755-768.
108. Feldhaus, M.J., Siegel, R.W., Opresko, L.K., Coleman, J.R., Feldhaus, J.M.W., Yeung, Y.A., Cochran, J.R., Heinzelman, P., Colby, D., and Swers, J., *Flow-cytometric isolation of human antibodies from a nonimmune Saccharomyces cerevisiae surface display library.* Nature biotechnology, 2003. **21**(2): p. 163-170.
109. Bowley, D., Labrijn, A., Zwick, M., and Burton, D., *Antigen selection from an HIV-1 immune antibody library displayed on yeast yields many novel antibodies compared to selection from the same library displayed on phage.* Protein Engineering Design and Selection, 2007. **20**(2): p. 81-90.
110. Shusta, E.V., Kieke, M.C., Parke, E., Kranz, D.M., and Wittrup, K.D., *Yeast polypeptide fusion surface display levels predict thermal stability and soluble secretion efficiency.* Journal of molecular biology, 1999. **292**(5): p. 949-956.
111. Blaise, L., Wehnert, A., Steukers, M.P., van den Beucken, T., Hoogenboom, H.R., and Hufton, S.E., *Construction and diversification of yeast cell surface displayed libraries by yeast mating: application to the affinity maturation of Fab antibody fragments.* Gene, 2004. **342**(2): p. 211-218.
112. Holler, P.D., Holman, P.O., Shusta, E.V., O'Herrin, S., Wittrup, K.D., and Kranz, D.M., *In vitro evolution of a T cell receptor with high affinity for peptide/MHC.* Proceedings of the National Academy of Sciences, 2000. **97**(10): p. 5387-5392.
113. Tillotson, B.J., de Larrinoa, I.F., Skinner, C.A., Klavas, D.M., and Shusta, E.V., *Antibody affinity maturation using yeast display with detergent-solubilized*

membrane proteins as antigen sources. Protein Engineering Design and Selection, 2012: p. gzs077.
114. Chen, C.-P., Hsieh, Y.-T., Prijovich, Z.M., Chuang, H.-Y., Chen, K.-C., Lu, W.-C., Tseng, Q., Leu, Y.-L., Cheng, T.-L., and Roffler, S.R., *ECSTASY, an adjustable membrane-tethered/soluble protein expression system for the directed evolution of mammalian proteins.* Protein Engineering Design and Selection, 2012. **25**(7): p. 367-375.
115. Kato, M., Maeda, H., Kawakami, M., Shiraga, S., and Ueda, M., *Construction of a selective cleavage system for a protein displayed on the cell surface of yeast.* Applied microbiology and biotechnology, 2005. **69**(4): p. 423-427.
116. de Araújo, A.D., Palomo, J.M., Cramer, J., Köhn, M., Schröder, H., Wacker, R., Niemeyer, C., Alexandrov, K., and Waldmann, H., *Diels–Alder Ligation and Surface Immobilization of Proteins.* Angewandte Chemie, International Edition, 2006. **45**(2): p. 296-301.
117. Khan, F., He, M., and Taussig, M.J., *Double-Hexahistidine Tag with High-Affinity Binding for Protein Immobilization, Purification, and Detection on Ni−Nitrilotriacetic Acid Surfaces.* Analytical Chemistry, 2006. **78**(9): p. 3072-3079.
118. Soellner, M.B., Dickson, K.A., Nilsson, B.L., and Raines, R.T., *Site-Specific Protein Immobilization by Staudinger Ligation.* Journal of the American Chemical Society, 2003. **125**(39): p. 11790-11791.
119. Junutula, J.R., Raab, H., Clark, S., Bhakta, S., Leipold, D.D., Weir, S., Chen, Y., Simpson, M., Tsai, S.P., and Dennis, M.S., *Site-specific conjugation of a cytotoxic drug to an antibody improves the therapeutic index.* Nature biotechnology, 2008. **26**(8): p. 925-932.
120. Liu, X.M., Thakur, A., and Wang, D., *Efficient synthesis of linear multifunctional poly(ethylene glycol) by copper(I)-catalyzed Huisgen 1,3-dipolar cycloaddition.* Biomacromolecules, 2007. **8**(9): p. 2653-2658.
121. Chen, I., Howarth, M., Lin, W., and Ting, A.Y., *Site-specific labeling of cell surface proteins with biophysical probes using biotin ligase.* Nature methods, 2005. **2**(2): p. 99-104.
122. Gaertner, H.F. and Offord, R.E., *Site-Specific Attachment of Functionalized Poly(ethylene glycol) to the Amino Terminus of Proteins.* Bioconjugate Chemistry, 1996. **7**(1): p. 38-44.
123. Huang, W., Wang, J., Bhattacharyya, D., and Bachas, L.G., *Improving the Activity of Immobilized Subtilisin by Site-Specific Attachment to Surfaces.* Analytical Chemistry, 1997. **69**(22): p. 4601-4607.
124. Fong, B.A., Wu, W.-Y., and Wood, D.W., *The potential role of self-cleaving purification tags in commercial-scale processes.* Trends in Biotechnology, 2010. **28**(5): p. 272-279.
125. Wang, D. and Cole, P.A., *Protein Tyrosine Kinase Csk-Catalyzed Phosphorylation of Src Containing Unnatural Tyrosine Analogues.* Journal of the American Chemical Society, 2001. **123**(37): p. 8883-8886.
126. Hyland, S., Beerli, R.R., Barbas, C.F., Hynes, N.E., and Wels, W., *Generation and functional characterization of intracellular antibodies interacting with the kinase domain of human EGF receptor.* Oncogene, 2003. **22**(10): p. 1557-67.

127. Gietz, R.D. and Schiestl, R.H., *High-efficiency yeast transformation using the LiAc/SS carrier DNA/PEG method.* Nature protocols, 2007. **2**(1): p. 31-34.
128. Muralidharan, V. and Muir, T.W., *Protein ligation: an enabling technology for the biophysical analysis of proteins.* Nature methods, 2006. **3**(6): p. 429-438.
129. Wörn, A. and Plückthun, A., *Stability engineering of antibody single-chain Fv fragments.* Journal of molecular biology, 2001. **305**(5): p. 989-1010.
130. Wang, X.X., Cho, Y.K., and Shusta, E.V., *Mining a yeast library for brain endothelial cell-binding antibodies.* Nature methods, 2007. **4**(2): p. 143-145.
131. Shusta, E.V., Holler, P.D., Kieke, M.C., Kranz, D.M., and Wittrup, K.D., *Directed evolution of a stable scaffold for T-cell receptor engineering.* Nature biotechnology, 2000. **18**(7): p. 754-759.
132. Bradbury, A.R.M., Sidhu, S., Dübel, S., and McCafferty, J., *Beyond natural antibodies: the power of in vitro display technologies.* Nature biotechnology, 2011. **29**(3): p. 245-254.
133. Parthasarathy, R., Bajaj, J., and Boder, E.T., *An Immobilized Biotin Ligase: Surface Display of Escherichia coli BirA on Saccharomycescerevisiae.* Biotechnology progress, 2005. **21**(6): p. 1627-1631.
134. Bundy, B.C. and Swartz, J.R., *Site-Specific Incorporation of p-Propargyloxyphenylalanine in a Cell-Free Environment for Direct Protein−Protein Click Conjugation.* Bioconjugate Chemistry, 2010. **21**(2): p. 255-263.
135. Li, M., De, P., Gondi, S.R., and Sumerlin, B.S., *Responsive polymer‐protein bioconjugates prepared by RAFT polymerization and copper‐catalyzed azide‐alkyne click chemistry.* Macromolecular Rapid Communications, 2008. **29**(12‐13): p. 1172-1176.
136. Chaisemartin, L., Chinestra, P., Favre, G., Blonski, C., and Faye, J.C., *Synthesis and Application of a N-1′ Fluorescent Biotinyl Derivative Inducing the Specific Carboxy-Terminal Dual Labeling of a Novel RhoB-Selective scFv.* Bioconjugate Chemistry, 2009. **20**(5): p. 847-855.
137. Angenendt, P., Glökler, J., Sobek, J., Lehrach, H., and Cahill, D.J., *Next generation of protein microarray support materials: Evaluation for protein and antibody microarray applications.* Journal of Chromatography A, 2003. **1009**(1): p. 97-104.
138. Olle, E.W., Messamore, J., Deogracias, M.P., McClintock, S.D., Anderson, T.D., and Johnson, K.J., *Comparison of antibody array substrates and the use of glycerol to normalize spot morphology.* Experimental and molecular pathology, 2005. **79**(3): p. 206-209.
139. Willats, W., Rasmussen, S., Kristensen, T., Mikkelsen, J., and Knox, J., *Sugar-coated microarrays: a novel slide surface for the high-throughput analysis of glycans.* Proteomics, 2002. **2**(12): p. 1666.
140. Adams, G., Shaller, C., Chappell, L., Wu, C., Horak, E., Simmons, H., Litwin, S., Marks, J., Weiner, L., and Brechbiel, M., *Delivery of the α-emitting radioisotope bismuth-213 to solid tumors via single-chain Fv and diabody molecules.* Nuclear medicine and biology, 2000. **27**(4): p. 339-346.
141. Kuimova, M.K., Bhatti, M., Deonarain, M., Yahioglu, G., Levitt, J.A., Stamati, I., Suhling, K., and Phillips, D., *Fluorescence characterisation of multiply-loaded*

anti-HER2 single chain Fv-photosesitizer conjugates suitable for photodynamic therapy. Photochemical & Photobiological Sciences, 2007. **6**(9): p. 933-939.

142. Nielsen, U.B., Kirpotin, D.B., Pickering, E.M., Hong, K., Park, J.W., Refaat Shalaby, M., Shao, Y., Benz, C.C., and Marks, J.D., *Therapeutic efficacy of anti-ErbB2 immunoliposomes targeted by a phage antibody selected for cellular endocytosis.* Biochimica et Biophysica Acta (BBA) - Molecular Cell Research, 2002. **1591**(1–3): p. 109-118.
143. Natarajan, A., Xiong, C.Y., Albrecht, H., DeNardo, G.L., and DeNardo, S.J., *Characterization of site-specific ScFv PEGylation for tumor-targeting pharmaceuticals.* Bioconjugate chemistry, 2005. **16**(1): p. 113-121.
144. Lu, R.M., Chang, Y.L., Chen, M.S., and Wu, H.C., *Single chain anti-c-Met antibody conjugated nanoparticles for in vivo tumor-targeted imaging and drug delivery.* Biomaterials, 2011. **32**(12): p. 3265-3274.
145. Marshall, C.J., Agarwal, N., Kalia, J., Grosskopf, V.A., McGrath, N.A., Abbott, N.L., Raines, R.T., and Shusta, E.V., *Facile chemical functionalization of proteins through intein-linked yeast display.* Bioconjugate chemistry, 2013. **24**(9): p. 1634-1644.
146. Valiyaveetil, F.I., MacKinnon, R., and Muir, T.W., *Semisynthesis and Folding of the Potassium Channel KcsA.* Journal of the American Chemical Society, 2002. **124**(31): p. 9113-9120.
147. Starwalt, S.E., Masteller, E.L., Bluestone, J.A., and Kranz, D.M., *Directed evolution of a single-chain class II MHC product by yeast display.* Protein Engineering Design and Selection, 2003. **16**(2): p. 147-156.
148. Piatesi, A., Howland, S.W., Rakestraw, J.A., Renner, C., Robson, N., Cebon, J., Maraskovsky, E., Ritter, G., Old, L., and Wittrup, K.D., *Directed evolution for improved secretion of cancer–testis antigen NY-ESO-1 from yeast.* Protein Expression and Purification, 2006. **48**(2): p. 232-242.
149. Rakestraw, J.A., Sazinsky, S.L., Piatesi, A., Antipov, E., and Wittrup, K.D., *Directed evolution of a secretory leader for the improved expression of heterologous proteins and full-length antibodies in Saccharomyces cerevisiae.* Biotechnology and bioengineering, 2009. **103**(6): p. 1192-1201.
150. Adam, E. and Perler, F.B., *Development of a positive genetic selection system for inhibition of protein splicing using mycobacterial inteins in Escherichia coli DNA gyrase subunit A.* Journal of molecular microbiology and biotechnology, 2002. **4**(5): p. 479-488.
151. Cann, I.K., Amaya, K.R., Southworth, M.W., and Perler, F.B., *Bacteriophage-based genetic system for selection of nonsplicing inteins.* Applied and environmental microbiology, 2004. **70**(5): p. 3158-3162.
152. Zeidler, M.P., Tan, C., Bellaiche, Y., Cherry, S., Häder, S., Gayko, U., and Perrimon, N., *Temperature-sensitive control of protein activity by conditionally splicing inteins.* Nature biotechnology, 2004. **22**(7): p. 871-876.
153. Buskirk, A.R., Ong, Y.-C., Gartner, Z.J., and Liu, D.R., *Directed evolution of ligand dependence: small-molecule-activated protein splicing.* Proceedings of the National Academy of Sciences of the United States of America, 2004. **101**(29): p. 10505-10510.

154. Lorimer, I.A., Keppler-Hafkemeyer, A., Beers, R.A., Pegram, C.N., Bigner, D.D., and Pastan, I., *Recombinant immunotoxins specific for a mutant epidermal growth factor receptor: targeting with a single chain antibody variable domain isolated by phage display.* Proceedings of the National Academy of Sciences, 1996. **93**(25): p. 14815-14820.
155. Zhou, Y., Drummond, D.C., Zou, H., Hayes, M.E., Adams, G.P., Kirpotin, D.B., and Marks, J.D., *Impact of Single-chain Fv Antibody Fragment Affinity on Nanoparticle Targeting of Epidermal Growth Factor Receptor-expressing Tumor Cells.* Journal of Molecular Biology, 2007. **371**(4): p. 934-947.
156. Marks, J.D. and Zhou, Y., *Mutant antibodies with high affinity for EGFR*. 2010, Google Patents.
157. Zaccolo, M., Williams, D.M., Brown, D.M., and Gherardi, E., *An approach to random mutagenesis of DNA using mixtures of triphosphate derivatives of nucleoside analogues.* Journal of molecular biology, 1996. **255**(4): p. 589-603.
158. Ness, J.E., Kim, S., Gottman, A., Pak, R., Krebber, A., Borchert, T.V., Govindarajan, S., Mundorff, E.C., and Minshull, J., *Synthetic shuffling expands functional protein diversity by allowing amino acids to recombine independently.* Nature biotechnology, 2002. **20**(12): p. 1251-1255.
159. Stemmer, W.P., Crameri, A., Ha, K.D., Brennan, T.M., and Heyneker, H.L., *Single-step assembly of a gene and entire plasmid from large numbers of oligodeoxyribonucleotides.* Gene, 1995. **164**(1): p. 49-53.
160. Wiepz, G., Guadaramma, A., Fulgham, D., and Bertics, P., *Purification and assay of kinase-active EGF receptor from mammalian cells by immunoaffinity chromatography.* Methods in molecular biology 2006. **327**: p. 25.
161. Cho, Y.K., Chen, I., Wei, X., Li, L., and Shusta, E.V., *A yeast display immunoprecipitation method for efficient isolation and characterization of antigens.* Journal of immunological methods, 2009. **341**(1): p. 117-126.
162. Boder, E.T., Midelfort, K.S., and Wittrup, K.D., *Directed evolution of antibody fragments with monovalent femtomolar antigen-binding affinity.* Proceedings of the National Academy of Sciences, 2000. **97**(20): p. 10701-10705.
163. Romanelli, A., Shekhtman, A., Cowburn, D., and Muir, T.W., *Semisynthesis of a segmental isotopically labeled protein splicing precursor: NMR evidence for an unusual peptide bond at the N-extein–intein junction.* Proceedings of the National Academy of Sciences of the United States of America, 2004. **101**(17): p. 6397-6402.
164. Klabunde, T., Sharma, S., Telenti, A., Jacobs, W.R., and Sacchettini, J.C., *Crystal structure of GyrA intein from Mycobacterium xenopi reveals structural basis of protein splicing.* Nature Structural & Molecular Biology, 1998. **5**(1): p. 31-36.
165. Wentz, A.E. and Shusta, E.V., *A novel high-throughput screen reveals yeast genes that increase secretion of heterologous proteins.* Applied and environmental microbiology, 2007. **73**(4): p. 1189-1198.
166. Guo, J.Q., Li, Q.M., Zhou, J.Y., Zhang, G.P., Yang, Y.Y., Xing, G.X., Zhao, D., You, S.Y., and Zhang, C.Y., *Efficient recovery of the functional IP10-scFv fusion protein from inclusion bodies with an on-column refolding system.* Protein Expression and Purification, 2006. **45**(1): p. 168-174.

167. Verma, R., Boleti, E., and George, A., *Antibody engineering: comparison of bacterial, yeast, insect and mammalian expression systems.* Journal of immunological methods, 1998. **216**(1): p. 165-181.
168. Southworth, M.W., Amaya, K., Evans, T.C., Xu, M.-Q., and Perler, F.B., *Purification of proteins fused to either the amino or carboxy terminus of the Mycobacterium xenopi gyrase A intein.* Biotechniques, 1999. **27**(1): p. 110-4, 116, 118-20.
169. Rostovtsev, V.V., Green, L.G., Fokin, V.V., and Sharpless, K.B., *A stepwise huisgen cycloaddition process: copper (I)-catalyzed regioselective "ligation" of azides and terminal alkynes.* Angewandte Chemie, 2002. **114**(14): p. 2708-2711.
170. Dennler, P., Chiotellis, A., Fischer, E., Brégeon, D., Belmant, C., Gauthier, L., Lhospice, F., Romagne, F., and Schibli, R., *Transglutaminase-Based Chemo-Enzymatic Conjugation Approach Yields Homogeneous Antibody–Drug Conjugates.* Bioconjugate Chemistry, 2014. **25**(3): p. 569-578.
171. Thomas, J.D., Cui, H., North, P., J, Hofer, T., Rader, C., and Burke Jr, T.R., *Application of Strain-Promoted Azide–Alkyne Cycloaddition and Tetrazine Ligation to Targeted Fc-Drug Conjugates.* Bioconjugate chemistry, 2012. **23**(10): p. 2007-2013.
172. Colombo, M., Sommaruga, S., Mazzucchelli, S., Polito, L., Verderio, P., Galeffi, P., Corsi, F., Tortora, P., and Prosperi, D., *Site-Specific Conjugation of ScFvs Antibodies to Nanoparticles by Bioorthogonal Strain-Promoted Alkyne–Nitrone Cycloaddition.* Angewandte Chemie, 2012. **124**(2): p. 511-514.
173. Kotagiri, N., Li, Z., Xu, X., Mondal, S., Nehorai, A., and Achilefu, S., *Antibody Quantum Dot Conjugates Developed via Copper-Free Click Chemistry for Rapid Analysis of Biological Samples Using a Microfluidic Microsphere Array System.* Bioconjugate Chemistry, 2014. **25**(7): p. 1272-1281.
174. Yarden, Y., *The EGFR family and its ligands in human cancer: signalling mechanisms and therapeutic opportunities.* European Journal of Cancer, 2001. **37**(Supplement 4): p. 3-8.
175. Herbst, R.S., *Review of epidermal growth factor receptor biology.* International Journal of Radiation Oncology*Biology*Physics, 2004. **59**(2, Supplement 1): p. S21-S26.
176. Sebastian, S., Settleman, J., Reshkin, S.J., Azzariti, A., Bellizzi, A., and Paradiso, A., *The complexity of targeting EGFR signalling in cancer: From expression to turnover.* Biochimica et Biophysica Acta (BBA) - Reviews on Cancer, 2006. **1766**(1): p. 120-139.
177. Arteaga, C.L., *Epidermal Growth Factor Receptor Dependence in Human Tumors: More Than Just Expression?* Oncologist, 2002. **7**(90004): p. 31-39.
178. Baselga, J., *The EGFR as a target for anticancer therapy--focus on cetuximab.* European Journal of Cancer, 2001. **37**(Supplement 4): p. 16-22.
179. Marchetti, A., Martella, C., Felicioni, L., Barassi, F., Salvatore, S., Chella, A., Camplese, P.P., Iarussi, T., Mucilli, F., Mezzetti, A., Cuccurullo, F., Sacco, R., and Buttitta, F., *EGFR Mutations in Non–Small-Cell Lung Cancer: Analysis of a Large Series of Cases and Development of a Rapid and Sensitive Method for Diagnostic Screening With Potential Implications on Pharmacologic Treatment.* Journal of Clinical Oncology, 2005. **23**(4): p. 857-865.

180. Lynch, T.J., *Activating Mutations in the Epidermal Growth Factor Receptor Underlying Responsiveness of Non Small-Cell Lung Cancer to Gefitinib.* New England Journal of Medicine, 2004. **350**(21): p. 2129-2139.
181. Pao, W., Miller, V., Zakowski, M., Doherty, J., Politi, K., Sarkaria, I., Singh, B., Heelan, R., Rusch, V., Fulton, L., Mardis, E., Kupfer, D., Wilson, R., Kris, M., and Varmus, H., *EGF Receptor Gene Mutations Are Common in Lung Cancers from "Never Smokers" and Are Associated with Sensitivity of Tumors to Gefitinib and Erlotinib.* Proceedings of the National Academy of Sciences of the United States of America, 2004. **101**(36): p. 13306-13311.
182. Paez, J.G., JÃ¤nne, P.A., Lee, J.C., Tracy, S., Greulich, H., Gabriel, S., Herman, P., Kaye, F.J., Lindeman, N., Boggon, T.J., Naoki, K., Sasaki, H., Fujii, Y., Eck, M.J., Sellers, W.R., Johnson, B.E., and Meyerson, M., *EGFR Mutations in Lung Cancer: Correlation with Clinical Response to Gefitinib Therapy.* Science, 2004. **304**(5676): p. 1497-1500.
183. Yu, J., Kane, S., Wu, J., Benedettini, E., Li, D., Reeves, C., Innocenti, G., Wetzel, R., Crosby, K., Becker, A., Ferrante, M., Cheung, W.C., Hong, X., Chirieac, L.R., Sholl, L.M., Haack, H., Smith, B.L., Polakiewicz, R.D., Tan, Y., Gu, T.-L., Loda, M., Zhou, X., and Comb, M.J., *Mutation-Specific Antibodies for the Detection of EGFR Mutations in Non-Small-Cell Lung Cancer.* Clinical Cancer Research, 2009. **15**(9): p. 3023-3028.
184. Shigematsu, H., Lin, L., Takahashi, T., Nomura, M., Suzuki, M., Wistuba, I.I., Fong, K.M., Lee, H., Toyooka, S., Shimizu, N., Fujisawa, T., Feng, Z., Roth, J.A., Herz, J., Minna, J.D., and Gazdar, A.F., *Clinical and Biological Features Associated With Epidermal Growth Factor Receptor Gene Mutations in Lung Cancers.* Journal of the National Cancer Institute, 2005. **97**(5): p. 339-346.
185. Rosell, R., Moran, T., Queralt, C., Porta, R., Cardenal, F., Camps, C., Majem, M., Lopez-Vivanco, G., Isla, D., Provencio, M., Insa, A., Massuti, B., Gonzalez-Larriba, J.L., Paz-Ares, L., Bover, I., Garcia-Campelo, R., Moreno, M.A., Catot, S., Rolfo, C., Reguart, N., Palmero, R., SÃ¡nchez, J.M., Bastus, R., Mayo, C., Bertran-Alamillo, J., Molina, M.A., Sanchez, J.J., and Taron, M., *Screening for Epidermal Growth Factor Receptor Mutations in Lung Cancer.* New England Journal of Medicine, 2009. **361**(10): p. 958-967.
186. Tetsuya, M., Satoshi, M., Yasushi, Y., Shunichi, N., Isamu, O., Junji, T., Takashi, S., Miyako, S., Hirohito, T., Tomonori, H., Kazuhiro, A., Nobuyuki, K., Minoru, T., Hiroshige, Y., Kazuhiko, S., Shinzoh, K., Eiji, S., Hiroshi, S., Shinichi, T., Kazuhiko, N., and Masahiro, F., *Gefitinib versus cisplatin plus docetaxel in patients with non-small-cell lung cancer harbouring mutations of the epidermal growth factor receptor (WJTOG3405): an open label, randomised phase 3 trial.* The Lancet Oncology. **11**(2): p. 121-128.
187. Maemondo, M., Inoue, A., Kobayashi, K., Sugawara, S., Oizumi, S., Isobe, H., Gemma, A., Harada, M., Yoshizawa, H., Kinoshita, I., Fujita, Y., Okinaga, S., Hirano, H., Yoshimori, K., Harada, T., Ogura, T., Ando, M., Miyazawa, H., Tanaka, T., Saijo, Y., Hagiwara, K., Morita, S., and Nukiwa, T., *Gefitinib or Chemotherapy for Nonâ€“Small-Cell Lung Cancer with Mutated EGFR.* New England Journal of Medicine. **362**(25): p. 2380-2388.

188. Mok, T.S., Wu, Y.-L., Thongprasert, S., Yang, C.-H., Chu, D.-T., Saijo, N., Sunpaweravong, P., Han, B., Margono, B., Ichinose, Y., Nishiwaki, Y., Ohe, Y., Yang, J.-J., Chewaskulyong, B., Jiang, H., Duffield, E.L., Watkins, C.L., Armour, A.A., and Fukuoka, M., *Gefitinib or Carboplatin-Paclitaxel in Pulmonary Adenocarcinoma.* New England Journal of Medicine, 2009. **361**(10): p. 947-957.
189. Mukherjee, B., McEllin, B., Camacho, C.V., Tomimatsu, N., Sirasanagandala, S., Nannepaga, S., Hatanpaa, K.J., Mickey, B., Madden, C., Maher, E., Boothman, D.A., Furnari, F., Cavenee, W.K., Bachoo, R.M., and Burma, S., *EGFRvIII and DNA Double-Strand Break Repair: A Molecular Mechanism for Radioresistance in Glioblastoma.* Cancer Research, 2009. **69**(10): p. 4252-4259.
190. Yoshimoto, K., Dang, J., Zhu, S., Nathanson, D., Huang, T., Dumont, R., Seligson, D.B., Yong, W.H., Xiong, Z., Rao, N., Winther, H., Chakravarti, A., Bigner, D.D., Mellinghoff, I.K., Horvath, S., Cavenee, W.K., Cloughesy, T.F., and Mischel, P.S., *Development of a Real-time RT-PCR Assay for Detecting EGFRvIII in Glioblastoma Samples.* Clinical Cancer Research, 2008. **14**(2): p. 488-493.
191. Furnari, F.B., Fenton, T., Bachoo, R.M., Mukasa, A., Stommel, J.M., Stegh, A., Hahn, W.C., Ligon, K.L., Louis, D.N., Brennan, C., Chin, L., DePinho, R.A., and Cavenee, W.K., *Malignant astrocytic glioma: genetics, biology, and paths to treatment.* Genes & Development, 2007(21): p. 2683-2710.
192. Gan, H.K., Kaye, A.H., and Luwor, R.B., *The EGFRvIII variant in glioblastoma multiforme.* Journal of Clinical Neuroscience, 2009. **16**(6): p. 748-754.
193. Mellinghoff, I.K., Wang, M.Y., Vivanco, I., Haas-Kogan, D.A., Zhu, S., Dia, E.Q., Lu, K.V., Yoshimoto, K., Huang, J.H.Y., Chute, D.J., Riggs, B.L., Horvath, S., Liau, L.M., Cavenee, W.K., Rao, P.N., Beroukhim, R., Peck, T.C., Lee, J.C., Sellers, W.R., Stokoe, D., Prados, M., Cloughesy, T.F., Sawyers, C.L., and Mischel, P.S., *Molecular Determinants of the Response of Glioblastomas to EGFR Kinase Inhibitors.* New England Journal of Medicine, 2005. **353**(19): p. 2012-2024.
194. Sonabend, A.M., Dana, K., and Lesniak, M.S., *Targeting epidermal growth factor receptor variant III: a novel strategy for the therapy of malignant glioma.(Report)(Clinical report).* Expert Review of Anticancer Therapy, 2007. **7**(12s): p. S45(1).
195. Pao, W. and Ladanyi, M., *Epidermal Growth Factor Receptor Mutation Testing in Lung Cancer: Searching for the Ideal Method.* Clinical Cancer Research, 2007. **13**(17): p. 4954-4955.
196. Hirsch, F.R., Varella-Garcia, M., McCoy, J., West, H., Xavier, A.C., Gumerlock, P., Bunn, P.A., Franklin, W.A., Crowley, J., and Gandara, D.R., *Increased Epidermal Growth Factor Receptor Gene Copy Number Detected by Fluorescence In Situ Hybridization Associates With Increased Sensitivity to Gefitinib in Patients With Bronchioloalveolar Carcinoma Subtypes: A Southwest Oncology Group Study.* Journal of Clinical Oncology, 2005. **23**(28): p. 6838-6845.
197. Gaiser, T., Waha, A., Moessler, F., Bruckner, T., Pietsch, T., and von Deimling, A., *Comparison of automated silver enhanced in situ hybridization and*

fluorescence in situ hybridization for evaluation of epidermal growth factor receptor status in human glioblastomas. Mod Pathol, 2009. **22**(9): p. 1263-1271.
198. Anderson, L. and Seilhamer, J., *A comparison of selected mRNA and protein abundances in human liver.* Electrophoresis, 1997. **18**(3‐4): p. 533-537.
199. Angenendt, P., *Progress in protein and antibody microarray technology.* Drug Discovery Today, 2005. **10**(7): p. 503-511.
200. Cappuzzo, F., Hirsch, F.R., Rossi, E., Bartolini, S., Ceresoli, G.L., Bemis, L., Haney, J., Witta, S., Danenberg, K., Domenichini, I., Ludovini, V., Magrini, E., Gregorc, V., Doglioni, C., Sidoni, A., Tonato, M., Franklin, W.A., Crino, L., Bunn, P.A., and Varella-Garcia, M., *Epidermal Growth Factor Receptor Gene and Protein and Gefitinib Sensitivity in Non-Small-Cell Lung Cancer.* Journal of the National Cancer Institute, 2005. **97**(9): p. 643-655.
201. Takano, T., Ohe, Y., Sakamoto, H., Tsuta, K., Matsuno, Y., Tateishi, U., Yamamoto, S., Nokihara, H., Yamamoto, N., Sekine, I., Kunitoh, H., Shibata, T., Sakiyama, T., Yoshida, T., and Tamura, T., *Epidermal Growth Factor Receptor Gene Mutations and Increased Copy Numbers Predict Gefitinib Sensitivity in Patients With Recurrent NonÂ–Small-Cell Lung Cancer.* Journal of Clinical Oncology, 2005. **23**(28): p. 6829-6837.
202. Brack, S.S., Silacci, M., Birchler, M., and Neri, D., *Tumor-targeting properties of novel antibodies specific to the large isoform of tenascin-C.* Clinical Cancer Research, 2006. **12**(10): p. 3200-3208.
203. Lorimer, I., Keppler-Hafkemeyer, A., Beers, R., Pegram, C., Bigner, D., and Pastan, I., *Recombinant immunotoxins specific for a mutant epidermal growth factor receptor: Targeting with a single chain antibody variable domain isolated by phageâ€‰display.* Proceedings of the National Academy of Sciences of the United States of America, 1996. **93**(25): p. 14815-14820.
204. Capper, D., Weißert, S., Balss, J., Habel, A., Meyer, J., Jäger, D., Ackermann, U., Tessmer, C., Korshunov, A., and Zentgraf, H., *Characterization of R132H Mutation‐specific IDH1 Antibody Binding in Brain Tumors.* Brain pathology, 2010. **20**(1): p. 245-254.
205. Döppler, H., Storz, P., Li, J., Comb, M.J., and Toker, A., *A Phosphorylation State-specific Antibody Recognizes Hsp27, a Novel Substrate of Protein Kinase D.* Journal of Biological Chemistry, 2005. **280**(15): p. 15013-15019.
206. Haab, B.B., Dunham, M.J., and Brown, P.O., *Protein microarrays for highly parallel detection and quantitation of specific proteins and antibodies in complex solutions.* Genome biology, 2001. **2**(2): p. research0004.
207. Gulmann, C., Sheehan, K.M., Kay, E.W., Liotta, L.A., and Petricoin, E.F., *Array-based proteomics: mapping of protein circuitries for diagnostics, prognostics, and therapy guidance in cancer.* The Journal of Pathology, 2006. **208**(5): p. 595-606.
208. Borrebaeck, C.A.K., *Antibodies in diagnostics - from immunoassays to protein chips.* Immunology Today, 2000. **21**(8): p. 379-382.
209. Abbott, N.L., Lowe, A.M., Bai, Y., Shusta, E.V., Agarwal, N., Raines, R.T., and Kalia, J., *Liquid Crystal-based Analytic Technology Enabling a Molecular View of Cancer.* BIOforum Europe, 2007. **11**: p. 42-45.

210. Tan, L.N., Wiepz, G.J., Miller, D.S., Shusta, E.V., and Abbott, N.L., *Liquid crystal droplet-based amplification of microvesicles that are shed by mammalian cells.* Analyst, 2014. **139**(10): p. 2386-2396.
211. Lowe, A.M., Ozer, B.H., Bai, Y., Bertics, P.J., and Abbott, N.L., *Design of Surfaces for Liquid Crystal-Based Bioanalytical Assays.* ACS Applied Materials & Interfaces, 2010. **2**(3): p. 722-731.
212. Mandell, J.W., *Phosphorylation state-specific antibodies: applications in investigative and diagnostic pathology.* The American journal of pathology, 2003. **163**(5): p. 1687-1698.
213. Cho, Y.K., *Antibody-based membrane proteomics*, in *Chemical and Biological Engineering*. 2010, University of Wiscosin-Madison.
214. Ubersax, J.A. and Ferrell Jr, J.E., *Mechanisms of specificity in protein phosphorylation.* Nat Rev Mol Cell Biol, 2007. **8**(7): p. 530-541.
215. Nelson, A.L., Dhimolea, E., and Reichert, J.M., *Development trends for human monoclonal antibody therapeutics.* Nature reviews drug discovery, 2010. **9**(10): p. 767-774.
216. Byrne, H., Conroy, P.J., Whisstock, J.C., and O'Kennedy, R.J., *A tale of two specificities: bispecific antibodies for therapeutic and diagnostic applications.* Trends in Biotechnology, 2013. **31**(11): p. 621-632.
217. Holliger, P. and Hudson, P.J., *Engineered antibody fragments and the rise of single domains.* Nat Biotech, 2005. **23**(9): p. 1126-1136.
218. Cuesta, Á.M., Sainz-Pastor, N., Bonet, J., Oliva, B., and Álvarez-Vallina, L., *Multivalent antibodies: when design surpasses evolution.* Trends in Biotechnology, 2010. **28**(7): p. 355-362.
219. Holmes, D., *Buy buy bispecific antibodies.* Nature Reviews Drug Discovery, 2011. **10**(11): p. 798-800.
220. Khatwani, S.L., Kang, J.S., Mullen, D.G., Hast, M.A., Beese, L.S., Distefano, M.D., and Taton, T.A., *Covalent protein–oligonucleotide conjugates by copper-free click reaction.* Bioorganic & medicinal chemistry, 2012. **20**(14): p. 4532-4539.
221. Meldal, M. and Tornøe, C.W., *Cu-catalyzed azide− alkyne cycloaddition.* Chemical reviews, 2008. **108**(8): p. 2952-3015.
222. Zheng, C.Y., Ma, G., and Su, Z., *Native PAGE eliminates the problem of PEG‐SDS interaction in SDS‐PAGE and provides an alternative to HPLC in characterization of protein PEGylation.* Electrophoresis, 2007. **28**(16): p. 2801-2807.
223. Wang, P., Na, Z., Fu, J., Tan, C.Y., Zhang, H., Yao, S.Q., and Sun, H., *Microarray immobilization of biomolecules using a fast trans-cyclooctene (TCO)–tetrazine reaction.* Chemical Communications, 2014.